PALEOCLIMATE SIGNAL FROM THE LATE EOCENE NEW JERSEY CONTINENTAL SLOPE: A MULTI-PROXY APPROACH

by

ROBERT H. APPLEBAUM

A dissertation submitted to the Graduate Faculty in Earth & Environmental Sciences in partial fulfillment of the requirements for the degree of Doctor of Philosophy, The City University of New York

2008

This manuscript has been read and accepted for the
Graduate Faculty in Earth and Environmental Sciences in satisfaction of the
Dissertation requirement for the degree of Doctor of Philosophy

Dr. Cecilia McHugh

Date — Chair of Examining Committee

Dr. Yehuda Klein

Date — Executive Officer

Dr. Yan Zheng

Dr. Jeffrey Steiner

Dr. Trevor Williams

Dr. John Chamberlain
Supervisory Committee

THE CITY UNIVERSITY OF NEW YORK

Abstract

PALEOCLIMATE SIGNAL FROM THE LATE EOCENE NEW JERSEY CONTINENTAL SLOPE: A MULTI-PROXY APPROACH

by

Robert Applebaum

Adviser: Professor Cecilia McHugh

Previous studies have documented that global climate cooled in the late Eocene at the million-year time scale. However, the precise details and timing of this cooling remain unresolved. This study proposes that the late Eocene million-year time scale cooling trend was punctuated by precessional Milankovitch cyclicity and that the cooling trend was interrupted by a warm pulse during the latest Eocene. The late Eocene paleoclimate was studied on the New Jersey Continental Margin from slope sediments recovered during Leg 150 of the Ocean Drilling Program. A multiproxy approach that included the following analyses was used: 1) grain size, 2) bulk mineralogy, 3) petrographic thin sections, 4) stable oxygen isotopes from planktonic foraminifera *Globigerina spp*., 5) geophysical FMS logs (Formation Microscanner; measuring conductivity), 6) spectral analysis, and 7) comparison to global records from previously published work.

A general cooling trend from the middle to the late Eocene is indicated by an increase in siliciclastic sediment, decrease in calcium carbonate, and grain size coarsening. These lithologic changes document the transition from carbonate to siliclastic sedimentation that accompanied the paleoclimatic cooling

and was previously documented for this margin. An increase in global ice volume through the late Eocene is also documented by stable oxygen isotopes obtained from the tests of *Globigerina spp*. Low resolution sampling at a 40 ka resolution showed $\delta^{18}O$ values increasing from -3.67 per mil up to -2.83 per mil over a span of 1,050,000 years between 35.3 Ma and 34.25 Ma. High resolution sampling, one sample every 5 ka, over the interval from 34.75 Ma to 34.25 Ma show $\delta^{18}O$ values ranging at -3.0 per mil and is interpreted as warming. These $\delta^{18}O$ values and interpretation are consistent with global composite stable isotope records and interpretations that document a warm period at the close of the late Eocene just before a dramatic short term global cooling in the early Oligocene. This cooling period lasted only a few hundred thousand years.

Orbital forcing of paleoclimate in the late Eocene is shown at high resolution by spectral analysis. Strong spectral peaks were found at intervals of 23.8 years and 19.2 years, which are very close to the Milankovitch precessional frequencies of 23ka and 19ka. Strong spectral peaks were also found at intervals of 23.4ka, and 18.7ka for the middle Eocene. The silica diagenesis found in the middle Eocene carbonates is thought to be the cause of the slight deviations in cyclicity. Precession within the late Eocene is also manifested by increases and decreases in planktonic foraminiferal productivity, measured directly by grain size analysis, and correlated to the oxygen isotope data.

AKNOWLEDGEMENTS

I would like to take this opportunity to thank my advisor Dr. Cecilia McHugh for her scientific mentoring, assistance with numerous software issues, moral support, and grant support for the oxygen isotope work phase of this study. I also thank my dissertation committee members Dr. Yan Zheng, Dr. Jeffrey Steiner, Dr. Trevor Williams, and Dr. John Chamberlain for their reviews and editing of early drafts of the manuscript. Thanks to Dr.'s Frederick Shaw, Jeffrey Osleeb, and Yehuda Klein who served as executive officers of the Earth and Environmental Sciences Department of the Graduate Center during my tenure in the PhD program. The EES department granted me a Science Fellowship my first two years in the PhD program for which I am most grateful and without which I would have never left my former job and entered the program.

Thanks to Lina McClain for administrative support and all her help through the years. Brendan Kennedy, one of my students at Westchester Community College, assisted me with sample preparation and foram separations in the lab. Thanks also to the Hunter College Geography Department and the Queens College School of Earth and Environmental Sciences for the adjunct teaching opportunities. Thanks to my friends and family for their encouragement, and finally most of all to my wife Rachyl for her patience all these years during my studies and her love and support through this difficult journey I embarked upon.

TABLE OF CONTENTS

LIST OF FIGURES

INTRODUCTION

The New Jersey continental margin can be studied within the following climatic framework. Deep-sea drilling researchers have identified three primary climatic intervals for the study of global sea level change: the Cretaceous (140 to 65 Ma) “Greenhouse World”, lacking significant ice sheets; the Paleocene-Eocene (65 to 33 Ma) “Doubthouse World” with questionable ice sheets; and the Oligocene to Holocene (33 Ma to 10,000 years ago) “Icehouse World”, dominated by worldwide changes in sea level driven by cooling and warming events, e.g. glaciations (Miller et al., 1994). Numerous investigations document a growing body of evidence for climate driven control of global sea level since the Middle Eocene (Miller, et al., 1991; Browning et al., 1996, and Miller, et al., 1998, Miller et al., 2002, and Miller et al., 2005).

The Late Eocene is generally recognized as a time of cooling on a global scale (Miller, et al., 1991; Browning, et al., 1996, and Miller, et al., 1998). The details of this cooling remain unresolved however (Bohaty and Zachos, 2003; DeConto and Pollard, 2003; Poag et al., 2003; Pearson et al., 2007). This study proposes that the Late Eocene general cooling trend was modified by Milankovitch cycles. Based on initial inspection of the Formation Microscanner logs, the hypothesis offered is that sedimentation changes along the NJ margin on the million year time scale were modified by a cyclicity controlled by Milankovitch orbital forcing.

Tectonically stable continental margins provide ideal locations for studying paleoclimate changes during the last 65 Ma (Miller et al., 1994; Mountain et al.,

1994; Miller et al., 1998; Steckler et al., 1999; Steckler, 2000). Such passive margins are uninterrupted by tectonic or volcanic disturbances since they are located far from plate boundaries (Miller et al., 1994; Miller et al., 1996). The results are relatively continuous sedimentary sections. This research focuses on the New Jersey Passive Continental Margin and its associated slope sediments. Only occasionally do the sediments include short hiatuses (diastems). Unconformities occur but they are usually widely separated in time (Miller et al., 1994; Aubry et al., 1996; Browning et al., 1996). In fact, unconformities serve to constrain major events along the margin, and in particular for the New Jersey case, provide us with a sequence stratigraphic framework upon which to build a deeper understanding of paleoclimatic changes (Miller et al., 1998).

This study reconstructs paleoclimatic changes during the Late Eocene recorded in sediment sections from Site 904, Leg 150 of the Ocean Drilling Program (ODP), Hole 904A (Miller et al., 1994; Mountain et al., 1994). The stratigraphic section extends upwards for 75 meters from an ejecta layer derived from a major meteorite impact in Chesapeake Bay dated at approximately 35.3 Ma to a major unconformity between the upper Eocene and upper Oligocene (Miller et al., 1994). This unconformity is dated using biomagnetostratigraphy at 34.25 Ma (Aubry, et. al. 1996). These two datums provide us with good age control and a total duration for the studied section of approximately 1,050,000 years.

The age for the ejecta was derived 330 km away from the study area (circa 35.2 ± 0.1 Ma, e.g. millions of years; Glass et al., 1998; McHugh et al.,

1998, citing personal communication of J.D. Obradovich, 11/6/97). Recent work by Pusz et al. (2006) on correlative layers of microtektites in Saint Steven's Quarry in Alabama and ODP Site 1090 in the South Atlantic fixes a rather precise magnetochronologic age of 35.426 ± 0.1 Ma for the tektite layer at these two localities. For the purposes of this study, an average value between these two dates of 35.3 Ma is applied to the tektite layer at Hole 904A.

The intent here is to document the specific nature of this paleoclimate change by applying a multi-proxy approach to the passive margin sediments. The study will develop several proxies to document the changing climatic conditions including: 1) grain size, 2) bulk mineralogy, 3) petrographic thin sections, 4) stable oxygen isotopes, 5) formation microscanner (FMS) geophysical borehole logs, 6) spectral analysis, and 7) comparison of the results to global oxygen isotope records.

1) ***Grain size***. Are there any significant grain size variations up-section? Coarser grain size is indicative of proximity to the shoreline, and grain size generally decreases with distance from the shoreline. An increase of coarser size fractions in the sediments on the slope indicates either a decrease in sea level with an associated regression of the shoreline seaward and sediment bypassing the shelf, or an increase in terrigenous transport across the shelf brought about by climate change and an increase in continental runoff rates.

2) ***Bulk Mineralogy***. What do mineralogical changes tell us about the changing paleoclimate? Changes in the relative amounts of quartz and calcite are expected to reveal paleoclimate shifts through the Late Eocene. Increased

quartz signals the shift to a siliciclastic dominated margin as the climate cools. Cooler climate means an increase in freeze-thaw cycles on land accelerating mechanical weathering rates and hence the removal of quartz grains from either crystalline or sedimentary bedrock. Warmer climate means an increase in carbonate production and hence calcite content in the sediments.

3) ***Petrographic Thin Sections***. The texture and diagenesis of the biosiliceous chalks were studied to evaluate their preservation and answer the following question: can the texture and composition of the sediments be used to extract a climatic signal? An increase of quartz, mica, and glauconite grains is seen in certain thin sections. These thin sections are then matched up with dark and light bands from the conductivity logs. The “signal” in the logs is thus linked directly to grain size and mineralogical variations in the sediments. A complete set of thin sections from borehole 904A, Leg 150 (Offshore Drilling Program) was examined for this study. The thin sections provide a sense of "ground truthing" for new proxy data from additional core sampling done for this study, and give us a standard to check our results against. A previous study by McHugh (1997) provides existing lithostratigraphic data and textural fabrics related to compactional history and diagenesis. Additionally, the petrographic thin sections were used to determine the diagenetic reactions of the chalks and guide the sampling intervals to avoid the noise that diagenesis could cause for the oxygen isotope and formation microscanner data.

4) ***Oxygen Isotopes***. How can oxygen isotopes help reveal paleoclimatic changes? Are there any important changes in ocean circulation recorded by the

oxygen isotope record? Also is there any cyclicity in the data? The relative proportion of the heavy oxygen isotope $\delta^{18}O$ in the calcite of foraminifera is an indicator of both temperature of seawater and global ice volume. When climate cools and global ice volume on land increases, more of the easily evaporated oxygen 16 is preferentially tied up in the ice on land, while more of the less easily evaporated heavier oxygen 18 remains behind in seawater increasing the oxygen 18/oxygen 16 ratio ($\delta^{18}O$) in seawater. Uncertainty exists in estimating the proportion of the oxygen isotope signal from just pure seawater temperature effects and that from global ice volume changes. Global ice volume changes are indicated when there is co-variance of oxygen isotopes from both benthonic and tropical planktonic forams (Miller et al. 1987; Miller at al., 1991).

5) ***Formation Microscanner (FMS) Geophysical Borehole Logs***. Are there significant changes in the conductivity of the slope sediments and how are they related to paleoclimate? What sedimentary factors are driving changes in conductivity? Dark bands on the FMS logs indicate high conductivity while light bands indicate low conductivity. Dark bands correlate with cooler climate intervals when decreased continental runoff brings less terrigenous quartz and mica silt to the slope. The result is a higher proportion of mud which conducts and is recorded as a high (dark-colored band) conductivity signature. Lighter bands correlate with warmer intervals when runoff rates are higher and terrigenous quartz and mica silts supplied to the slope increase. These minerals do not conduct which results in a low (light-colored band) conductivity signature.

6) ***Spectral Analysis and Potential Cyclicity of FMS Logs***. Is there cyclicity in the climate signal recorded by the FMS logs and do Milankovitch periodicities play a role? The rhythmicity of paleoclimate signals using time-series and coherence analysis was also one of the research goals of ODP Leg 150 of the Ocean Drilling Program (Mountain, et al., 1994). This includes the integration of lithostratigraphic, biostratigraphic, paleomagnetic, and geochemical data. The goal of Mountain et al. (1994) was to establish a credible set of datum levels in order to interpret layer thicknesses within the time domain. This means establish reliable sedimentation rates. Reliable magnetostratigraphy and biostratigraphy is already available from previous ODP Leg 150 studies (Aubry, 1996; Aubry, et. al. 1996; Snyder, et al., 1996, and McHugh, 1998).

7) ***Comparison to the Global Record***. Using all previous proxies, how does the New Jersey continental margin record compare to other Ocean Drilling sites throughout the world focusing on the Late Eocene? Why is the New Jersey record important to study?

STUDY AREA

Deep Sea Core Location

The study area is on the continental slope in the New Jersey continental margin. The ODP Leg 150, 904 Site is located in the continental slope approximately 150 kilometers east of Atlantic City, New Jersey at 38^{o} 51.81' N, 72^{o} 46.08' W in 1123 m. of water depth (Figure 1). The paleodepth in the late Eocene was approximately 1020-1120 m. (Katz and Miller 1996). This depth is

transitional from middle (600-1000 m.) to lower (1000-2000 m.) bathyal zones (Katz and Miller 1996). The continental slope here has a gradient greater than 1:40 , or >1.6^{o} (Miller et al., 1994). More recently, extensive high-resolution, multibeam bathymetry (Pratson and Haxby 1996) measured a 2.5^{o} slope along the New Jersey continental margin.

Other Regional New Jersey Margin Study Sites

This study is one of a group of studies collectively termed the New Jersey Mid-Atlantic Sea-level Transect (MAT, see Figure 1 below). Leg 150 and the slope drilling sites (including Hole 904A, this study) were the first step in characterizing the New Jersey Continental Margin (Miller, et al., 1994; Miller et al. 1996; Miller et al. 1998, and Mountain et al., 1994). Later work centered on coastal plain sites (**Leg 150X**) at Island Beach, Atlantic City, and Cape May (Browning et al., 1996; Browning, Miller, and Olsson, 1997, and Browning et al., 1997). Most recently ODP Legs 174A (Austin, J.A. et al., 1998) and 174AX (Miller et al., 1998) were drilled on the continental shelf. ODP Leg 174A drilled Sites 1071 and 1072 on the outer continental shelf and Site 1073 on the upper continental slope. The Bass River Site was drilled during ODP Let 174AX on the New Jersey Coastal Plain (Miller et al., 1998). Sedimentology and stratigraphy from this study (**Hole 904A**) will be compared to the coastal plain sites noted above from Leg 150X (Browning, et al., 1996; Browning et al., 1997a; Browning

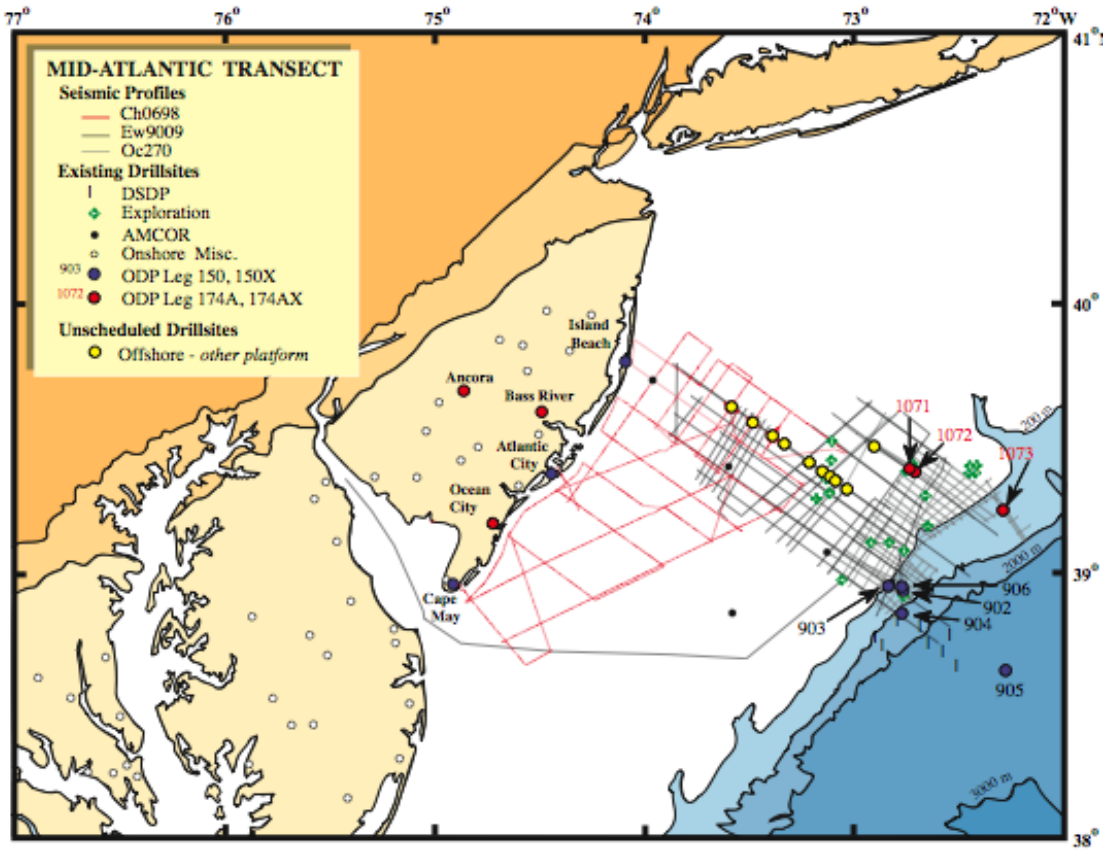

FIGURE 1: New Jersey Margin Drill Sites (Miller et. al., 1998). Note site 904 just down slope from the 1000 m. bathymetric contour in about 1,200 m. of water depth. Leg 150 sites also include Site 905 on the continental rise. Leg 150X coastal plain sites include Cape May, Atlantic City, and Island Beach. Leg 174A shelf and upper slope sites are numbered 1071, 1072 and 1073 respectively. Leg 174AX sites include two additional boreholes onshore at Ancora and Bass River.

et al., 1997b, and Browning et al., 1997). All the New Jersey Continental Margin study sites together have provided us with one of the most complete Eocene stratigraphic records in the world. The results from this study will also be compared to other Late Eocene records from around the globe (Abreu and Anderson, 1998; Diester-Haass and Zachos, 2003; Zachos, et al., 2004, and Pearson et al., 2007).

BACKGROUND LITERATURE

LATE EOCENE GLOBAL COOLING

The Late Eocene is a critical time in Earth history and is extensively studied by geologists and oceanographers (Liu and Yang, 1999; Bestland, 2000; Palike et al., 2001; Kvacek, 2002; Bohaty and Zachos, 2003; Nilsen et al., 2003; Prothero et al., 2003; Bodiselitsch et al., 2004; Pearson et al., 2007). The above studies document a complex series of events recorded by the deterioration (cooling) of the climate into the current "Ice House" conditions. Currently the world is characterized by Antarctic and Greenland ice sheets coupled with northern hemisphere glaciations (Miller et al., 2005). Numerous Late Eocene studies have documented climatic deterioration and a general cooling trend throughout the world (Katz and Miller, 1996; Lavelle, 2000; Wade et al., 2001; Barrett, 2003, and DeConto and Pollard, 2003).

There is a broad consensus of results indicating a general global cooling of the climate through the Late Eocene based on fossil pollen assemblages. In China, the flora takes on a modern appearance by the Late Eocene (Liu and Yang, 1999). Floras of the Yuanqu Basin in China show a shift from temperate and humid subtropical climate to a mild temperate zone climate (Wang, 1999). Palynofloras of east Texas show major changes in land plant assemblages through the Middle Eocene to Oligocene interval. The trend shows a gradual disappearance of tropical humid elements and the appearance of cooler drier elements in the palynofloras (Yancey and Elsik, 1999; Elsik and Yancey, 2000). In southeastern Mississippi and southwestern Alabama, a major floral turnover

(species change) also occurred well before the early Oligocene, probably at the end of the Middle Eocene (Oboh-Ikuenobe and Jaramillo, 2003). Their early Oligocene palynofloral assemblage is indicative of a cooler temperate climate in comparison with warmer more tropical elements in Early and Middle Eocene assemblages.

A cooling trend in the Late Eocene is argued for based on distinct changes in clay assemblages in the Southern Ocean (Kerguelen Plateau and Maud Rise; ODP sites 744 and 689). The clay mineral trends show a step by step evolution of marine and continental Antarctic environments that eventually resulted in permanent ice coverage and dense cold water formation (Robert et al., 2002). A cooling trend is also shown by an increase in biogenic silica production or preservation after the Eocene/Oligocene boundary at ODP site 925 on the Ceara Rise in the western equatorial Atlantic (Nilsen et al., 2003).

A drawdown in atmospheric CO_2 on a global basis in the Late Eocene has been linked to changes in continental weathering rates, ocean circulation and paleoproductivity in the oceans (Pearson et al., 2000; DeConto and Pollard, 2001; Way and DeConto, 2002; DeConto and Pollard, 2003, and Barrett, 2003). Modeling results indicate Late Eocene global cooling while the declining CO_2 content in the atmosphere and orbital parameters were the major forcing factors in the rapid build-up of East Antarctic ice (DeConto and Pollard, 2001).

Fluegeman (2003) suggests that Late Eocene global cooling is a factor in the benthic foraminiferal succession for the Gulf Coastal Plain. He found that benthic foraminiferal turnover patterns there are similar to neritic benthic

foraminiferal faunas from southern Australia. Fluegeman (2003) studied planktonic and benthic foraminifera and found an inverse correlation between planktonic : benthonic ratios and $\delta^{18}O$ data from *Cibicidoides spp* in the Mossy Grove Core (upper Eocene through Oligocene) from western Mississippi. Presumably then, during cooling periods (oxygen isotope **increases**), sea-level will drop as continental ice builds up and then planktonic: benthonic ratios **decrease** since there is less water column through which to accumulate planktonic individuals; hence the inverse relationship between $\delta^{18}O$ and planktonic: benthonic ratio (**p/b**). Based on the temporal resolution, he attributed this relationship to glacioeustatic cycles for this interval in the Late Eocene.

A climate change from warm humid Late Eocene conditions to cooler drier Early Oligocene conditions is recorded by a decrease in weathering rates of paleosols from the mid-latitude setting of central Oregon (Bestland, 2000). Precise age control from Cascade Arc volcanic rocks and ash falls make these paleosol sequences ideal for global age comparisons with other regions. Resolution of paleoclimatic trends is comparable with deep sea cores (Retallack 2002). Paleosol sequences from areas in Oregon, Montana, and Nebraska-South Dakota agree with such landmarks of deep-sea records as terminal Eocene warm-wet conditions followed by earliest Oligocene cold-dry conditions (Retallack, 2002) and thus record global climate rather than local tectonic effects.

Climatic cooling coupled with eustacy-related events best explains the timing and mechanisms of extinctions and appearances of mollusk groups across the Eocene/Oligocene boundary in both North America and Europe (Dockery III

and Lozouet, 2003). Additionally, biotic patterns of mollusks along the Carolinas of the southeast Atlantic Coastal Plain are similar to the Gulf Coastal Plain (Campbell and Campbell, 2003). Campbell and Campbell (2003) found that substantial species-level extinctions across both the mid-Bartonian (middle upper Eocene) and the Eocene/Oligocene boundary suggest a gradual or stepwise decline (cooling) rather than an abrupt Eocene-Oligocene extinction.

Along the Gulf Coastal Plain, temperature decreases ranging from 25° to 30° C in the Paleocene down to 15° to 20° C across the upper Eocene / Oligocene boundary are recorded by oxygen-18 isotope data collected from fish otoliths or “ear stones” (Ivany et al., 2003). The researchers also found increased seasonality across the Eocene / Oligocene boundary with markedly cooler winter temperatures recorded by the otoliths.

In contrast to the general climatic deterioration and global cooling through the Late Eocene, a more pronounced decrease of 3° to 4° C for ocean bottom waters signaling increased Antarctic ice volume is recorded by a sharp increase in marine oxygen isotope ratios toward heavier values near the Oligocene-Eocene boundary. This dramatic early Oligocene cooling event (Zachos et al., 1996) heralds the appearance of permanent ice sheets on Antarctica during the Oligocene and the inception of the modern "Ice House" world. An ice sheet with half the mass of present day Antarctic ice has been proposed (Miller et al., 1987; Zachos et al., 1994).

A review of the literature shows that Late Eocene global cooling is far from a simple or regular trend though and may have proceeded through several

phases (Bohaty and Zachos, 2003). Poag et al. (2003) studied a Late Eocene section in southeastern Virginia just above the Chesapeake Bay impact horizon. They infer three separate Late Eocene warming events or sub-pulses from the oxygen isotope record there. They attribute these to successive bolide impacts during a comet shower. A warm pulse in the Late Eocene is recorded by the high-resolution oxygen isotope record gathered for this study.

Orbital Forcing in the Late Eocene

Milankovitch cycles in the Eocene have also been examined in several important studies from around the world. Orbital forcing in the Middle to Late Eocene was found by Palike et al. (2001) for sediments from ODP Leg 171B, Site 1052 from Blake Nose along the Atlantic margin of northern Florida. Precessional forcing was resolved by Wade et al. (2001) in stable oxygen isotope records from benthic foraminifera living at Blake Nose, western North Atlantic waters for the late Middle-Eocene. Clear Milankovitch-scale paleoclimate oscillations were found by Retallack (2002) in exceptional Late Eocene (40.0-40.5 Ma) paleosol sequences in Oregon. Near 400-kyr cycles of productivity and clay mineral composition were found by Robert et al. (2002) suggesting that orbital frequencies played a role in small-scale variations of both continental and marine Antarctic environments of the late Paleogene at ODP Sites 744 and 689, the Kerguelen Plateau and Maud Rise of the South Atlantic. High frequency variations in sedimentation rate approximating Milankovitch frequencies of 10^4 to

10^5 years (Shipboard Scientific Party, 2000) were also found in the preliminary results from LEG 189 of the Ocean Drilling Project.

THE NEW JERSEY CONTINENTAL MARGIN

Margin Tectonics

The New Jersey and more generally the U.S. Atlantic margin is a classic passive continental margin (Mountain et al., 1994). Passive continental margins are ideal for studying paleoclimate change because sedimentation is relatively continuous with few or no tectonic disturbances. The New Jersey continental margin began its evolution following the rifting apart of Europe and North America in the Late Triassic (Mountain et al., 1994). Rifting opened up the modern Atlantic Ocean as North America drifted slowly westward away from Europe. For this reason, passive margins are also referred to as trailing margins since the location of the margin trails behind the direction of plate motion.

The North Atlantic sedimentary basin formed by a process that involves sudden stretching, followed by slow cooling of the lower part of the plates that are separating (McKenzie 1978). This thermal cooling of the ocean plate causes subsidence along the periphery of the basin. The Atlantic-type margin (New Jersey margin) of the East Coast, U.S., is characterized by up to 12 km. of seaward-dipping Mesozoic and Tertiary sediments (Steckler and Watts, 1978). Steckler and Watts (1978) examined the origin of subsidence along the East Coast of the U.S. by applying a simple thermal model for the cooling lithosphere. They accomplished this after removing the effects of sediment loading,

compaction, water depth, and sea level changes (Steckler and Watts, 1978). Lister et al. (1986) point out the role of detachment faulting in producing marginal asymmetry on either side of a developing basin. The New Jersey margin, as part of the East Coast of the U.S., resembles their "Upper-plate margin" type. The Upper-plate type (Lister et al., 1986) is characterized by seaward-dipping normal faults in the upper part of the crust above the basal detachment fault.

The New Jersey margin was responding to gradual lithospheric subsidence (post-Mesozoic rifting) and gradual sediment loading (McKenzie, 1978; Steckler and Watts, 1978, and Lister et al., 1986). Clinoform progradation probably began during the latest Eocene and continued into the Oligocene. Clinoforms averaged approximately 20 meters thick for the Late Eocene. The youngest Eocene to early Oligocene sequences formed a wedge-shaped geometry (Pekar et al., 2000). Because subsidence was slow and gradual, a limited amount of accommodation space was created.

Present Margin Physiography and Sedimentation

The New Jersey continental margin today is tectonically quiescent. Currently the Holocene sea-level highstand means most modern river sediment is trapped close to shore near major river mouths such as the Hudson, Delaware, and Susquehanna. Little, if any, terrigenous sediment reaches the outer shelf or slope (Mountain et al., 1994). Modern sedimentation on the slope is primarily hemipelagic and sediments are derived from muds carried as suspended

material from river discharge or from resuspended shelf sediments carried off the shelf (Mountain et al., 1994**)**.

Continental Slope Physiography and Sediments

The modern continental slope can be subdivided into the upper slope (200 to 1500 m of water depth) and the lower slope from 1500 to 2500 m (Mountain et al., 1994). Overall, the present continental slope averages a gradient of 2.5^{o} (Pratson and Haxby, 1996). The upper slope (< 1500 m.) contains semi-lithified to unconsolidated Tertiary to Quaternary muds (Pratson and Haxby, 1996). Lithified Eocene biosiliceous chalks and biosiliceous porcellanitic chalks crop out on the lower slope and submarine canyons incise into the chalks (McHugh et al., 1993). McHugh et al. (1993) found that upper slope submarine canyons have a "V-shaped" profile while lower slope canyons are "U-shaped".

Late Eocene Margin Physiography and Sedimentation

Bathymmetric slope and sedimentation along the New Jersey continental margin were quite different during the Late Eocene. During this time, the margin was a relatively steeply dipping carbonate ramp with a paleogradient between 1 : 300 and 1 : 500 and a shelf edge in at least 500 meters of water depth (Steckler et al., 1999). This configuration changed in the Oligocene and Miocene as the margin shifted from carbonate to siliciclastic sedimentation. These sediments formed a series of prograding clinoform wedges (Steckler et al., 1999). Terrigenous input to the margin increased as the climate cooled and erosion

rates increased, along with possible tectonic rejuvenation in the Appalachian source area (Pazzaglia and Gardner, 2000). This progradation was most accentuated during the Miocene and built the shelf edge out to its current position in about 130 meters of water (Steckler et al., 1999). The margin was transformed from a seaward-dipping, deep carbonate ramp to a flatter shelf with a sharp edge at present (Steckler 2000).

During the Late Eocene sedimentation was dominantly open ocean pelagic to hemipelagic calcareous and siliceous oozes (McHugh 1997). The climate was warmer than today, but it is recognized from Ocean Drilling Program studies, sequence stratigraphic approaches, and stable isotope studies (Miller et al., 1991; Browning et al., 1996, and Miller et al., 1998) that the Late Eocene is a time of cooling. Important regional to global climatic coolings are documented during and at the close of the Eocene (Browning et al., 1996) and during the early Oligocene (Zachos et al., 1996).

Middle to upper Eocene sediments of the New Jersey slope consist of semi-indurated, moderately to intensely bioturbated biosiliceous nannofossil chalks with clay and foraminifers (Aubry et al., 1996). The Eocene slope setting was deeper and quieter than the coastal plain. The dominant sedimentary process during the Eocene was open ocean pelagic settling of fine-grained sediment. (Shipboard Scientific Party, Site 904, In Mountain et al., 1994). The greater depth at the slope means that sedimentary sequences are much more complete than for the coastal plain (continental shelf). Problems of erosion and exposure due to eustatic sea-level falls rarely occur in the slope. The slow

rainout of fine pelagic oozes was occasionally interrupted though. Although a minor process at slope sites, McHugh (1997) describes horizons in the upper Eocene rich in glauconite that correlate with detrital quartz, and interpreted this as transport of terrigenous sediment from shallow water. McHugh (1997) further points out that the influx of terrigenous material predominantly in the Late Eocene signals the shift from carbonate to siliciclastic sedimentation also recorded at correlative sites on the coastal plain. This shift is marked by a major unconformity between upper Eocene pelagic biosiliceous chalks and upper Oligocene hemipelagic silty clays.

Coastal Plain Physiography and Sediments

According to Browning et al. (1996), beginning in the late-middle Eocene (43-42 Ma), a shift from carbonate-dominated to siliciclastic-dominated sedimentation began along the coastal plain near to the shoreline. Middle Eocene (Browning, Miller, et. al. 1997, and Browning, Miller, and Olsson, 1997), and upper Eocene stratigraphic sequences (Browning, Miller, and Bybell, 1997) are identified within the New Jersey coastal plain. Typical Eocene sequences consist of thin glauconite-rich clay at the base followed by clays above which become slightly sandy at the top (Browning, Miller, and Olsson 1997). Glauconite forms in the ocean shelf regions (60 to 1,000 meters deep) when there is very little or no sediment being supplied to the shelves by rivers from the continents. This allows the glauconite minerals to grow, taking from 10,000 up to a million years to reach sand size (>63μ). Generally, the presence of glauconite signals

that terrestrial transport of sediments has slowed down or stopped due to climate changes, or perhaps sea level has risen resulting in the capture of these sediments closer to the shoreline nearer major river mouths.

Sequence Stratigraphy

Eocene coastal plain sequences (Vail and Mitchum, 1977) are bounded by unconformities or gaps. The strata within each sequence are part of a genetically related sedimentary package deposited during a single cycle of sea level fall and rise. Eocene sequences have been dated by combining lithostratigraphy, magnetostratigraphy, and biostratigraphy (Browning, Miller, and Bybell, 1997). Faunal trends of microfossils include abundance of planktonic foraminifera, calcareous nannofossils, dinocysts, diatoms and their relative proportions (Miller, et al., 1998).

In terms of sequence stratigraphy, coastal plain sequences are characterized by transgressive systems tracts (**TST**) and highstand systems tracts (**HST**); lowstand systems tracts (**LST**) are absent. Sequence bases are characterized by reworked quartz, micas, and glauconite indicating transgressive surfaces. The tops of these sequences are sometimes coincident with the maximum flooding surface, indicated by peak occurrences of the benthic foraminifera *Uvigerina spp.* (Browning, Miller, and Bybell, 1997). These are followed upward by silty-clays and foraminiferal chalks of the highstand, deposited during deeper water phases as sea level was rising. Sometimes these

beds are capped by sands indicating limited progradation and terrigenous input at the close of highstand phases.

Some components of the typical upper Eocene sequences may be lacking at a given locality along the shelf (Miller et al., 1998). Due to erosion or variation in the relative rate of sea level falls and rises, not all the typical kinds of sediments and fossils normally associated with a single sequence or sea level cycle are necessarily represented in the sedimentary record. Erosion may even remove entire sequences. Sequences are more likely to be complete for slope sediments. In order to compare sediments from widely spaced localities (coastal plain vs. slope), extreme care must be taken in order to recognize where erosion has removed part of the record.

Upper Eocene sequences contain burrowed clay throughout with little sand, and again thin glauconitic intervals at the bases (Browning, Miller, and Bybell, 1997). Miller, et al. (1998) generally describe Eocene sequences as containing thin basal glauconitic clay or clayey sand overlain by carbonate-rich foraminiferal/radiolarian clay. Paleowater depths from coastal plain drilling sites are in the range from 75 to 125 meters based on benthic foraminiferal biofacies analysis (Browning, Miller, and Bybell, 1997).

Age Control for Studied Interval

This study is focused within the Late Eocene, presently defined as from 41.3 to 33.7 million years ago according to the time scale of Berggren et al. (1995). New Jersey slope sediments studied here were laid down during the end

of this time interval. We have good age control for this interval from several reliable sources. A tektite (glass micro-spherules) layer has been radiometrically dated at 35.1 to 35.2 Ma (million years) for slope drill Site 904 (McHugh et al., 1998, citing personal communication of J.D. Obradovich, 11/6/97). This tektite layer was deposited in response to a large meteorite impact at Chesapeake Bay (Poag et al., Glass et al., McHugh et al., 1998). Recent work by Pusz et. al. (2006) on correlative layers of microtektites in Saint Steven's Quarry in Alabama and ODP Site 1090 in the South Atlantic fixes a rather precise magnetochronologic age of 35.426 ± 0.1 Ma for the tektite layer at these two localities. For the purposes of this study, an average value between these two dates of 35.3 Ma is applied to the tektite layer at Hole 904A. Aubry et al., (1996) have precisely dated the upper surface of the upper Eocene for the slope by combining the occurrences of a number of planktonic microfossils and the time scale of Berggren et al., (1995). They estimate the age of the boundary at 34.25 Ma. This presents us with an interval of approximately 1,050,000 years (35.3 minus 34.25 Ma) to work with for the youngest Eocene strata recorded at our drilled site 904A.

DETAILED LITHOSTRATIGRAPHY, BIOSTRATIGRAPHY, AND MAGNETOSTRATIGRAPHY OF HOLE 904A

Lithostratigraphy

A complete Eocene section is available from ODP Leg 150, drill hole 904A. The drilling also penetrated Neogene and Recent deposits above the

Eocene. Figure 2 below shows a generalized lithologic column with available magnetostratigraphy and biostratigraphy. Cores (each 9 meters length) are designated by numbers 36 through 62 on the left of the column. Note the three major unconformities; first one at 341.20 meters below the sea floor (mbsf), separating the upper Eocene from upper Oligocene; second at 420 mbsf, separating the middle Eocene from the upper Eocene; and third at approximately 560 mbsf, separating the lower middle Eocene from the middle middle Eocene. Note also the tektite layer at 416.1 mbsf, approximately 4 meters above the second unconformity.

Biostratigraphic zones (Aubry et. al., 1996) are delineated by solid lines where the boundaries were based on good marker species and by dotted lines where inferred (see Figure 2 below). The only nannofossil interval not successfully subdivided is the upper NP15-lower NP16 zonal interval (note dotted line on Figure 2). Only two of the planktonic foraminiferal zones shown are subdivided, the P11/P12 and P14/P15 boundaries; all other zonal boundaries are inferred (dotted lines).

Eocene chalks are overlain at the first unconformity (Figure 2, 341.2 mbsf) by dark brown glauconitic sandy silty-clays (McHugh, 1997). Diagenetic effects and less common non-carbonate grains are most pronounced just at and below the major unconformities shown below in Figure 2. At the first unconformity (Figure 2, 341.2 mbsf), McHugh (1997) noted the presence of glauconite, forams with dark halos, fluid pathways, and detrital quartz. The dark halos and fluid pathways indicated diagenesis. Possibly the lowstand of sea-level permitted for

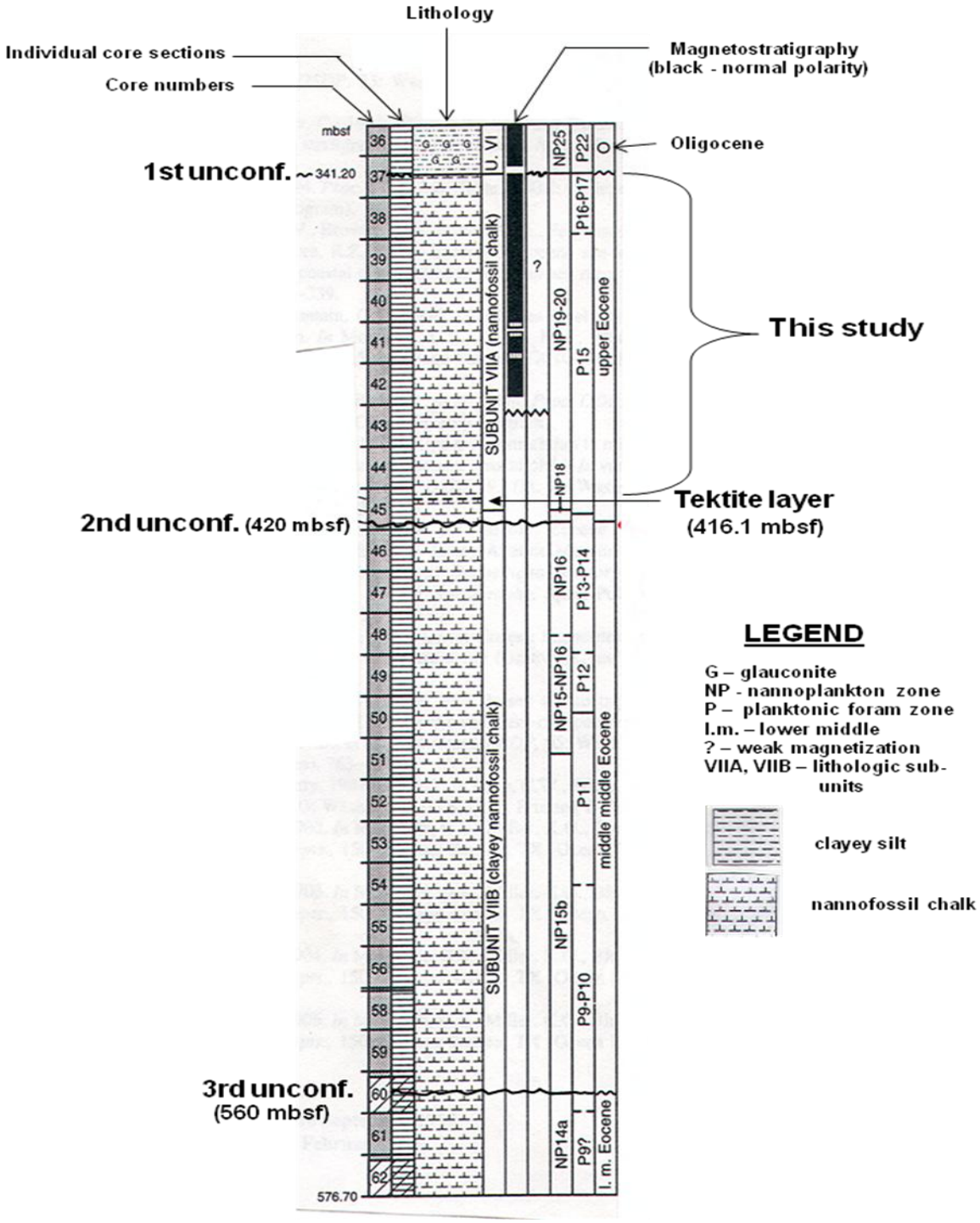

FIGURE 2: Lithostratigraphy of Hole 904A (after Figure 1 from Aubry, 1996). Note the 3 major unconformities at 341, 420, and 560 mbsf. The 1st unconformity separates nannoplankton (NP) zone NP19 below from NP25 above, and planktonic foram zone P17 below from P22 above. Biostratigraphic zonal boundaries are dashed lines where inferred. The 2nd unconformity separates nannoplankton zones NP16 below and NP18 above (NP17 is missing). The 3rd unconformity separates zones NP14a below from NP15b above. Note also the tektite layer at 416.1 mbsf.

increased pore fluid pressure to reach the shelf and perhaps the upper slope, leading to diagenetic reactions. The quartz grains and glauconite (dark brown) indicate transport. McHugh (1997) interpreted these grains as evidence of terrigenous transport from shallower waters across the shelf to the continental slope since glauconite does not form in the deeper waters of the continental slope. All these features decrease systematically downward from the unconformity (McHugh 1997). At the second unconformity (Figure 2, 420 mbsf), well-preserved forams are found just below and constitute reworked clusters (McHugh, 1997). Diagenetic fluid pathways and staining are also evident from thin sections. At the third unconformity (Figure 2, 560 mbsf), abundant diagenetic fluid pathways constitute 90% of the matrix, which is unusual for the Lower Eocene (McHugh, 1997). The matrix is rich in silica, and just above the unconformity McHugh (1997) found reworked forams altered to re-crystallized quartz. The present author found peculiar re-crystallized quartz-pyrite composite grains in two samples just above the tektite layer at 416.1 mbsf (see Figure 2 above). These are quite different from the reworked forams described by McHugh (1997), and are interpreted to be reworked ejecta materials from the Chesapeake Bay meteorite impact. This means that the ejecta continued to fall through the water column for quite some time after the impact event. The texture of these grains is brecciated and looks like the quartz and pyrite fragments were fused together during impact.

Biostratigraphy

Snyder et al. (1996) provided a comprehensive biostratigraphy based on planktonic foraminifera for all drill holes from ODP Leg 150 including Hole 904A. The foram work in the current study closely follows the framework laid out in Snyder et. al. (1996) published as part of the ODP Scientific Results from Leg 150. Key planktonic species were identified using the range zone chart from Snyder, et. al. (1996) and several standard microfossil references including Van Morkoven et al. (1987), Loeblich and Tappan (1988), and Bolli et al. (1994). Two other important papers with applicability to the fauna on the New Jersey slope were used. These include the work of Poag and Commeau (1995) that outlines and richly illustrates important planktonic species from the Salisbury embayment in Virginia and Maryland, and Snyder and Waters (1985), focusing on the Goban Spur region off southwestern Ireland from DSDP Leg 80. The current study relies principally on these important references and draws heavily from the work of Snyder et al. (1996).

Snyder et. al. (1996), indicate that zonal and chronozonal boundaries for Site 904 are often inferred based on the highest common occurrence of diagnostic taxa in conjunction with changes in the quality of preservation. Chronozonal assignments are tentative due to problems with reworking of middle Eocene taxa up into the upper Eocene part of the section. Lab work with planktonic forams during this study did encounter a few middle Eocene individuals in samples close to the tektite layer but they were rare (Figure 2 above, core sections 44 and 45). The vast majority of planktonic foram

individuals seen were in fact upper Eocene taxa and this simplified problems of identification.

According to Snyder et. al. (1996), the P14/P15 zonal boundary is placed 4.1 meters below the tektite layer at 416.1 mbsf (see Figure 2 above). The base of zone P16 is placed within the study section for this paper near the bottom of core section 38 (Figure 2). Chronozones P16 and P17 could not be differentiated reliably (Snyder et al., 1996). Individual species used during the current study are discussed below under the methods and results sections.

Snyder et al. (1996) also presented abundance patterns of planktonic foraminifera for Hole 904A. The number of planktonic foraminifers per gram of sediment revealed dramatic changes from the Eocene through the Miocene. The changes are complex and probably related to a number of factors including sea-level changes, diagenesis, paleoproductivity, and local sedimentation rate.

Katz and Miller (1996) present a rigorous study using benthic foraminifera and place the sediments from the New Jersey slope within a sequence stratigraphic context. This study included all the drill holes of ODP Leg 150 including Hole 904A. Paleodepths were estimated using backstripping methods, which take into account thermal subsidence of the crust and loading of the sediment pile. Once these effects are removed, a paleodepth was determined. Benthic foraminiferal distributions were used to evaluate paleodepths for sections lacking independent depth estimates. Paleodepth for the slope Site 904 was estimated at 1020 to 1120 meters of water depth.

Katz and Miller (1996) found that upper Eocene bathyal faunas on the New Jersey transect contain high abundances of *Bulimina alazanensis* (up to 50%) similar to peak *B. alazanensis* abundances reported from other Atlantic locations. They speculated that this uniform biofacies indicated that circum-Atlantic (including Site 904, this study) and Gulf of Mexico sites were ventilated by similar intermediate to upper deep-water masses in the Late Eocene.

Eocene benthic foraminifers on the New Jersey transect represent cosmopolitan deep-water faunas (Katz and Miller, 1996). They split benthic taxa up into five principle factors using Q-mode principal component and varimax factor methods. The five factors are recognized by certain major taxa that together constitute unique benthic foraminiferal biofacies. Early to middle Eocene bathyal biofacies were characterized by *Lenticulina spp*., *A. wilcoxensis*, and *Osangularia spp*. Bathyal biofacies shifted to one dominated by *B. alazanensis*, *Osangularia spp*. and *P. bulloides* by the upper Eocene. Katz and Miller (1996) suggest that this major bathyal faunal change near the end of the middle Eocene at New Jersey reflects a global event that is also recorded at other bathyal and abyssal sites. Several other important studies also looked at benthic foraminifera to evaluate sequences along the New Jersey transect (Browning, Miller and Olsson, 1997; Browning, Miller and Bybell, 1997, and Miller et. al., 1998).

Magnetostratigraphy

No reliable magnetostratigraphic record was obtained in Hole 904A. The normal signature obtained at the top of Figure 2 was not identified with a

specific magnetic chron due to the weakly magnetized chalks and correlation uncertainties (Aubry et. al., 1996).

GLACIOEUSTACY AND LATE EOCENE CLIMATE

General Framework

It is important to place the New Jersey Passive margin into the overall glacioeustatic context of the early Cenozoic. Cenozoic paleoclimate studies have relied heavily on results from stable oxygen and carbon isotopes gathered using planktonic and benthonic foraminifera or both (Miller et al., 1987; Prentice and Mathews, 1988; Miller et al., 1991, and Zachos et al., 1994). These studies have also related the results of stable isotope series to the eustatic curves of Haq et al. (1987). Using Neogene sea level cycles, Haq et al. (1987) noticed deep sea sedimentation gaps correspond with either condensed sections (marine flooding surfaces) or sequence boundaries. They relate these boundaries to changes in deep water masses brought about by eustatic sea level changes. Highstand phases correspond with dissolution hiatuses in deeper water due to a lowering of the calcium compensation depth (CCD) as carbonate sediments are trapped near shore. Lowstand phases correspond to sequence boundaries and erosional hiatuses in deeper water due to stronger thermal gradients brought about by enhanced climatic inequitability (Haq et al., 1987). At a paleodepth of 1020 to 1120 meters (Katz and Miller, 1996), the New Jersey slope was well above the CCD so carbonate dissolution was driven by cooler drier periods when primary production was lowered.

Unconformities are an important part of the sedimentary record at New Jersey and serve to frame the temporal resolution of the current study. Therefore, Haq's et. al. (1987) paper is applicable to all passive margins including New Jersey where exceptional sedimentary sequences are available. However, recent work (Miller et al., 2005) has brought into question the magnitude of Haq's eustatic falls for the last 100 My. The timing of those sea level changes is not questioned. Miller et al. (2005) suggest that the amplitudes of Haq's sea level curve are at least 2.5 times too high when compared to their eustatic estimates.

As mentioned previously, multi-proxy climatic data from numerous studies document the Late Paleogene and in particular the Late Eocene as a time of global cooling (Miller et al., 1991; Browning et al., 1996, and Miller et al., 1998). Taking into account this global cooling trend, many stable isotope studies have considered the question of whether sea level changes in the early Tertiary and near the Eocene/Oligocene boundary were related to glacioeustatic changes (Miller et al., 1987; Miller et al., 1991; Zachos et al., 1994; Abreu and Anderson, 1998, and Hurley and Fluegeman, 2003). A critical factor in unlocking the glacioeustatic signal during this time is the timing of glaciation on Antarctica and the first true appearance of ice sheets there.

Stable isotope studies can be used as a proxy for glaciation in Antarctica. According to Miller et al. (1991), the best indicator of ice growth is a coeval increase in global benthic and western equatorial planktonic $\delta^{18}O$ records. They document up to a dozen such oxygen isotope increases during the Oligocene

and Miocene from global scale Deep Sea Drilling records and attribute these to glacioeustacy. However, it is unclear if ice sheets existed on Antarctica during the Middle to Late Eocene "Doubt House" world, and oxygen isotope increases during this time are not presently linked unequivocally with glacioeustatic sea level lowerings.

Evidence from Antarctica

Direct evidence for expansion of an East Antarctic ice sheet comes from fossil bivalve fragments recovered from glacial diamictites occurring in Prydz Bay (Lavelle 2000). Strontium isotope stratigraphy suggests an age of approximately 33 million years for these glacial sediments. Lavelle (2000) also found West Antarctic glacial sediments on King George Island dated by strontium isotopes to 30 million years. The earliest glacial marine deposits from Seymour Island, Antarctic Peninsula, date to just at or very close to the Eocene / Oligocene boundary at 33.7 Ma and suggest the presence of a regionally extensive West Antarctica ice sheet (Ivany et al., 2006). These dates suggest that permanent ice sheets were not present in Antarctica prior to the Early Oligocene. Magnetostratigraphic records of Oligocene glaciomarine sediments from the Victoria Land Basin also corroborate Lavelle's findings of no major East Antarctic ice sheet growth in the Late Eocene (Wilson et al., 1999). Their results show no major ice sheet until well into the Oligocene. Other less precise estimates of Middle to Late Eocene Antarctic glaciation come from studies of clay mineral assemblages in McMurdo Sound (Ehrmann 1998), the presence of floating ice in

association with a terrestrial flora stunted by cold temperatures (O'Brien et al., 2000; ODP Leg 188), or quartz grain micro textures in fluvio-deltaic sands from Prydz Bay ODP Site 1166 (Strand et al., 2003).

Ocean Gateways

It is also important to consider the configuration of major ocean gateways and their effect on global ocean circulation and deep-water masses. In the Late Eocene (40 Ma), the Caribbean Seaway extended westward to an open ocean gateway between North and South America (Iturralde-Vincent, 2003). Crucial to an understanding of surface and deep water flow across the New Jersey continental slope is the possible closing of this gateway during the Latest Eocene-Early Oligocene (35-32 Ma) by the formation of the land bridge Gaarlandia east of present Central America (Iturralde-Vincent, 2003). This would have enhanced the western boundary current in the north Atlantic forming the ancestral Gulf Stream flowing north past New Jersey.

Of particular importance in evaluating the presence of an Antarctic ice sheet in the Late Eocene are the Southern Ocean gateways including the Tasmanian Gateway and the Drake Passage. The conventional argument links the formation of the Antarctic Circumpolar Current (ACC) and isolation and cooling on Antarctica to a fully open Drake Passage and Tasmanian Gateway. Fully open gateways allow deep-water circulation that detaches the ACC from warmer western boundary currents moving southward, in particular along the eastern margins of Australia and South America. This reduces ocean heat

transport south to Antarctica and promotes the growth of ice sheets. According to Lawver and Gahagan (2003), major plate motions based on dated seafloor spreading anomalies and distinct fracture zone lineations constrain the age of the opening of a seaway between the South Tasman Rise and Antarctica as very close to the Eocene-Oligocene boundary, with an unrestricted opening deeper than 2000 meters dating from approximately 32 Ma. Also based on plate tectonic reconstructions, Lawver and Gahagan (2003) suggest that the Drake Passage was open to deep-water circulation by approximately 31 plus or minus 2 million years.

The Role of CO_2

More recently, studies have considered the opening of the Southern Ocean gateways and changes in ocean heat transport to have a smaller effect than previously thought (Hay et al., 2002; Barrett, 2003, and DeConto and Pollard, 2003). These authors have looked at the role of declining atmospheric CO_2 from the Cretaceous into the early Cenozoic and during the Eocene-Oligocene transition. Hay et al. (2002) contend that the decline in CO_2 was a major factor in the Eocene-Oligocene decline. DeConto and Pollard (2002) provide a model with an alternative explanation for the sudden build-up and subsequent variations of Antarctic ice near the Eocene/Oligocene boundary, emphasizing atmospheric CO_2, orbital forcing, and ice-climate feedbacks. Their model shows that a 20% change in southward ocean-heat convergence had a significant effect on the timing of glacial inception on Antarctica, but only within a

relatively narrow range of CO_2 (2.5 to 3X the present value). The model also shows that the exact timing of the glaciation can be paced by orbital variations that lead to cooler winters and snow accumulation on the Antarctic continent.

The debate over the triggering mechanism for Antarctic glaciation at the Eocene-Oligocene boundary is ongoing and will require more work in the future. Most likely the solution will involve a combination of plate tectonic considerations, ocean heat transport, Milankovitch cycles, and global atmospheric circulation models considering CO_2. At any rate, according to Lawver and Gahagan (2003), the complete opening of the two main Southern Ocean gateways (32 Ma or younger) took place just after the time interval for this study along the New Jersey margin between 35.3 Ma and 34.25 Ma. The current author considers this close enough in time that we must consider these Southern Ocean changes and their possible effect on deep-water masses that may have affected the New Jersey margin and its sediments.

Eustacy and the New Jersey Margin

The global $\delta^{18}O$ record for the Eocene suggests only limited eustatic rises and falls on the order of 10 to 20 meters (Miller et. al., 1998); slightly larger values are estimated at 27 to 55 meters for the Middle Eocene from a benthic foraminiferal $\delta^{18}O$ record at ODP Site 527 (Browning, et. al. 1997). At New Jersey, with a relatively flat ramp margin (slope 1:300 to 1:500; Steckler et al., 1999) and limited accommodation space, these relatively small sea-level changes could have meant exposure of the shelf and generation of type-1

unconformities (sequence boundaries). Steckler et. al. (1999) did modeling suggesting lowering of sea-level and reduction of shelf water depths are sufficient to cause bypassing and erosion of the shelf without complete exposure.

Presently at New Jersey, only late middle Eocene and late Eocene sequences correlate with global oxygen isotope increases attributed to glacioeustacy (Browning, Miller and Bybell, 1997). For the lower Eocene and early to middle-middle Eocene, glacioeustacy cannot be invoked from the sequences or the global $\delta^{18}O$ record. The eustatic changes at New Jersey agree reasonably well with other Atlantic margins including the Carolinas Coast, Bahamas Bank, Gulf Coast, and North Sea. All suggest sea-level changes of no more than tens (10s) of meters (Miller et al., 1998).

GLOBAL CENOZOIC COMPOSITE ISOTOPE RECORD

As seen above, oxygen isotope records have been among the most widely used proxy indicators of glaciation (Abreu and Anderson, 1998). Abreu and Anderson (1998) present an excellent composite oxygen isotope record for the Cenozoic. Their record is reproduced on Figure 3 below. The record for the Cenozoic presented on Figure 3 aims at preserving the chronostratigraphic position and amplitude of higher frequency, one million year positive isotope events. Abreu and Anderson's reconstruction attempts to integrate the deep-sea record with the terrestrial and continental margin record while emphasizing the latter. Their data is taken from 19 sites around the world (Abreu and Anderson, 1998).

According to the authors, the first evidence for the existence of an ice sheet in East Antarctica occurs near the lower-middle Eocene boundary (base of the Lutetian stage). There is no evidence for a large ice sheet on

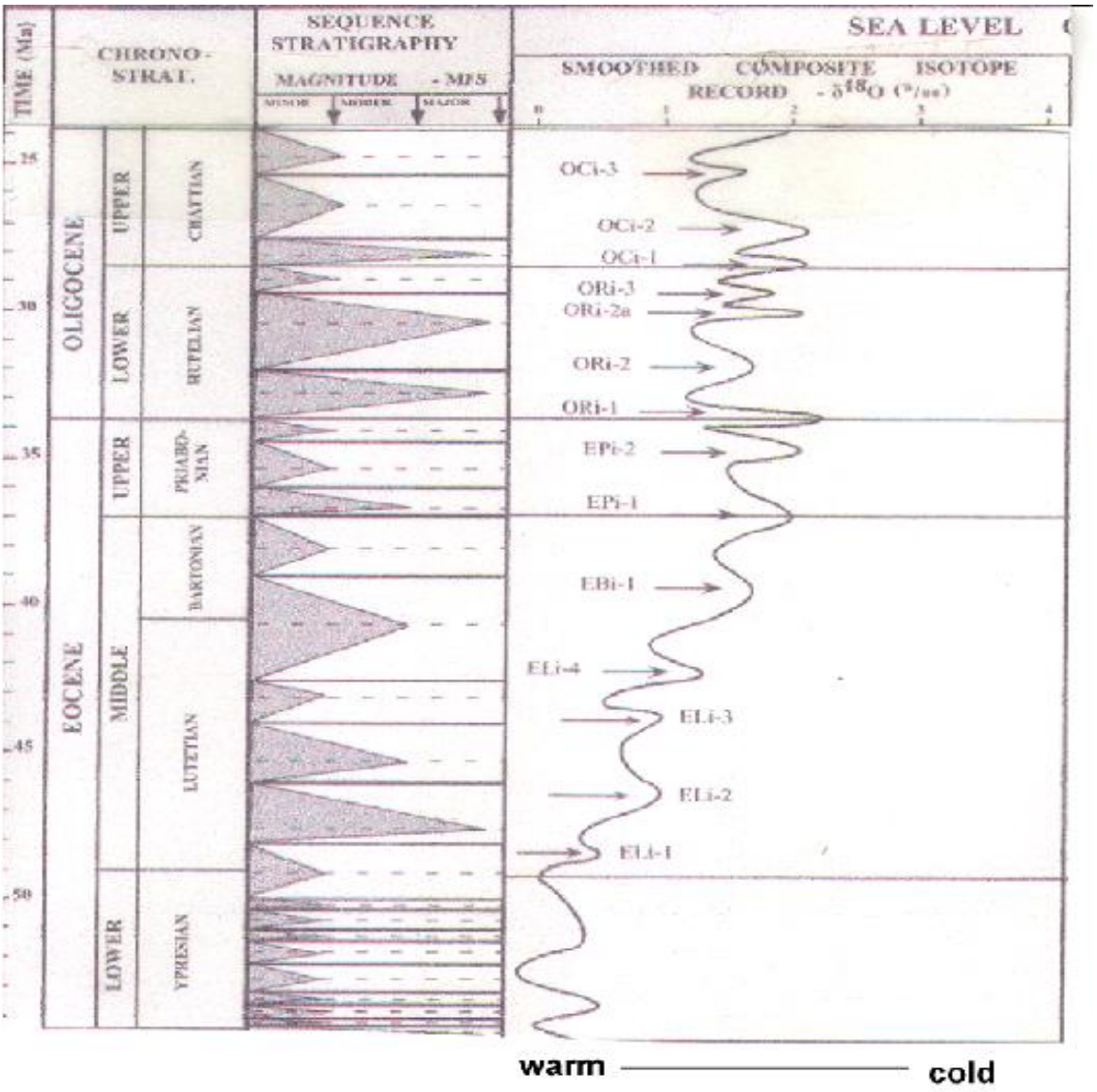

FIGURE 3: Composite Oxygen Isotope Curve for the Cenozoic (Part of Figure 4 from Abreu and Anderson, 1998). Note that $\delta^{18}O$ increases from the lower to the upper Eocene indicating a cooling trend. Note also that during the upper Eocene Priabonian stage, there are two main oxygen isotope increases denoted by the lettering EPi-1 and Epi-2. Note also that the amplitude of the $\delta^{18}O$ fluctuations also increases into the upper Eocene culminating with the sharp lower Oligocene boundary event (ORi-1).

Antarctica prior to this time (Abreu and Anderson, 1998). Their isotope curve also indicates that the ice sheet experienced phases of growth during the Late Eocene and Middle Oligocene, followed by a decrease in volume in the Early Miocene. The global cooling through the Middle Eocene and into the Late Eocene is shown on the composite oxygen curve by a stepwise increase, with the last two positive events shown as Epi-1 and Epi-2 within the Priabonian stage. It is this last event (Epi-2) that is of most concern to this study and how it applies to the New Jersey margin. Abreu and Anderson (1998) dated this event at 34.7 Ma by integrating the oxygen curve with the record from Deep Sea Site 689, Southern Ocean at Maud Rise. This correlates very closely to our age for the Late Eocene New Jersey slope sediments at Site 904 (34.25 to 35.3 Ma). The composite curve is thus important to this research in that the global record can be compared to the regional record for New Jersey. The sequence stratigraphic record for New Jersey can also be compared to other regions on the basis of the three main unconformities discussed earlier under the stratigraphy of Site 904 (See Figure 2 above). The upper two unconformities separating the middle and upper Eocene and the upper Eocene and upper Oligocene in the New Jersey sequence are recognized from other margins around the world.

METHODS

1. Grain Size Separation

A total of 99 samples were analyzed for grain size from 336.5 meters below sea floor (mbsf.) to 380.8 mbsf. These high resolution samples (1 every 0.4 m., see Appendix A) extend from the upper Oligocene down into the upper Eocene. Only the third major unconformity for Hole 904A at 341 mbsf. (see Figure 2, page 23 above) is present within this sampling interval. The coarse (>.063 mm.) and fine (<.063 mm.) fractions were separated by wet-sieving with distilled water. The coarse fraction was then dry-sieved into three size classes including: coarse silt to medium sand (0.0625 mm. – 0.25 mm.); medium to coarse sand (0.25 – 0.5 mm.), and coarse sand (>0.5 mm.). Frequency percent was calculated as weight of the medium to coarse sand 0.25 – 0.5 mm. fraction divided by total weight of all three size fractions dry-sieved. Mud content or the <0.0625 mm. size fraction is not reflected in this calculation.

2. Bulk Mineralogy by X-Ray Diffraction

Equipment

Standard X-Ray diffraction procedures were performed at the Earth & Environmental Sciences Department of Queens College (City University of New York) using a Phillps PW1710 machine with Cu anode and monochrometer. The X-Ray diffractometer was warmed up for approximately one half hour and power was slowly ramped up to 40 Kv and 39 mAmp's. The coolant recirculating system was checked periodically during the start of the diffraction procedure.

Sampling

Sixty three samples were analyzed by X-ray diffraction analysis extending from just below the lower Eocene / middle Eocene boundary at 564 meters below sea floor up to the upper Eocene / upper Oligocene boundary at 341.22 meters below sea floor. These two boundaries constitute the first and third unconformities in the stratigraphic section (see Figure 2, page 23 above). No samples were collected from above the top unconformity. Samples comprising this X-ray data were taken approximately every 3 meters (see Appendix B), considerably lower resolution than the 0.4-meter sample interval used for the stable oxygen isotope data set of 99 samples discussed below.

Sample Preparation

The following procedure was used: 1) ground the sediment in agate mortar with pestle for 3 to 5 minutes, 2) only rolling motion, no sliding to avoid damage to clay mineral plates, 3) stirred with metal tong to fine out powder; avoid clumps, 4) attached glass plate to the back of stainless steel sample holding plate, 5) pressed in powder and compress with second glass plate, 6) attached small metal cover plate over compressed sample powder, and 7) removed back glass plate to open up sample surface.

Each individual stainless steel sample tray was then inserted into an automatic sample feeder holding 35 samples. Extreme care was exercised as each individual tray was placed into position within the sample holder so as not to cross-contaminate any samples. The sample holder was then attached to the

sampling feeder port on the Phillips PW-1710. The software was programmed to scan each sample at 2θ angles from 2 to 70 degrees at scan steps of 0.02 2θ per second.

Diffractogram Analysis

The interpretation of the X-ray diffractor analysis was conducted using the Ocean Drilling Program procedure (Miller et al., 1994). This procedure uses the software package MacDiff 3.0.6c (R. Petschick, 1995). Raw diffractogram files are generated on the Phillips PW-1710 and inputted directly into the MacDiff program. The user within the MacDiff software package generates a custom analyses program.

For this study, as in ODP Legs 150 and 174A, nine minerals with associated d-spacings (dÅ) were entered into the program as follows: pyrite; 2.71Å, siderite; 2.79Å, amphibole; 8.45Å, dolomite; 2.89Å, feldspar (albite); 3.19Å, calcite; 3.04Å, feldspar (microcline); 3.24Å, quartz; 3.34Å, and opal-CT; 4.11Å. The analyses program then searches each diffractogram's numerous peaks for which the critical minerals have been programmed for.

Individual peak analysis is initiated by double clicking a single reflection of the profile. During a short calculation period the position (in d[Å] and °2θ), the intensity (counts minus background, I[c]), the area (integration of all counts of the peak frame above the background, F[∑]) and the half-heigth-width (or FWHM = full width at half maximum, shown as H[Δ] which means Δ°2θ) will be displayed in

a frame on the right side of the view (Petschick 1995). These parameters are illustrated in Figure 4 below.

Peaks can be manually adjusted by moving the peak limit lines sideways. The software also has a command to adjust the profile to remove small overlapping peaks or aberrant reflections to make a peak area calculation more exact. After these minor adjustments, if a peak is close to the right d-spacing for that mineral, the peak can be saved by the user for the completed file which is later outputted to excel for plotting.

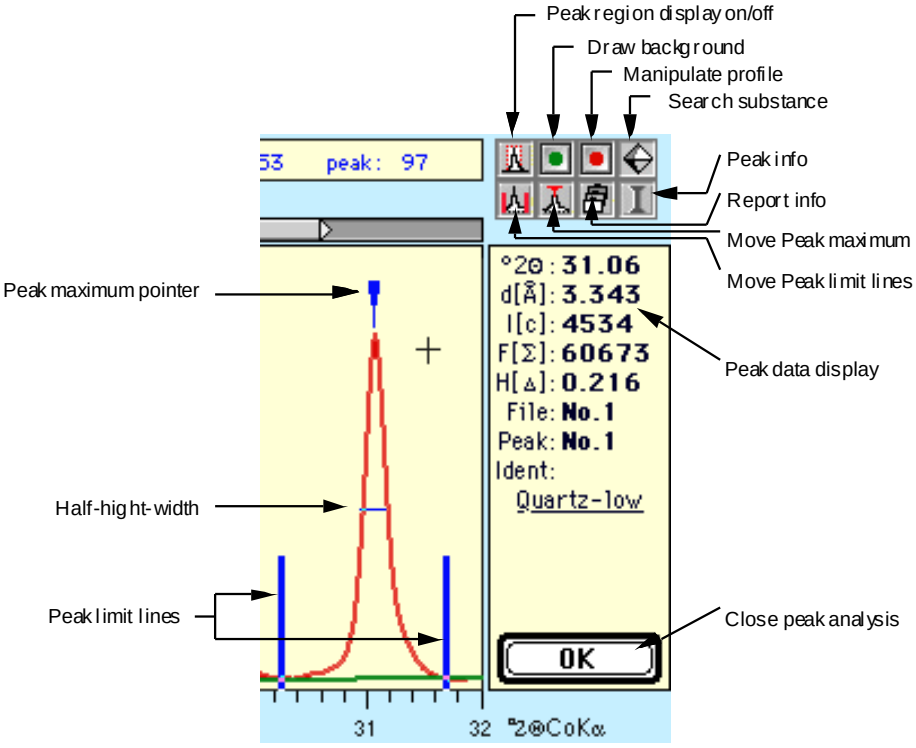

FIGURE 4: Figure 3 from Petschick (1995). Peak analysis window from MacDiff software package. Minor adjustments can be made to each peak during this stage of the analysis, but care should be taken to limit these changes since they amount to a manipulation of the data.

3. Petrographic Thin Sections

A complete set of thin sections spanning the study interval from Site 904 was examined using a standard polarizing petrographic microscope. Slides were examined under 50X, 100X, and 200X power magnifications in both plane and polarized light. Semi-quantitative observations were compiled by categories and included the following:

a. texture: size, size range, sorting, and roundness

b. grain descriptions: skeletal and non-skeletal

c. other features including replacement fabrics, extinction, diagenesis

d. minerals present

e. details of any glauconites such as color, shape, and size.

4. Stable Oxygen Isotopes from Planktonic Foraminifera: *Globigerina spp.*

Sampling

Preliminary low-resolution sampling was done first with a frequency of approximately every three meters or 38,000 years spanning the entire upper Eocene. This data set contained 23 total samples (see Appendix C). High-resolution sampling with a frequency of every 0.4 meters or about 5,000 years was conducted from the upper Eocene at 382 mbsf. up to the upper Oligocene at 341.2 mbsf. (see Appendix C and Figure 8 below).

Temperature and Ice Volume

To interpret the results of $\delta^{18}O$ analyses from *Globigerina spp*. in this study, temperature and global seawater compositional (ice volume) changes were calculated using the following paleotemperature equation:

$$T = 16.9 - 4.38 (\delta_c - \delta_w) + 0.10 (\delta_c - \delta_w)^2$$

where T is paleotemperature, δ_w is global seawater composition, and δ_c is the measured value in calcite assuming equilibrium calcification (O'Neil et al., 1969; Shackleton, 1974).

Foram Washing

The following procedure was used: 1) dissolved 0.4 g. KOH (4 tablets) in 100 ml. distilled water in a 600 ml. beaker, 2) weighed the raw sample on triple beam balance, 3) gently broke the sample with fingers using rubber gloves to prevent contamination of the samples. The sample was broken into pieces of 1 cm. wide or less, 4) soaked samples in KOH solution overnight, 5) the saturated samples were left in the KOH solution until dissolved, 6) the excess clayey residue was washed out from the solution with distilled water, 7) the solution was wet-sieved to separate >63μm. fractions using a soft paintbrush to assist in the wet-sieving. The fine fraction (<63μm) was saved in a container and used for clay analyses, 8) the >63μm. size fraction was decanted and dried in a conventional lab oven at 200^o F., and 9) once dried the clay fraction was weighed on triple beam balance.

Foram Picking Procedure

The following picking procedure was used: 1) *Globigerina spp* foraminifers were picked from the 250 - 500 micron sand size fraction using a microscope examining tray, 2) the samples were spread to coat the tray, and 3) ten foraminifers were picked and placed onto 1mm thick cardboard standard micropaleontology slide with circular viewing depression.

Quality Control for Selecting Individual Foram Specimens

The following guidelines were adhered to: 1) larger specimens approaching 0.4 to 0.5 mm were picked to avoid juveniles, 2) of the larger specimens, only those with non-cemented open apertures were picked and whose outer test walls were clean and free of overgrowth cements, and 3) avoided any specimens that show clear signs of dissolution, boring, or silica diagenesis. This usually appeared as a slightly clear, hyaline or glassy luster. Fresh carbonate tests appeared white and totally opaque.

5. FMS Logs (Formation Microscanner, measuring conductivity)

The FMS logs were interpreted by correlating directly to the thin section observations. High conductivity dark bands on the logs corresponded with high clay content and little quartz silt observed in thin sections. Low conductivity light bands on the logs corresponded with thin sections showing more detrital quartz and micas.

Un-normalized and normalized data sets (see Appendix D) were examined for this study. Processing of the normalized data set was done to improve the local contrast in the formation microscanner image as seen in Figure 9 below. This image enhancement aids in the accurate interpretation of small scale sedimentological features such as inclined laminations, burrows, faults, or altered horizons. The normalization process is called dynamic normalization (Serra, 1989). A linear transform is applied to the input data in order to keep a constant mean and standard deviation within a sliding window. The window is kept larger than the thickest event in the stratigraphic section, i.e. laminations or burrows (Serra, 1989). Conductivity values were also mathematically smoothed using the Mac software package Analyseries 2.0.3.).

6. Spectral Analysis on FMS Logs

In order to interpret the variability in the logs a statistical analysis was performed. This time-series analysis is referred to as spectral analysis. The goal was to take a time series and quickly assess how many regular component oscillations were present (Weedon 2003). To put it in another way, what is the cyclicity in the data? The approach used in this study was a power-spectral analysis that showed the relative amplitudes (strictly squared amplitudes) and wavelengths or periods of all the regular components in the time series (Weedon 2003).

The conventional spectral analysis plot or power spectrum consists of an x-y graph. The horizontal axis is plotted as frequency with highest frequencies

appearing on the right. For this study, frequency is expressed in cycles per meter since the original formation microscanner logs measured conductivity against depth below the seabed. The vertical axis of the spectrum is usually plotted as squared amplitude and by analogy with physics it is described as 'power' (energy per time interval), hence the name power spectrum (Weedon 2003).

For this study, the software used is termed 'Analyseries' (Paillard et al., 1996). It was developed for use on Mac platforms. A G4 Apple Power Book laptop with 12 inch LCD screen was used with version 2.0.3 of Analyseries. Analyseries is a Macintosh application that follows graphically oriented menu-driven applications (Paillard et al., 1996). Analyseries was specifically designed to study paleoclimatic records and addresses the problem of transforming "data versus depth" records into "data versus age" records (Paillard, et al., 1996).

The specific spectral analysis method used is the Blackman-Tukey method (Blackman and Tukey 1958). The Blackman-Tukey method (BTM) is based on the Fourier transform of part of the autocovariance sequence. The autocovariance represents the autocorrelation sequence multiplied by the time series variance. Autocorrelation is calculated by comparing the time series with itself with varying numbers of offset steps. The number of offsets is termed the lag (Weedon 2003). An advantage of the BTM is that the frequencies at which spectral estimates are obtained do not need to be restricted to the traditional Fourier harmonic frequencies. In BTM spectra, the amount of power associated with each peak is determined by the area under the curve rather than from peak heights (Weedon 2003).

7. Comparison to Global Records

Oxygen isotope data and the age model produced in this study were correlated to other oxygen isotope records and age models for global correlation. Overall trends and magnitude of changes were compared.

RESULTS

Grain Size Data

Grain size data show an overall coarsening upwards trend through the upper Eocene (Figure 5). Foraminifers dominate the samples within the medium to coarse sand (0.25 – 0.5 mm.) size fraction. Most of the planktonic and benthonic foraminifera were found in this size fraction. Rarely a few forams were seen in the coarse sand (>0.5 mm) size fraction. Juvenile forams and an abundance of radiolarians and diatoms were seen in the coarse silt to medium sand (0.0625 mm. – 0.25 mm) size fraction. Quartz is most abundant in the coarse silt to medium sand size fraction.

The data shows a slight increase in medium to coarse sand from an average of 10% at 380 mbsf. to about 17 – 18% at 341 mbsf (Figure 5). There is a sharp increase to almost 30% at 366 mbsf. Medium to coarse sand remains elevated above 20% until about 355 mbsf. where it drops to below 10%. From there up to 341 mbsf., percent levels show a slight increase with values fluctuating from below 10% to above 20%. At 341 mbsf. percent levels rise rapidly to a value of 55.8% at 338 mbsf. This increase is due to the presence of glauconite that makes up more than 95% of grains for the sandiest samples. The sandy glauconite-rich samples are all in the upper Oligocene above the unconformity at 341 mbsf.

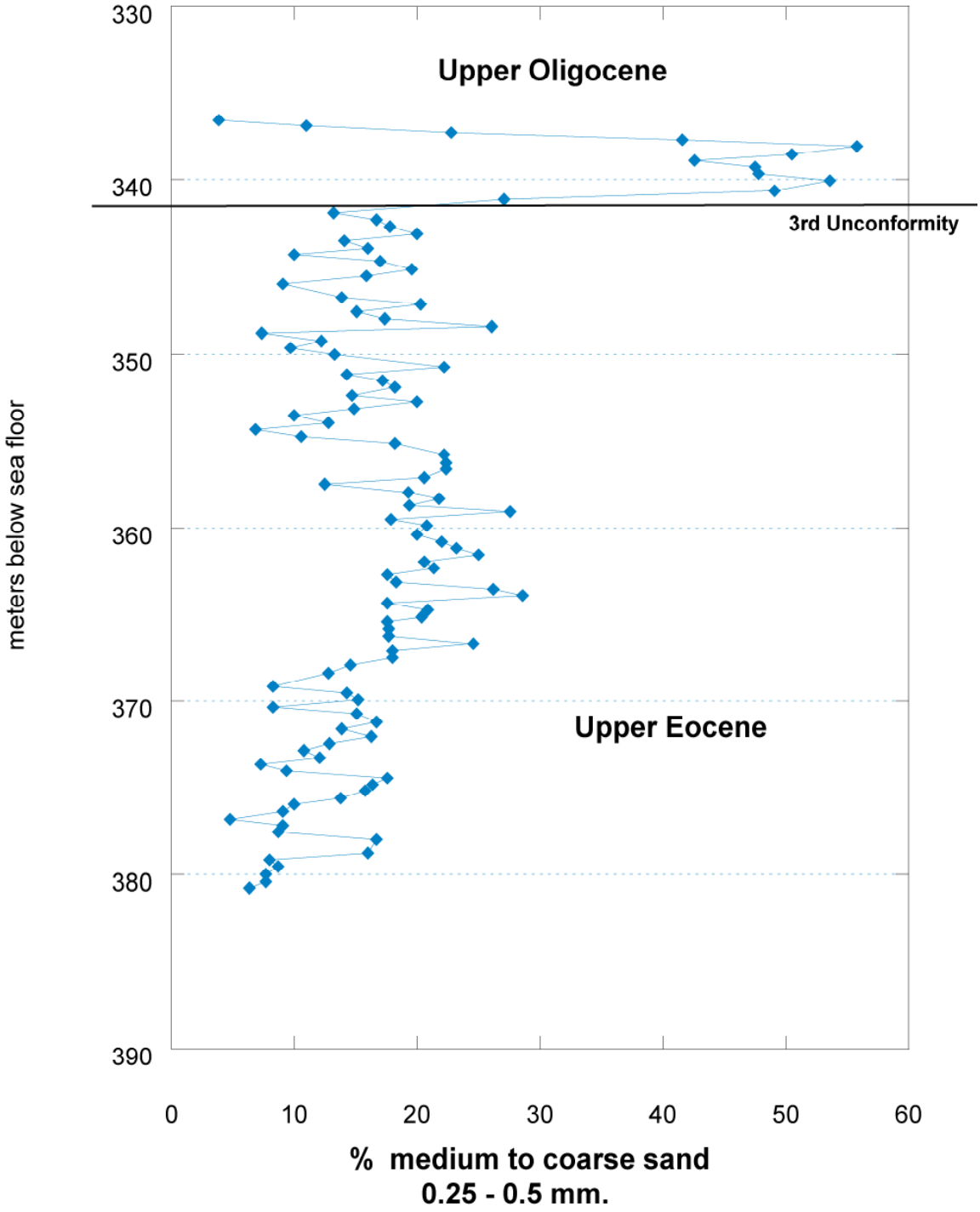

FIGURE 5: Grain size data. Graph above shows the medium to coarse, 0.25 to 0.50 mm. size fraction plotted as frequency percent of total sand against depth (mbsf.). The uppermost unconformity is shown near the top of the section and separates the upper Eocene from the upper Oligocene. Note the slight increase in grain size towards the unconformity and the dramatic increase above the unconformity. Above the unconformity the sediments are dominated by glauconite and the increase in grain size represents the abundance of glauconite.

Bulk Mineralogy

MInerals are dominated by calcite and quartz with minor opal CT, siderite, and pyrite, and they show very distinct patterns (Figure 6). Total calcite varies about a mean of 2500 counts per second (cps.) through the middle Eocene (560 to 420 mbsf, Figure 6) and begins to decrease toward the top of the middle Eocene. Then during the upper Eocene the calcite intensity continues to drop gradually to a mean of approximately 1500 cps. No clear cut cyclicity is visible in the data, although crude 500 to 1000 count per second fluctuations are present in the upper Eocene (Figure 6). A sharp drop in calcite intensity occurs just above the second unconformity at 420 mbsf.

Quartz intensity shows a sharp increase from 100 up to approximately 600 cps. at the second unconformity. Pyrite and siderite intensity also shows a sharp increase at the 2nd unconformity to values of 45 and 25 cps. respectively (see Figure 6). This increase is possibly related to iron replacement brought about during diagenesis. Under low oxygen conditions, organic matter is reduced and iron carbonate (siderite) is produced. Otherwise quartz intensity is fairly constant at about 100 cps. from 560 up to 480 mbsf. From 480 up to 420 mbsf., quartz intensity is up slightly with maximum values of 200 cps. during this interval (middle Eocene). Above the sharp increase at 420 mbsf., quartz values remain elevated around a mean of approximately 300 cps. throughout the remainder of the upper Eocene. Fluctuations in quartz intensity between 200 and 400 cps. are present throughout the upper Eocene but have not been linked to any type of cyclicity.

Sixty eight percent of samples show trace amounts of pyrite with amounts slightly higher in the upper Eocene than the middle Eocene. Intensity values range from 9 cps. up to a maximum of 43 cps. for the sample point just above the

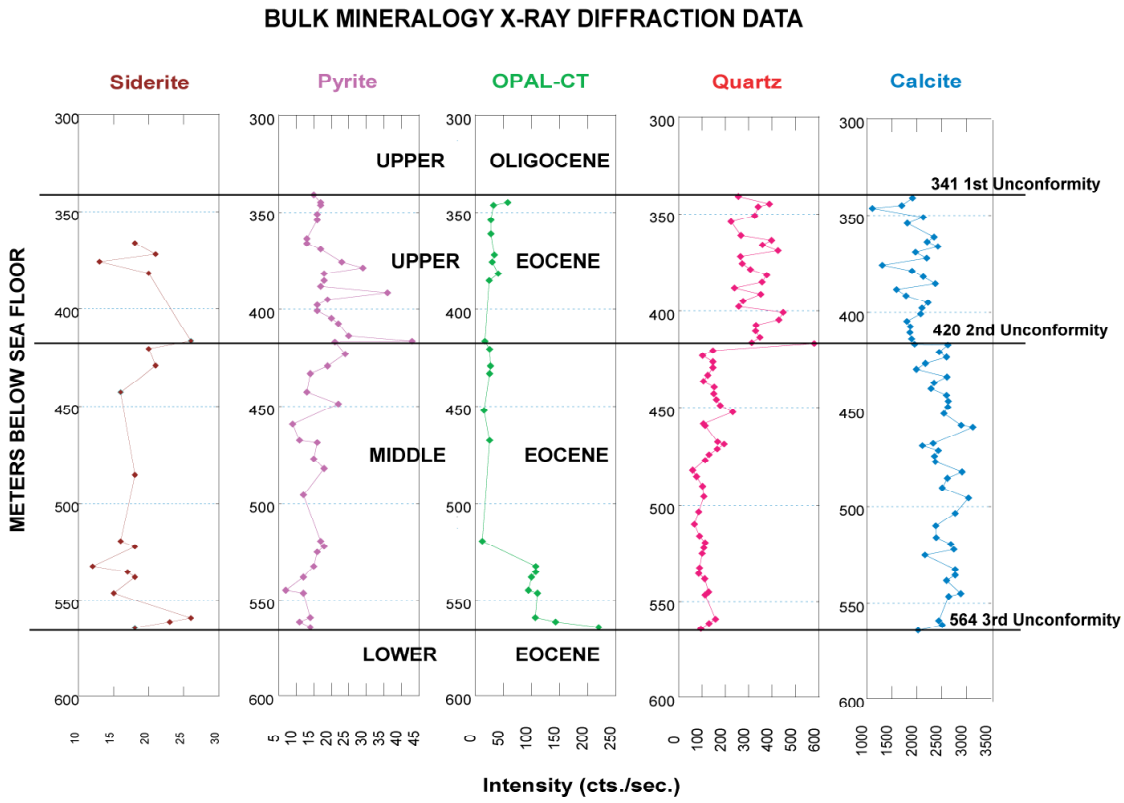

FIGURE 6 : Bulk Mineralogy X-ray Diffraction Data. Relative amounts of each mineral are plotted as intensity in counts per second (cps.) recorded by the diffractometer against depth in meters below the sea floor (mbsf.). Major divisions of the Eocene and Oligocene are separated by the three major unconformities recognized for Site 904.

second unconformity at 420 mbsf. (Figure 6). Siderite is much rarer and was detected in only 28 percent of samples with intensity ranging from 12 to 26 cps.

Opal-CT was detected at the bottom of the stratigraphic section in eight consecutive samples from 564 mbsf. up to 533 mbsf. These samples represent a 30 meter interval just above the third unconformity which marks the lower Eocene / middle Eocene boundary (See Figure 2, page 23). Intensity values for

this interval average about 100 cps. with a maximum of 220 cps. for a sample at 564 mbsf. Opal-CT intensity values for this interval are well above the trace amounts detected for siderite and pyrite, and equivalent to quartz intensity values at about 100 cps. This increase in opal-CT is significant and probably related to diagenetic pore fluid flow. This release of fluids is due to the release of crystallographic water during the opal-A to opal-CT transformation (McHugh, 1997). Opal-CT occurrence is very spotty up through the rest of the middle Eocene and into the upper Eocene (Figure 6). There is a slight increase in intensity at about 380 mbsf up to the first unconformity at 341.2 mbsf. Intensity values here range from 28 to 58 cps.

Summing up then, a trend in the data is displayed by the gradual decrease in calcite content beginning in the middle middle Eocene at about 470 mbsf. and extending up section into the upper Eocene. Below this calcite content is fairly constant. Relative quartz content clearly delineates the middle Eocene from the upper Eocene with a sharp increase at the second unconformity at 420 mbsf. The reason for this inverse relationship between calcite and quartz content is treated below in the discussion section. Siderite and pyrite diagenesis are associated to the 2nd unconformity at 420 mbsf. and siderite diagenesis to the 3rd unconformity at 564 mbsf. Opal-CT diagenesis is prevalent in the lower portion of the middle Eocene due to deeper water and greater compaction (McHugh, 1997), and this validates the fact that foraminifers within the studied interval (upper Eocene) are stratigraphically high up enough to be well preserved. For this

reason they have not undergone major diagenetic changes that may alter the stable oxygen isotope record.

Bulk mineralogy XRD results for opal and calcite from this study are corroborated by a previous study reporting absolute weight-percents for calcium carbonate and opal by wet chemical methods (McHugh, 1997). Both studies reveal decreasing carbonate content from the middle through the upper Eocene (Figure 7 below). Coupled with increasing quartz content noted above, the

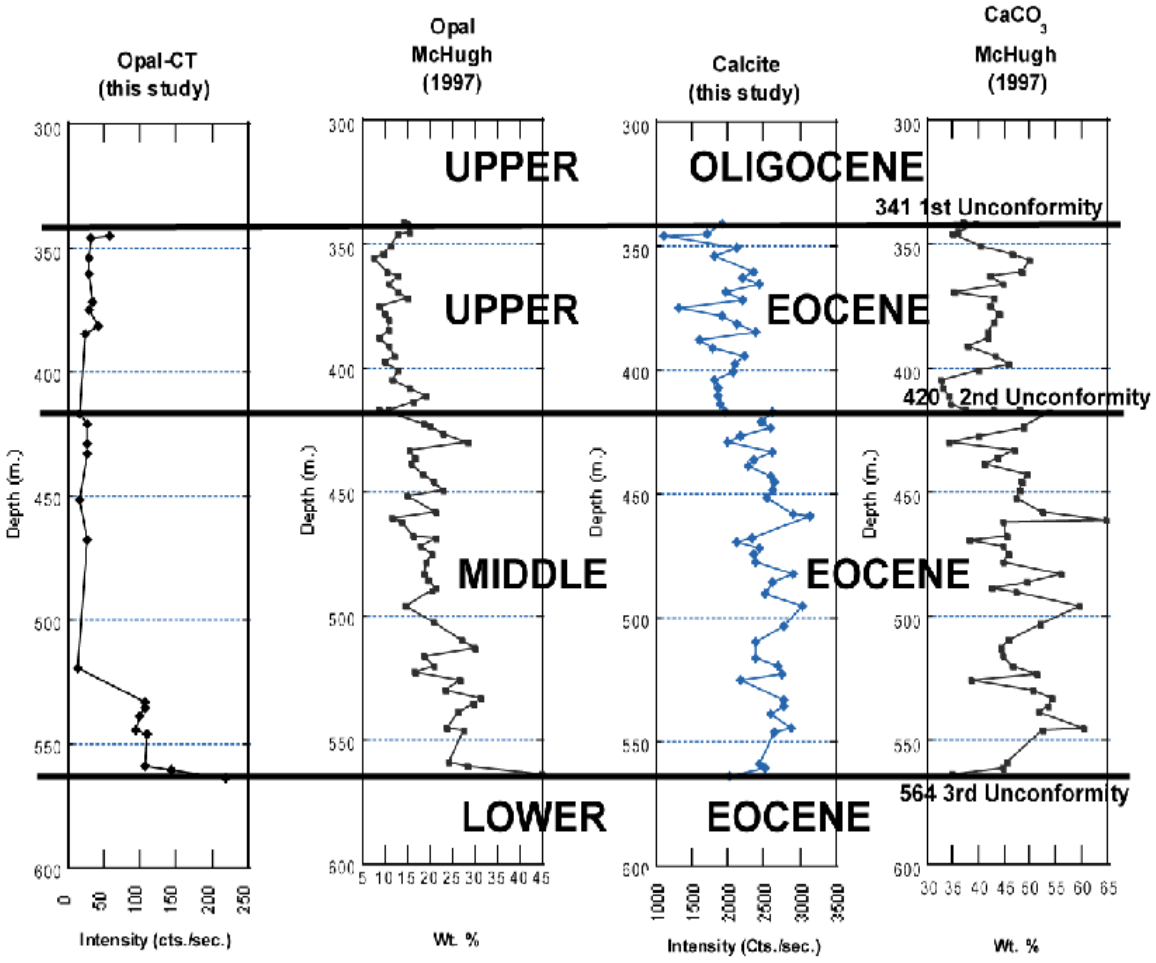

FIGURE 7: Calcite and Opal Data. Note the strong correlation of peaks and troughs between the calcite curve XRD data (this study) and the measured $CaCO_3$ wt. % curve of McHugh (1997). Both these curves also show decreasing carbonate content from the middle into the upper Eocene. Note also decreasing opal wt. % (McHugh 1997) from the middle to upper Eocene. The XRD opal curve for this study shows mostly trace amounts of opal but does show a distinct decrease at the base of the middle Eocene.

carbonate trend is consistent with a margin shifting from carbonate to siliciclastic sedimentation into the Oligocene. The decreasing opal weight-percent recorded by McHugh (1997) also clearly records this shift in the New Jersey margin.

Stable Oxygen Isotope Data

Results of the low resolution (44,000K) stable oxygen isotope chemical analyses show a slight increase in $\delta^{18}O$ up section through the upper Eocene from -3.67 per mil up to -2.83 per mil at the top of the upper Eocene (Figure 8). These analyses were conducted as a test to evaluate if a high-resolution record could be obtained.

The higher resolution results (5,000K) span from the upper Eocene to the upper Oligocene and show $\delta^{18}O$ values fluctuating between -3.25 per mil and -2.75 per mil throughout the upper Eocene between 380 and 340 mbsf. (Figure 9). In the upper Oligocene above the third unconformity at 341.22 mbsf., $\delta^{18}O$ values increase to almost –2.0 per mil and then drop off slightly again to -2.5 per mil at the very top of the stratigraphic section at 336 meters depth. Spectral analysis was run on this oxygen isotope high-resolution data set but no cyclicity was detected.

Formation Microscanner Logs

Interpretation of the FMS logs by correlating the sediment to the FMS images shows apparent cyclic fluctuations at the meter scale and longer-term

changes at the 10-meter scale. The low conductivity signal (lighter sepia tones) was correlated to coarser grain size and more terrigenous minerals such as

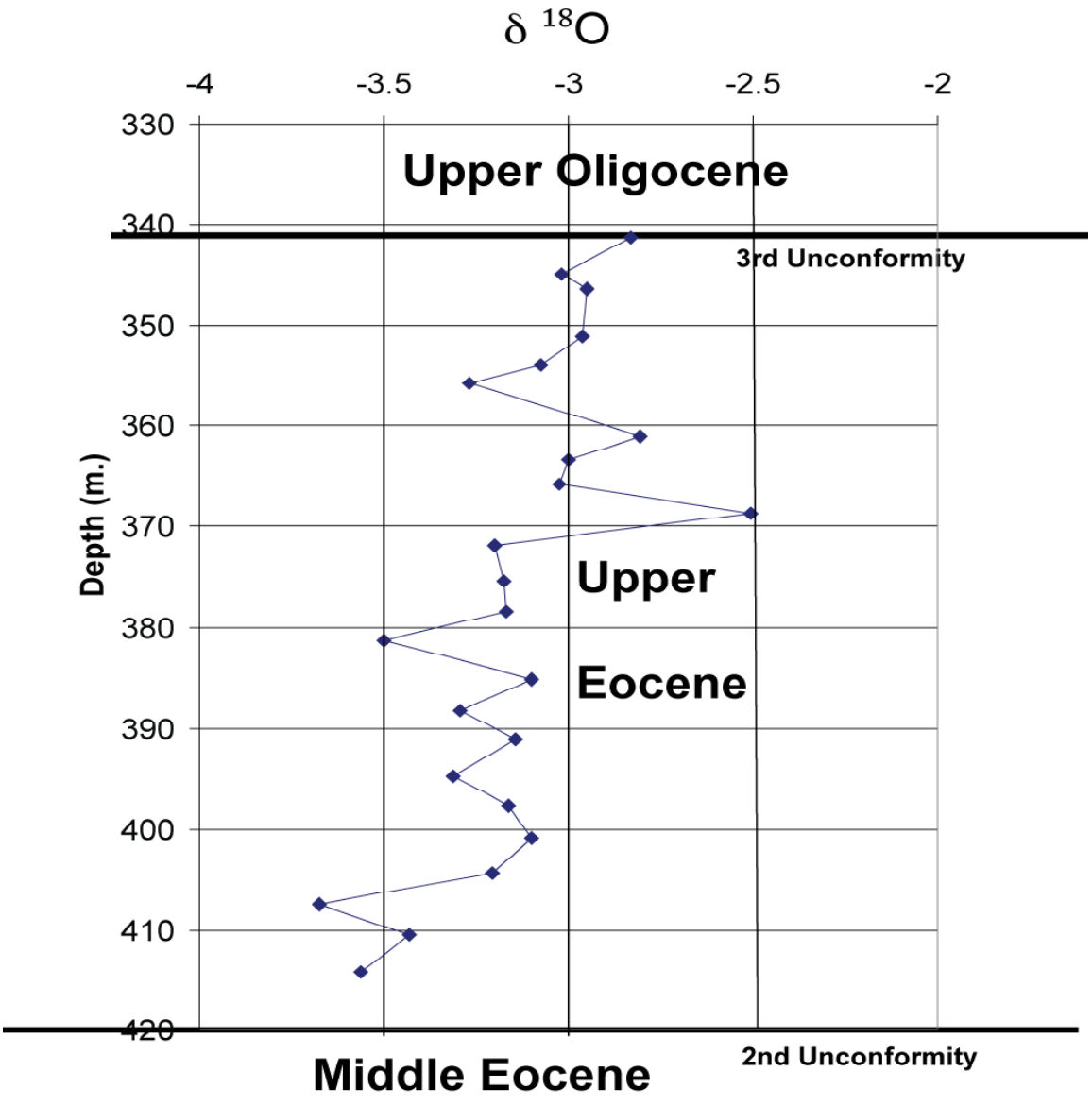

FIGURE 8: Low Resolution Stable Isotopes. $\delta^{18}O$ in per mil PDB is plotted against depth in meters below sea floor (mbsf.). Note a slight increase in $\delta^{18}O$ up section from a minimum of –3.67 at 414.1 mbsf. to –2.83 at 341.22 mbsf. The 2nd and 3rd unconformities are plotted for reference (See Figure 2, page 23 above)

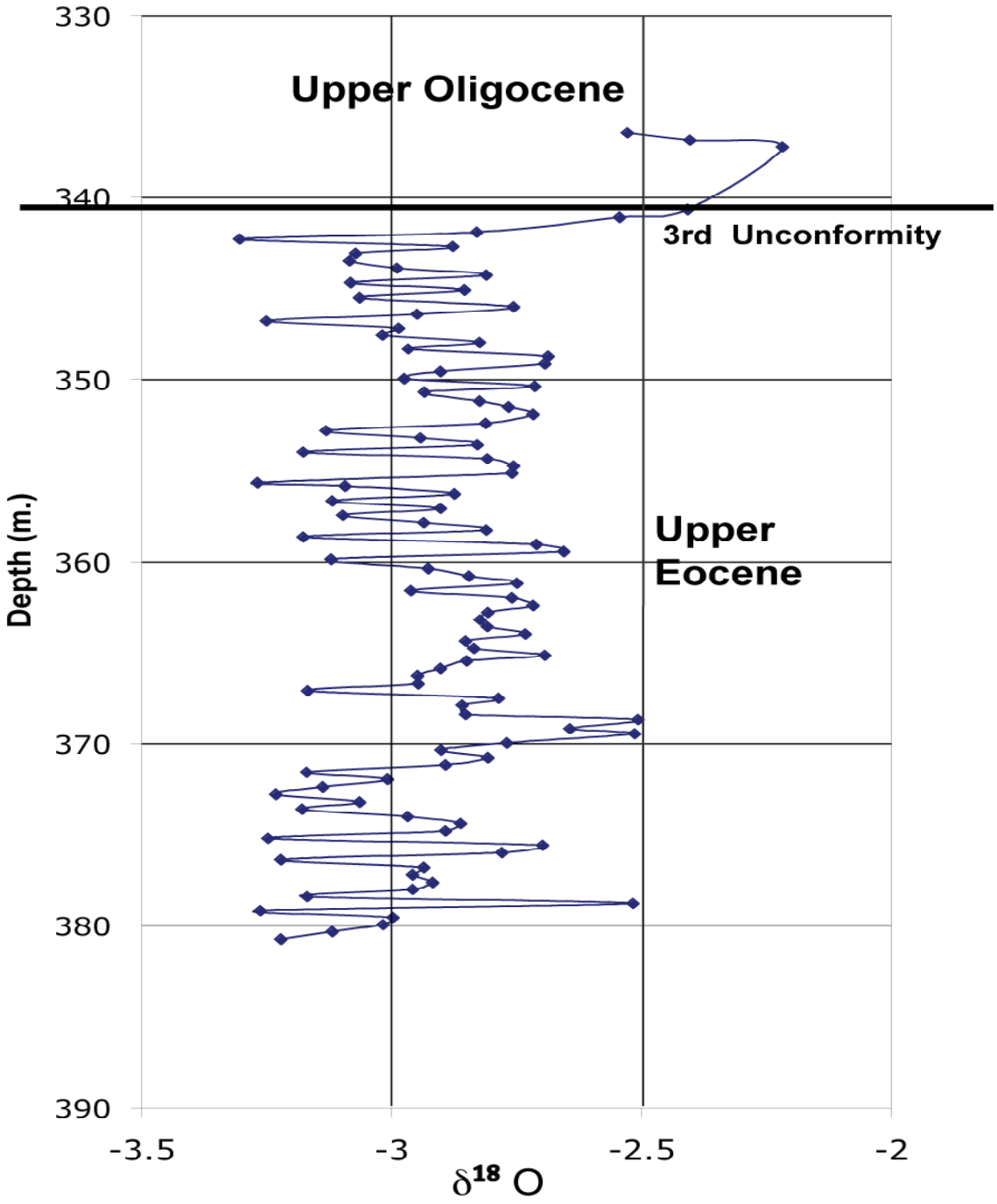

FIGURE 9: High Resolution Stable Isotopes. $\delta^{18}O$ in per mil PDB is plotted against depth in meters below sea floor (mbsf.). Note values are steady around –3.0 per mil throughout the upper Eocene and then rise in the upper Oligocene to almost –2.0 per mil.

quartz and mica. The high conductivity signal (dark tones) was correlated to finer silt and clay content (Figure 10 below).

Conductivity data is presented below in the next two figures. Un-normalized conductivity data shows readings at about 7 for most of the section with the exception of a sharp increase to a maximum of 13 at 390 mbsf (Figure 11). This sharp increase coincides with the location of a pyrite-filled burrow. Conductivity increases at 352 mbsf. to about 11.5 before dropping back below 7 at the third unconformity. Conductivity then rises again into the upper Oligocene above the third unconformity. No clear cut cyclicity is apparent from visual inspection of Figure 11. Symmetrical peaks and troughs are easily visible in the plot of the normalized conductivity data with consecutive peaks separated by approximately 1.7 meter intervals (Figure 12).The third unconformity is again plotted for reference near the top of the section and separates the upper Eocene from the upper Oligocene.

Spectral Analysis

Spectral analysis is first presented for runs on both the normalized and un-normalized conductivity data sets for the late Eocene. Spectral analysis was used as a tool to examine the data sets for any signs of cyclicity. The spectral analysis method is also a rigorous mathematical approach to determining the frequency of cyclic variations in the conductivity data and shows if multiple frequencies are present. Stratigraphically the normalized and un-normalized data

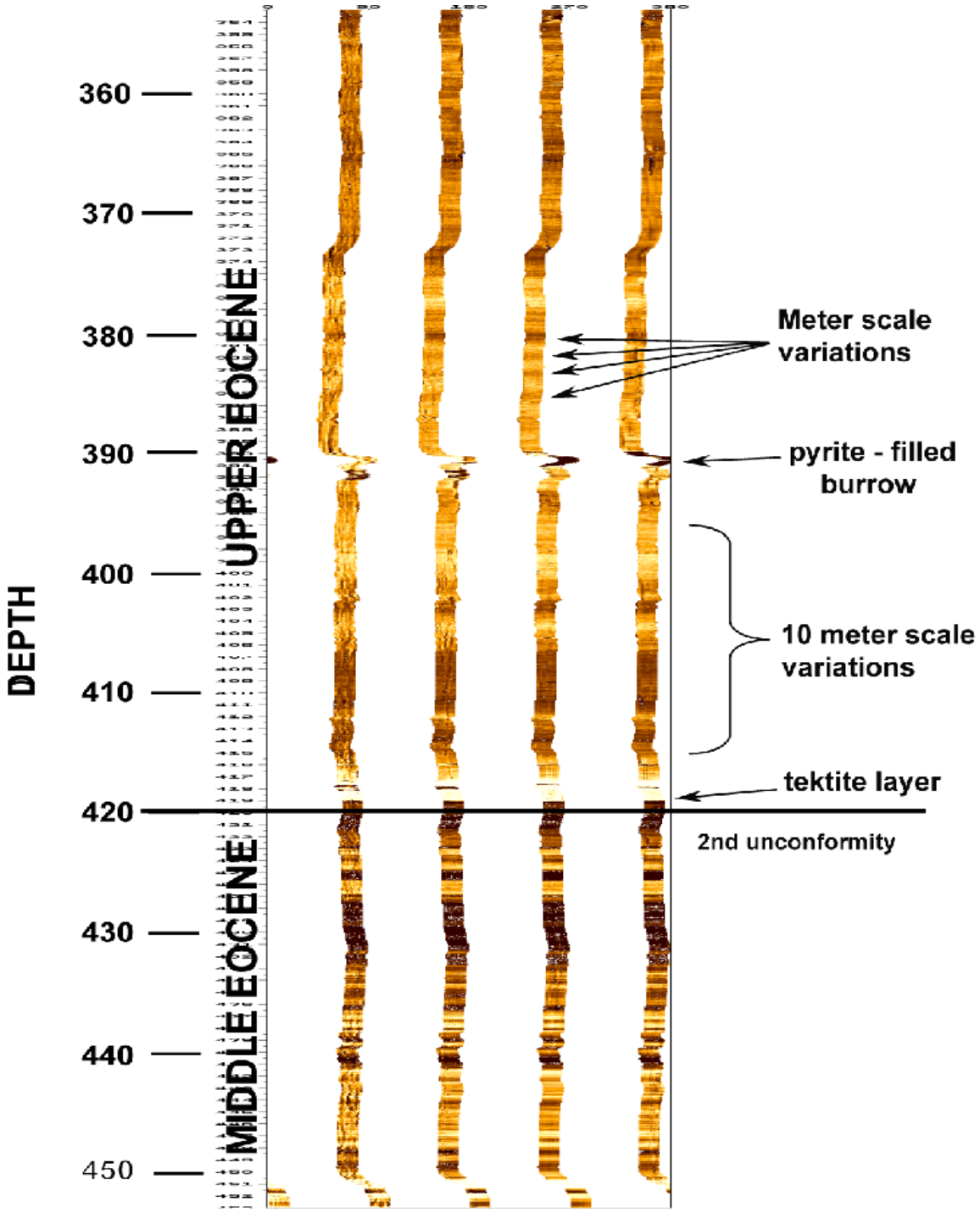

FIGURE 10: Formation Microscanner Log Image. Light tones indicate low conductivity, coarser grain size (sand and coarse silt) and more quartz and mica, while dark tones indicate high conductivity and finer grain size (fine silt and clay). The four colored columns correspond to electrical pads of the FMS instrument located at ninety degree intervals around the borehole. Light and dark color bands can be seen as meter-scale variations. Note also the pyrite-filled burrow, tektite layer, and the 2nd unconformity at 420 m. depth separating the middle and upper Eocene. The 3rd unconformity separating the upper Eocene from the upper Oligocene at 341 m. depth is just above the top of this image.

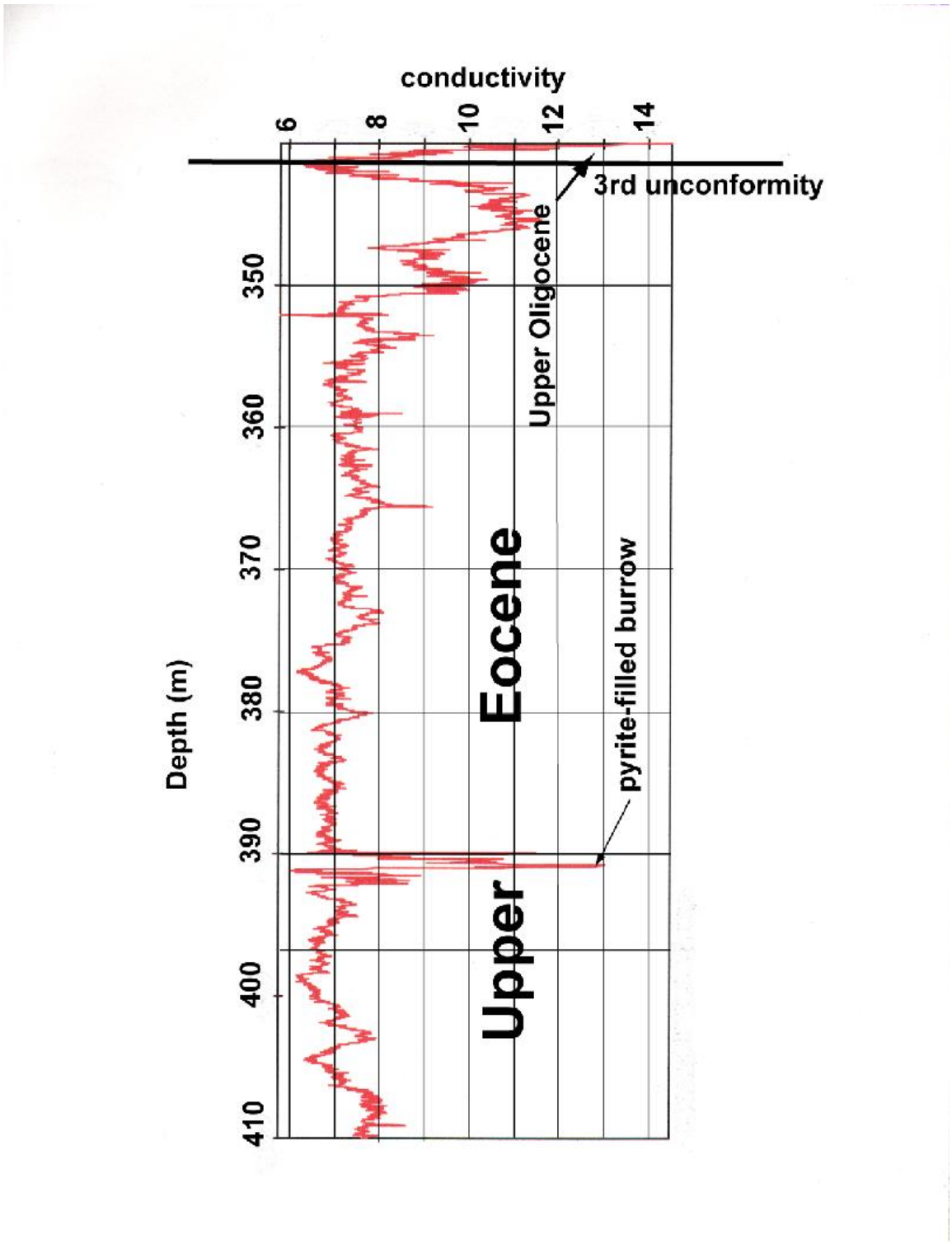

FIGURE 11: Un-normalized Conductivity Data. Uncalibrated conductivity is plotted against depth in meters below the sea floor (mbsf.) The sharp increase at 390 mbsf. coincides with a distinct pyrite-filled burrow at that horizon. Note the increase in conductivity toward the top of the section as the 3rd unconformity is approached. Note the sharp drop in conductivity at the 3rd unconformity.

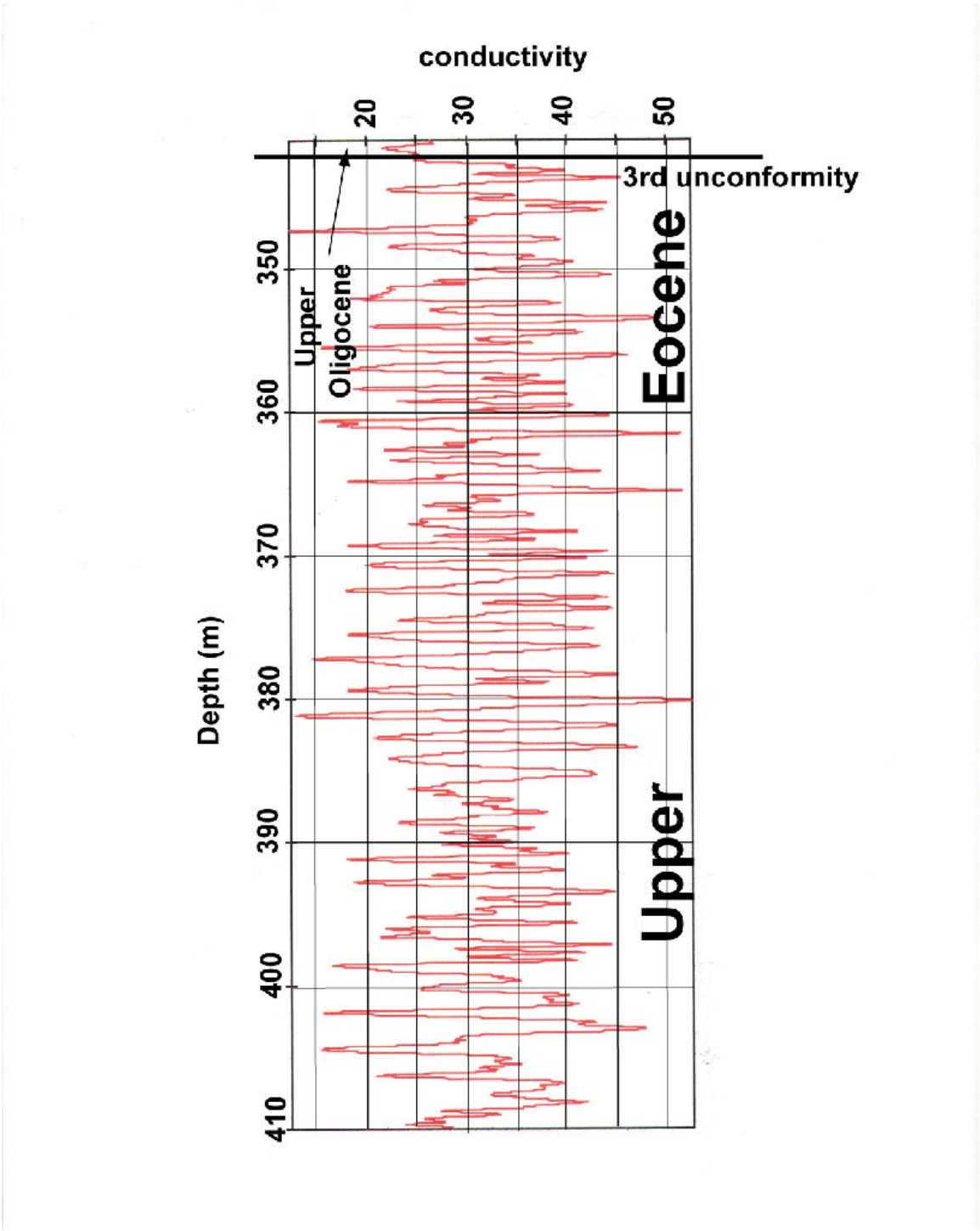

FIGURE 12: Dynamically Normalized Conductivity Data. Conductivity is plotted against depth (mbsf.). Data was smoothed in Analyseries 2.0.3 prior to plotting. Smoothing was done with a simple moving window averaging using the fast Fourier transform. Note the 3rd unconformity at the top of the section separating the upper Oligocene from the upper Eocene. Note also regularly spaced peaks about every 1.7 meters strongly suggestive of cyclicity.

sets correspond closely but not exactly to the interval between the 2nd and 3rd unconformities or between 420 and 341 mbsf. (see Figure 6 above). The actual data set chosen for upper Eocene spectral analysis is from 410 to 341 mbsf. and therefore begins ten meters above the 2nd unconformity. This was done to avoid complications in the data caused by reworking above the tektite layer located at 416.1 mbsf.

Spectral analyses were also conducted for the middle Eocene to constrain test the age model for the late Eocene. The formation microscanner image for the middle Eocene also showed apparently cyclic light and dark banding at a similar scale to the late Eocene and this suggests a similar climatic influence on sedimentation. The middle Eocene sediments are very similar in terms of composition and texture and thus the sedimentation model for the late Eocene can be extended down into the middle Eocene.

Analyses of the power spectrum from the normalized conductivity data indicates two strong peaks that are very close to the Milankovitch precessional frequencies of 23,000 and 19,000 years (Figure 13). Both peaks are well above the background and as such cannot be confused with any white noise in the data. The shifting of both peaks slightly off the exact precessional frequencies may be a result of uncertainty in sedimentation rate during the late Eocene. In spite of this complication, there is no doubt that the analysis shows a strong precessional signal in the normalized conductivity data collected by the Formation Microscanner.

Peaks are more subdued for the un-normalized data than those for the

normalized data set. Analysis of the peak at 0.31 cycles per meter reveals it is somewhat close to the obliquity Milankovitch frequency of 41,000 years (Figure 14). The obliquity frequency is missing in the spectral plot for the normalized data set (Figure 13). The weak obliquity signal was probably masked by the much stronger precessional signal once the dynamic normalization of the conductivity data was applied.

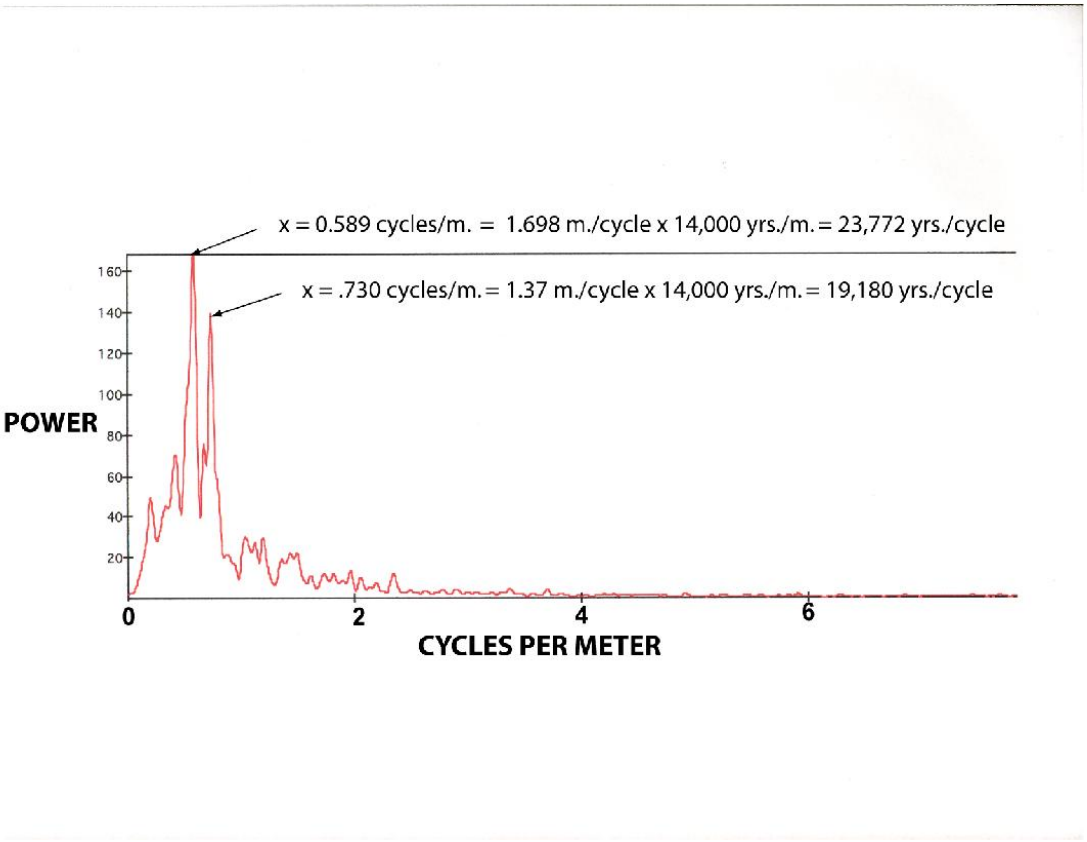

FIGURE 13: Normalized Data, 341 to 410 mbsf. Above plot shows the power spectrum for the late Eocene. The horizontal scale is frequency in cycles per meter and the vertical scale is raw power (strictly squared average amplitude). Two very prominent peaks are present. The first peak occurs at a frequency of 0.589 cycles per meter. Taking the reciprocal results in 1.698 meters per cycle. This value is converted to time using a sedimentation rate of 7.14 cm. per 1,000 yrs. or 14,000 years per meter. The result is 23,772 years per cycle. (Note: 14,000 years per meter comes from dividing the entire time duration, 1,050,000 years, of the studied section, by its stratigraphic thickness of 75 meters). The same analysis was done for the peak at 0.730 cycles per meter resulting in 19,180 years per cycle. The first peak is very close to the Milankovitch precessional frequency of 23K, and the second peak is essentially at the 19K frequency. A slight change in sedimentation rate through the late Eocene may explain the shifting of the upper peak off the exact precessional frequency of 23K.

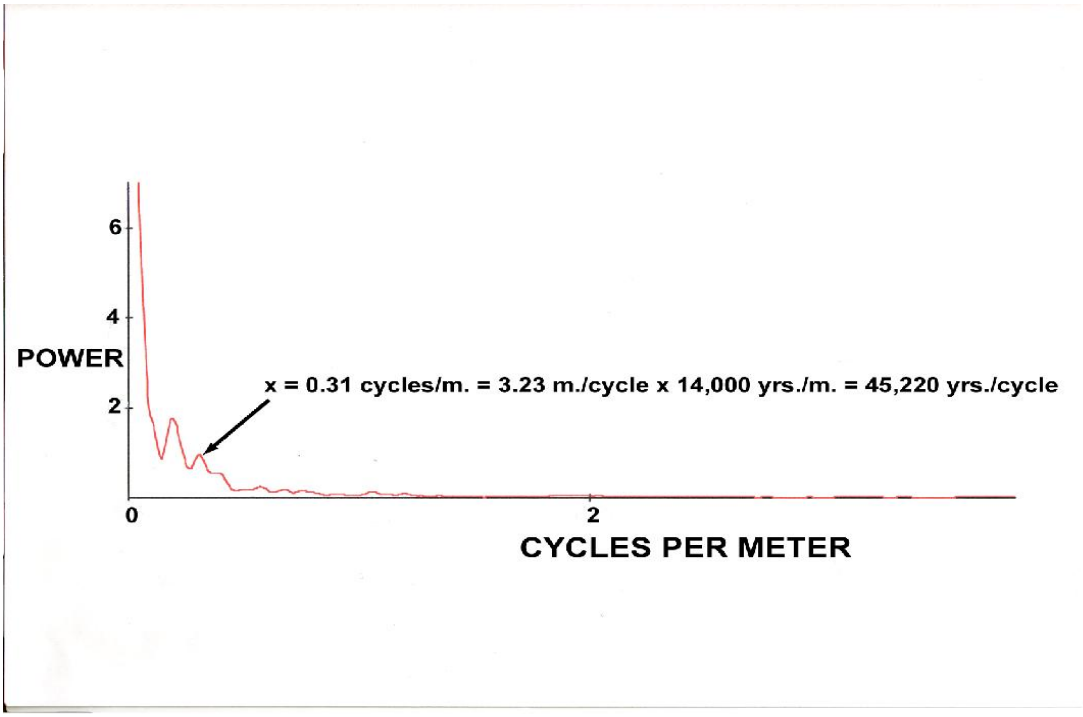

FIGURE 14: Un-normalized Data, 341 to 410 mbsf. Above plot shows the power spectrum for the late Eocene. The horizontal scale is frequency in cycles per meter and the vertical scale is raw power (strictly squared average amplitude). Note the relatively weak peak at 0.31 cycles per meter. Taking the reciprocal results in 3.23 meters per cycle. This value is converted to time using a sedimentation rate of 7.14 cm. per 1,000 yrs. or 14,000 years per meter. The result is 45,220 years per cycle. This is not exact but somewhat close to the obliquity Milankovitch frequency of 41,000 years. No precessional signal is present in this spectrum.

Spectral analysis was also performed on conductivity data from the middle Eocene to compare it to the late Eocene. Borehole 904A on the continental slope off New Jersey was drilled well into the lower Eocene and formation microscanner data was collected down into the middle Eocene. Results of the spectral analysis for the normalized conductivity data from the middle Eocene(420 to 552 mbsf.) show that the middle Eocene spectrum is much noisier (Figure 15). Analysis of two of the four strong spectral peaks showed frequencies of 23,366 and 18,690 years per cycle respectively. Both peaks show a strong Milankovitch precessional signal. It is important to point out here that these

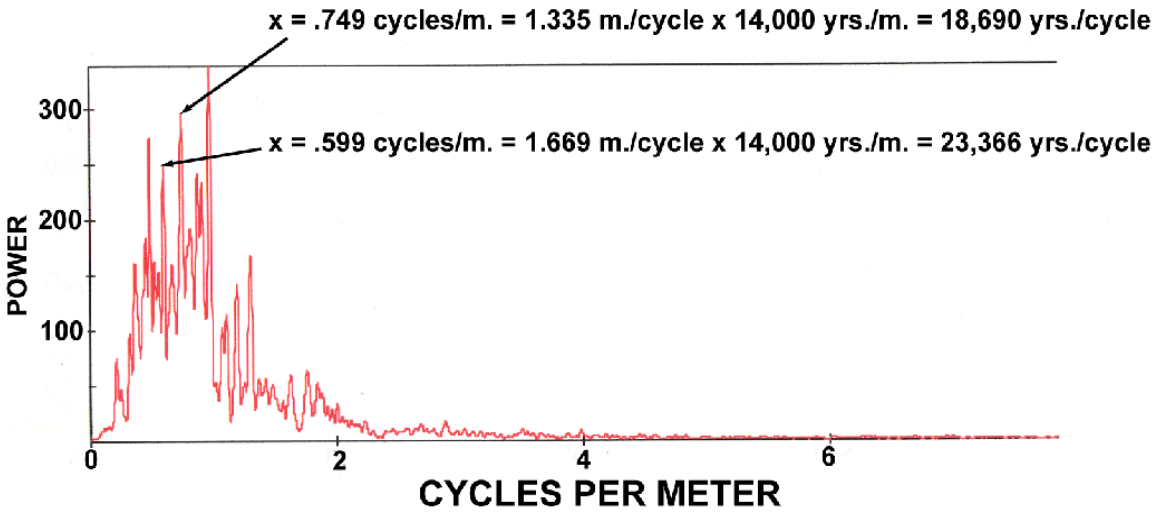

FIGURE 15: Normalized Data, 420 to 552 mbsf. Above plot shows the power spectrum for the middle Eocene. Again the horizontal scale is frequency in cycles per meter and the vertical scale is raw power (strictly squared average amplitude). The power spectrum is somewhat noisier than the upper Eocene with four strong peaks instead of two. The second strong peak occurs at 0.599 cycles per meter. Taking the reciprocal equals 1.669 meters per cycle. This value is converted to time by applying the late Eocene sedimentation rate of 7.14 cm. per 1,000 years or 14,000 years per meter. The result is 23,366 years per cycle or very close to the precessional Milankovitch frequency of 23K. The same analysis of the third peak above at 0.749 cycles per meter results in a frequency of 18,690 years per cycle that is almost right at the 19K year precessional frequency.

results were obtained by applying the late Eocene sedimentation rate to the Middle Eocene for Hole 904A. There is no age control available for the middle Eocene for Hole 904A, however visual inspection of the formation microscanner logs for this interval strongly suggested cyclicity. Based on what the logs looked like, it was decided to run the spectral analysis on the middle Eocene as well just to see if the results would be similar to the late Eocene. Since sedimentation rates can be expected to vary throughout the entire Eocene and no age control is available for the middle Eocene, the results of spectral analysis for the middle Eocene should be viewed with caution.

DISCUSSION

Long Term Cooling and Shift from Carbonate to Siliciclastic Sedimentation

The Late Eocene is generally recognized as a time of cooling on a global scale (Miller, et al., 1991; Browning, et al., 1996, and Miller, et al., 1998; DeConto and Pollard, 2003; Diester-Haass and Zachos, 2003; Prothero et al., 2003; Zachos, et al., 2004; Pearson et al., 2007, and Lear et al., 2008). The changing climatic conditions during the late Eocene are reflected on the New Jersey slope by changes in the mineralogical character of the sediments. It was previously documented that the New Jersey margin experienced a transformation from a steeply dipping carbonate ramp during the middle to late Eocene into a flatter siliciclastic shelf with prograding clinoform wedges into the early Oligocene (Steckler et al., 1999). This shift from carbonate to siliciclastic sedimentation began along the New Jersey coastal plain in the late-middle Eocene at about 43 to 42 Ma (Browning et. al. 1996). The shift from carbonate to siliciclastic sedimentation at the New Jersey slope began later at about 37 to 36 Ma (this study).

The cooling trend through the late Eocene is backed up by evidence from two of our climate proxies including mineralogy and conductivity logs (Figure 16). Age control has also been included for reference to other global deep-sea records. Bulk mineralogy data gathered in this study clearly shows the beginning of this trend. Cooling climate led to a decrease in calcite and increased

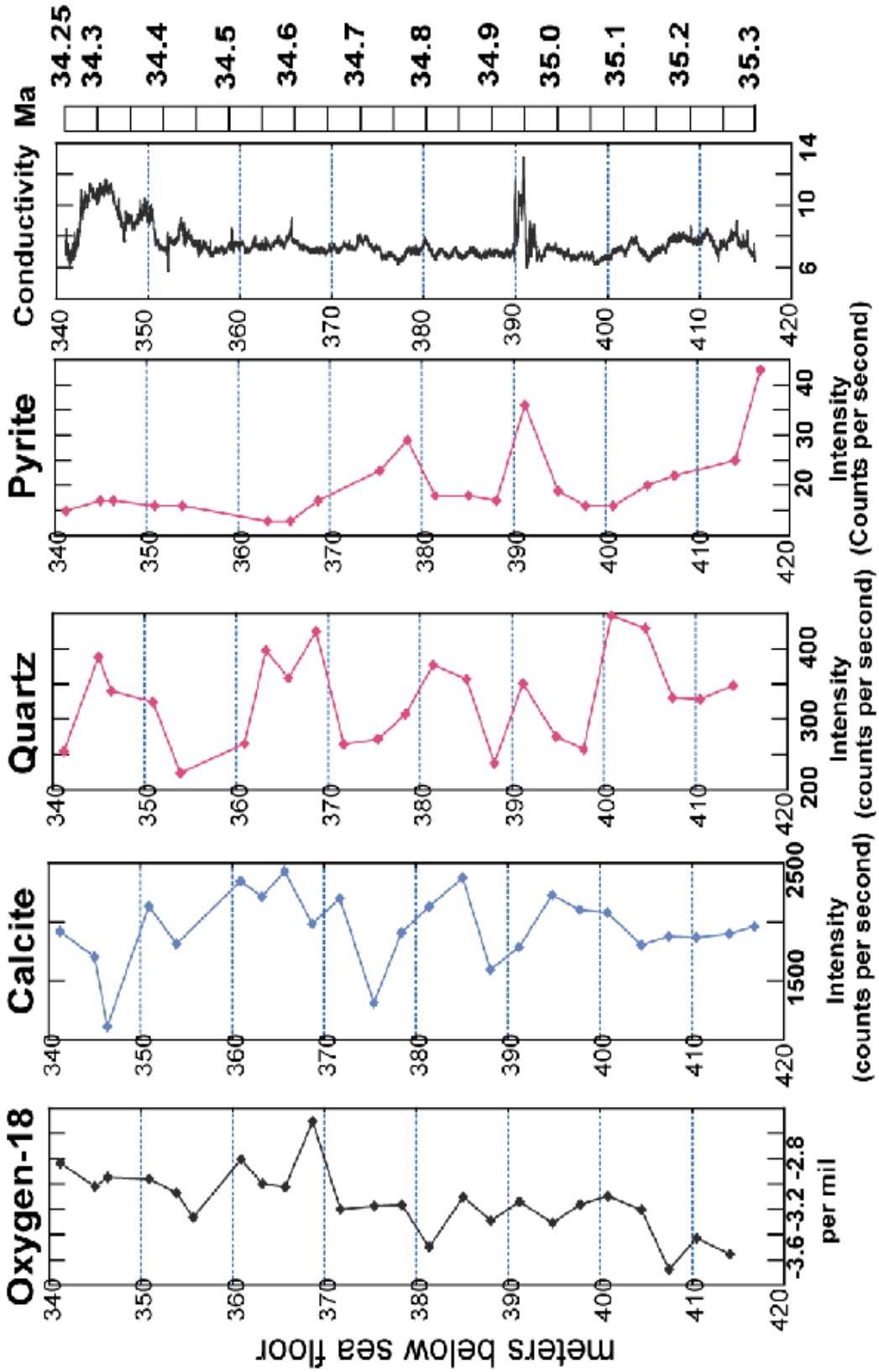

FIGURE 16: Proxy Comparison Showing Low Resolution Stable Isotopes, Mineralogy, and Conductivity. Note age control has been added; 34.25 Ma representing the upper Eocene / upper Oligocene unconformity, and 35.3 represents the tektite layer at 416 mbsf, just above the middle Eocene / upper Eocene unconformity at 420 mbsf.

sediment transport led to an increase in quartz (see also Figure 6, page 50; last column). This is followed upward by a sharp decrease in calcite content at the unconformity separating the middle from the upper Eocene (Figure 6, 2nd unconformity at 420 mbsf.). Less calcite means cooler climate as primary production decreases. Calcite content continues to decrease through the upper Eocene. Over the same stratigraphic interval the quartz signal is the inverse. Quartz content begins to increase at 460 mbsf. and shows a sharp increase at the middle / upper Eocene unconformity at 420 mbsf. Quartz content clearly remains elevated through the remainder of the upper Eocene (see Figure 6, page 50, quartz column). This trend is consistent with an increasing siliciclastic margin across the Eocene - Oligocene boundary. Note also the strong correlation of the peak in pyrite intensity at 390 mbsf. with a sharp increase in conductivity. There is strong diagenesis associated with a pyrite-filled burrow at this horizon.

The calcite, quartz, and conductivity data from this study thus corroborates the findings of earlier New Jersey margin studies that show a cooling in the late Eocene (Katz and Miller, 1996; McHugh, 1997; Browning, Miller, et. al. 1997; Browning, Miller, and Olsson, 1997; Browning, Miller, and Bybell, 1997, and Miller et al., 1998). Clearly the calcite and quartz XRD data indicate that a cooling climate change was underway in the late-middle Eocene, continued through the late Eocene, and culminated in the early Oligocene cooling event documented globally (Zachos et al., 1996; Diester-Haass and Zahn, 1996; Diester-Haass and Zachos, 2003, and Zachos et al., 2004; see also Figure 3, page 35, this study, positive oxygen isotope event ORi-1: Oligocene-Rupelian isotope 1).

Spectral Analysis Reveals Late Eocene Strong Precessional Cyclicity and Weak Obliquity

Orbital forcing of late Eocene paleoclimate was a dominant factor along the New Jersey continental slope. Spectral analysis confirmed the presence of a strong precessional signal in the conductivity data. A weaker obliquity signal was also detected (see Figure 14, page 62). Figure 17 below presents a comparison of the power spectra for the late and middle Eocene. The late Eocene signal is clearer with only two spectral peaks. The noisier signal in the middle Eocene may be the result of increased silica diagenesis as biogenic opal-A of radiolaria is transformed to opal-CT, foraminifera are replaced by opal-CT, and the matrix is also subject to increased silica cementation (McHugh, 1997). Increased silica content will affect porosity and hence the conductivity signature of the sediment column, and therefore will alter the apparent cyclicity recorded by the FMS. McHugh (1997) documented an increase in porcellanite chalks as one goes down section through the middle Eocene at Drill Site 904A.

Dividing the two late Eocene spectral peaks of 23,772 and 19,180 years yields a ratio of 1.239, very close to the true ratio of 1.2105 when dividing the true precessional frequencies (23,000 ÷ 19,000 years). This amounts to a very low percent error of 2.35%. This result confirms that the calculated spectral frequencies for this study (23.8K and 19.2K) are significant and not the result of any random fluctuations in the data.

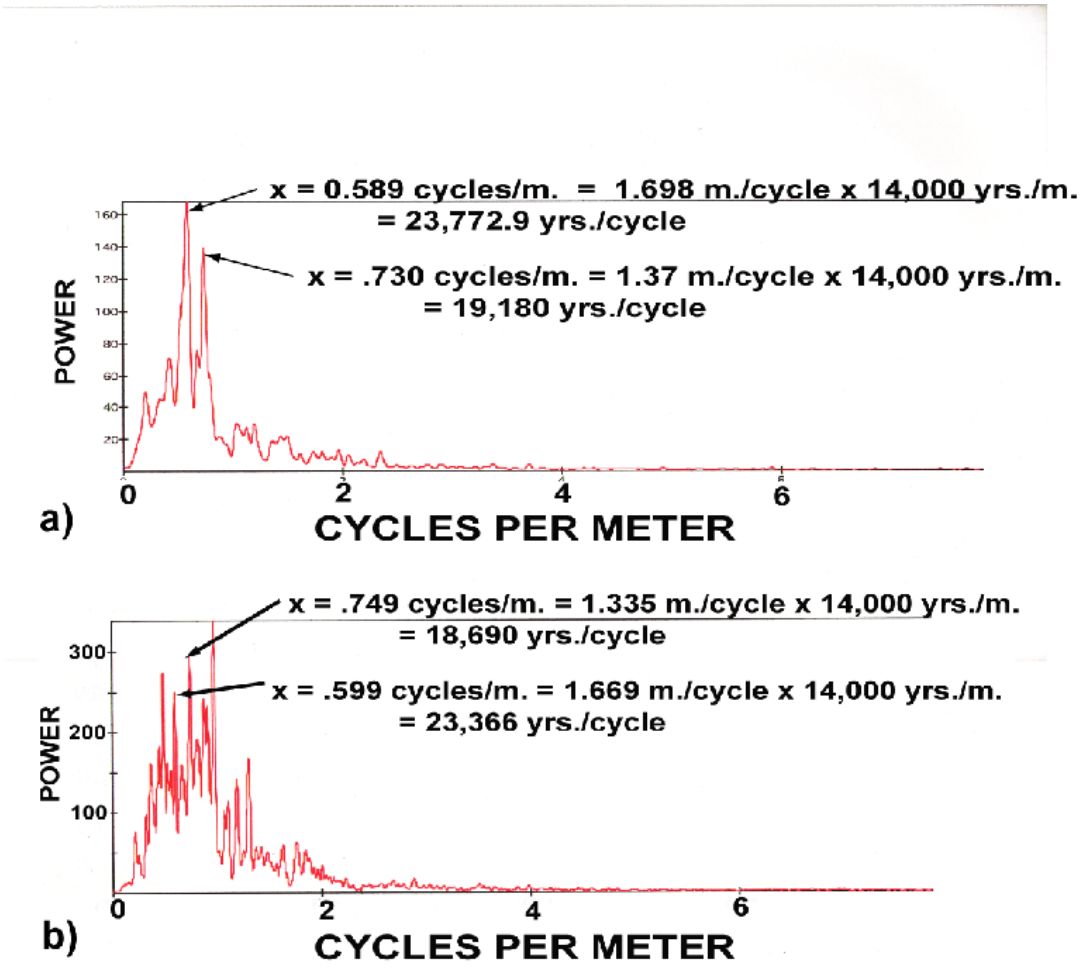

FIGURE 17: Comparison of Power Spectra. Spectral analysis (Blackman-Tukey method, 1959) was performed on normalized conductivity data generated by the formation microscanner in Hole 904A, New Jersey slope. a). Power spectrum for the upper Eocene (341 to 410 mbsf.). Note two strong peaks at 23.8K and 19.2K, close to the precessional Milankovitch frequencies of 23 and 19K. b). Power spectrum for the middle Eocene (420 to 552 mbsf.). Note there are four strong peaks, with two at close to precessional frequencies of 23.4K, and 18.7K.

Orbitally Driven Climate Cycles Dominated by Precession

The three orbital cycles that cause climate changes over tens of thousands of years are precession (direction earth's axis points into space), obliquity (tilt of earth's axis), and eccentricity (circularity of earth's orbit). The

orbital cycles influence climate by affecting the amount of solar radiation received at different latitudes, and by exceeding certain temperature thresholds (Weedon, 2003). These small variations in Earth-Sun geometry change how extreme the seasonal changes are throughout the year and hence affect the climate. In precession, the earth's axis points out into space and an observer outside the earth would see this axis point through different directions like the wobble of a spinning top over the span of 19,000 to 23,000 years. All three orbital cycles have been resolved from the geologic record of the late Eocene (Palike et al., 2001, precession and obliquity; Wade et al., 2001, precession; Robert et al., 2002, eccentricity, and Retallack, 2002). The discovery of precessional cycles in the New Jersey slope sediments (this study) confirms that the New Jersey margin was at a high enough latitude to have been affected by precessional scale climate changes in the late Eocene.

At the New Jersey slope, correlation of the grain size to the conductivity data shows similar fluctuations at comparable scales (Fig. 18). The interpretation is that variations in the medium sand size fraction reflecting foram abundance and conductivity are being driven by the same climatic cycles, i.e. precessional cycles. Low conductivities from the FMS (formation microscanner) plot (Figure 19, light bands) correspond to warm climate intervals with increased continental run-off and terrigenous input to the continental slope. Periodic shifts from cool dry conditions to warmer, wetter conditions are also invoked to explain increases and decreases in terrigenous material delivered to the Ceara Rise (ODP Site 925) off

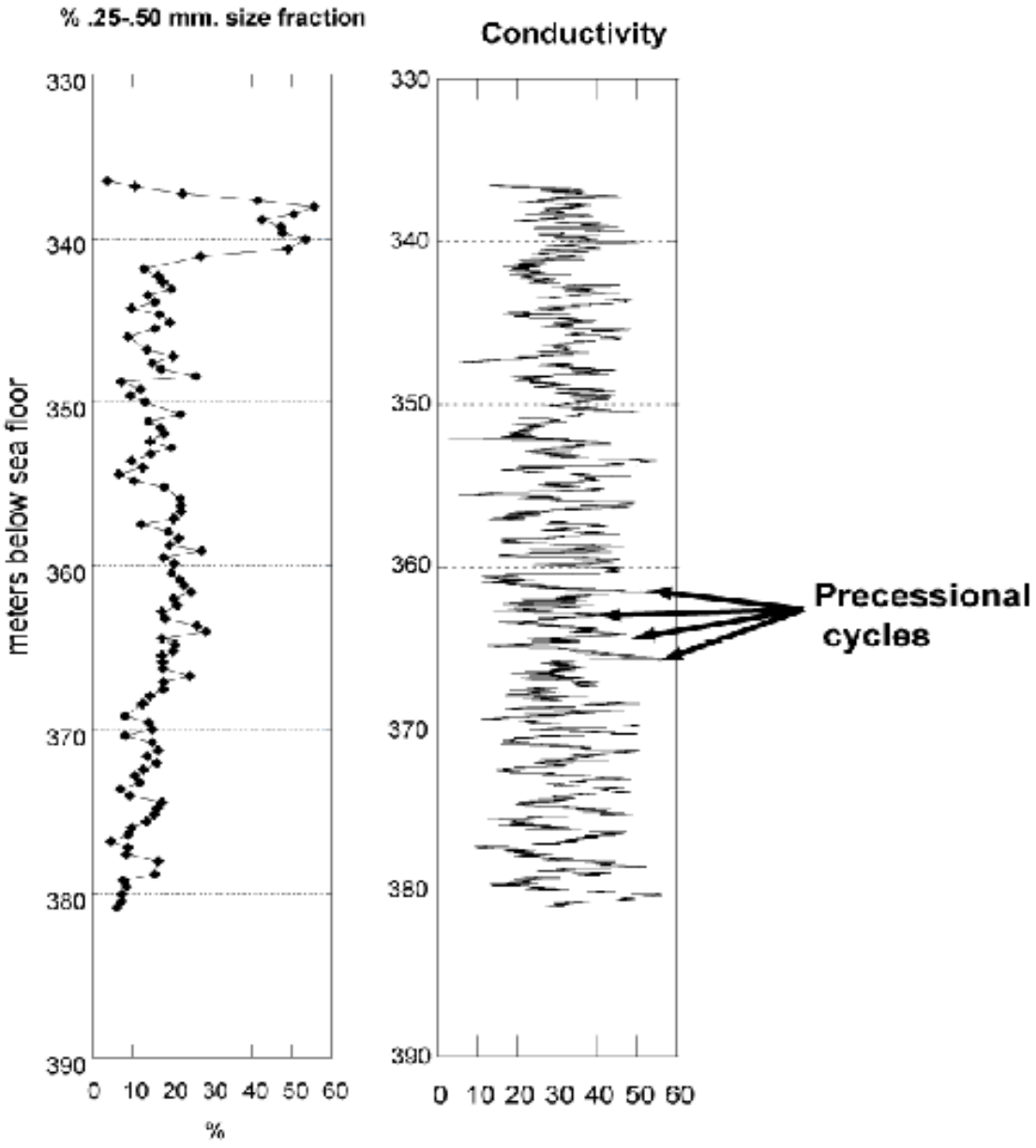

FIGURE 18: Grain Size and Conductivity Data; 336 – 381 mbsf. Note precessional cycles at regular intervals. Warm periods are shown by low conductivities (minimums at approximately 10) and cooler periods by high conductivities (maximums at about 50).

the northeast coast of South America in the late Eocene (Diester-Haass and Zachos, 2003). During these warmer, wetter periods along the New Jersey slope, more quartz, micas, and glauconite are transported across the shelf to the slope and the relative amount of mud in the sediment decreases. Direct evidence for

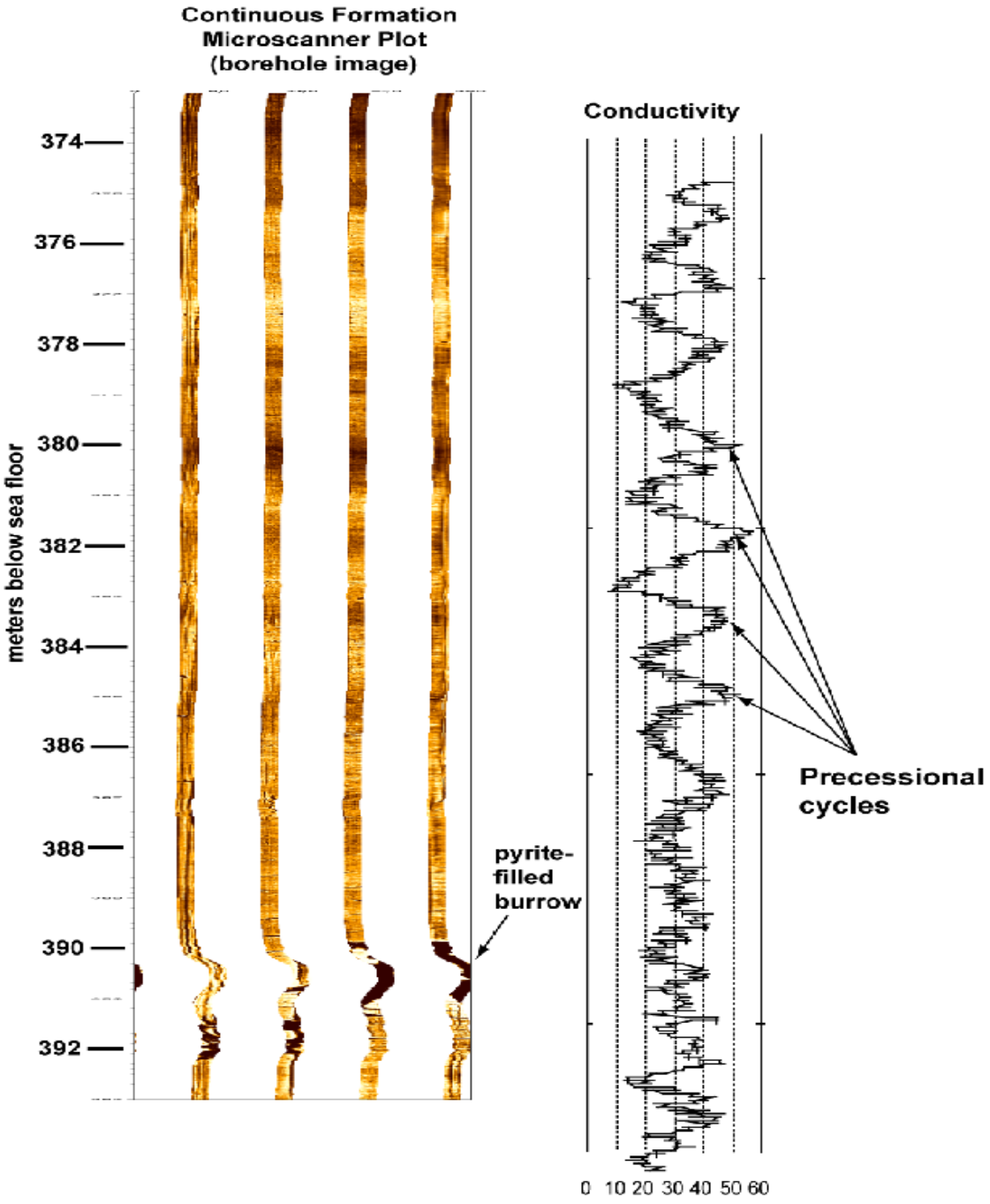

FIGURE 19: Correlation of Conductivity Curve with Borehole Image. On the left is a brown tone view of the borehole, with intensity of color proportional to conductivity level. The image is statically normalized. Light color is low conductivity, dark color is high conductivity. The 4 color columns coincide with the locations of electrode pads at 90 degree intervals around the circumference of the borehole. Note the pyrite-filled burrow near the bottom of the section. Dynamically normalized average conductivity data is presented to the right. The higher the number, the higher the average conductivity. Note precessional cycles about every 1.7 meters or 23,000 years. Precessional cycles are obscured in lower section by diagenesis near the pyrite-filled burrow.

this was seen as increased terrigenous grains in the thin section samples corresponding to low conductivity bands on the FMS (note troughs on conductivity curves in Figures 18 and 19). In other words, the FMS logs are directly recording sedimentation changes along the slope driven by climate changes. During these warmer intervals, planktonic foraminifera respond to increased surface water temperatures by an increase in productivity and so their numbers in the medium sand size fraction increase. Higher foram abundances are recorded by the peaks in the medium sand size fraction shown in Figure 18. During cooler, dryer climate intervals, continental run-off decreases due to less precipitation and hence terrigenous input across the shelf to the slope also decreases. As a result, relative mud content increases in the sediment that now has a high conductivity signature on the FMS plot (Figure 19, dark bands). These cooler, dryer periods are also reflected by lower planktonic foram abundances due to decreased surface water temperatures. Also, note the presence of cycles at regular intervals every 1.7 meters. As mentioned above, spectral analysis has shown these are precessional Milankovitch cycles at frequencies of every 23.8K and 19.2K years. In Figure 19 this becomes evident as a slight variation in depth between successive peaks on the conductivity plot.

Orbitally driven climate change paced at precessional Milankovitch frequencies is thus driving the regional sedimentation changes along the New Jersey slope. Conductivity fluctuations measured by the FMS directly record the increases and decreases in terrigenous grains supplied to the continental slope and the thin section observations back up this assertion. These relatively short

term (10^4 K) orbitally driven climate changes are superimposed on the longer term million year scale late Eocene cooling trend.

Sloan and Huber (2001) modeled the effects of precessional scale orbital forcing on Eocene oceanic processes including surface temperature, upwelling intensity and location, net surface moisture balance, and amount of continental runoff. The results of their model indicate that continental runoff is highly variable at all latitudes in response to the prescribed orbital forcing (Sloan and Huber, 2001). Stated another way, precessional orbital forcing taken together with the regional factors stated above is enough to cause climate change of a magnitude large enough to drive detectable and quantifiable sedimentation changes along a margin. Thus, the New Jersey slope can be viewed as an example of predictable and expected regional margin changes brought about by the global phenomenon of orbital forcing.

The sedimentation model for this study is also corroborated by Palike et al. (2001), namely that orbital forcing at precessional frequencies is pacing fluctuations between wetter, warmer and cooler, dryer periods which in turn are driving increases and decreases in terrigenous runoff rates. They studied late Eocene sediments from ODP Site 1052 (Blake Nose, Atlantic margin of northern Florida). The proximity of their site to the New Jersey margin makes it ideal for comparison. Their upper limit on sedimentation rate of 5 cm/kyr compares well to 7.14 cm/kyr for this study. They performed spectral analysis on XRF measurements of Ca/Fe ratio in sediments and found strong obliquity and precessional signals in their data as well. It is likely that both margins were

responding to the same orbitally driven climate changes.

Oxygen Isotopes and Correlation to the Global Record

Part of the hypothesis for this study was that stable isotope analysis should show a cooling trend within the late Eocene. As mentioned previously, numerous late Eocene studies have documented a general cooling or cooling pulses in the late Eocene (Katz and Miller, 1996; Nesbitt, 1999; Yancey and Elsik, 1999; Wang, 1999; Bestland, 2000; Bohaty et al., 2000; Elsik and Yancey, 2000; Lavelle, 2000; Terry, 2001; Wade et al., 2001; Retallack, 2002; Barrett, 2003, and DeConto and Pollard, 2003; Roth-Nebelsick et al., 2004). A summary of the oxygen isotope data obtained from the samples in this study did not unequivocally indicate a cooling trend. Only the lower resolution data set (see Figure 8, page 54 and Figure 16 above) showed an increase in $\delta^{18}O$ but not a very strong one. $\delta^{18}O$ values went from –3.67 per mil at the start of the late Eocene to –2.83 per mil at the end of the late Eocene (Figure 16). Although this is not a strong trend, it does agree with $\delta^{18}O$ increases from benthic *Cibicidoides spp*. in the late Eocene from other deep sea sites (Miller et al., 1991 and Zachos et al., 2004). Figure 20 below compares the $\delta^{18}O$ records of benthic *Cibicidoides spp.* from ODP Site 612 (Miller et al., 1991; New Jersey slope) and planktonic *Globigerina spp.* from Site 904 (this study). Both records show comparable increases in $\delta^{18}O$ during the late Eocene.

There are two interpretations for an increase in $\delta^{18}O$ from foraminiferal calcite: 1) an increase in ice volume on land or, 2) an absolute decrease in ocean

water temperature. Using the paleotemperature equation defined in the methods section (see page 42), $T = 16.9 - 4.38 (\delta_c - \delta_w) + 0.10 (\delta_c - \delta_w)^2$ we can estimate the change in surface water temperature through the late Eocene. Assuming an ice-free world for the late Eocene, global mean δ_w is -1.2 per mil (Ken Miller, personal communication, 2007). Using the measured δ_c values of -3.6 and -2.8 per mil, and plugging in the ice-free δ_w value of -1.2, the resulting mean surface water temperature changes from 28.5°C (83.3°F) at the beginning of the late Eocene to 24.1°C (75.4°F) at the close of the late Eocene. The value 28.5°C (83.3°F) is probably too high for this latitude, and an absolute temperature drop of 4.4°C (7.9°F) during the late Eocene without ice sheet growth may be too much. This suggests that the cooling of surface water temperatures may be related to ephemeral ice sheets on Antarctica as previously documented for the late Eocene (Miller et al., 1998; Miller et al., 2005). This is further supported by the $\delta^{18}O$ signals obtained from benthonic *Cibicidoides spp.* from Site 612 (Miller et al., 1991) and planktonic *Globigerina spp.* from Site 904 that taken together strongly suggest an increase in Antarctic ice volume. The late Eocene $\delta^{18}O$ increase is also documented globally at several ODP sites including the north and south Atlantic and Indian Oceans (Miller et al., 1991; Diester-Haass and Zahn, 1996; Zachos et al., 1996; Zachos et al., 2001; see Figure 20 below) further supporting global ice volume change.

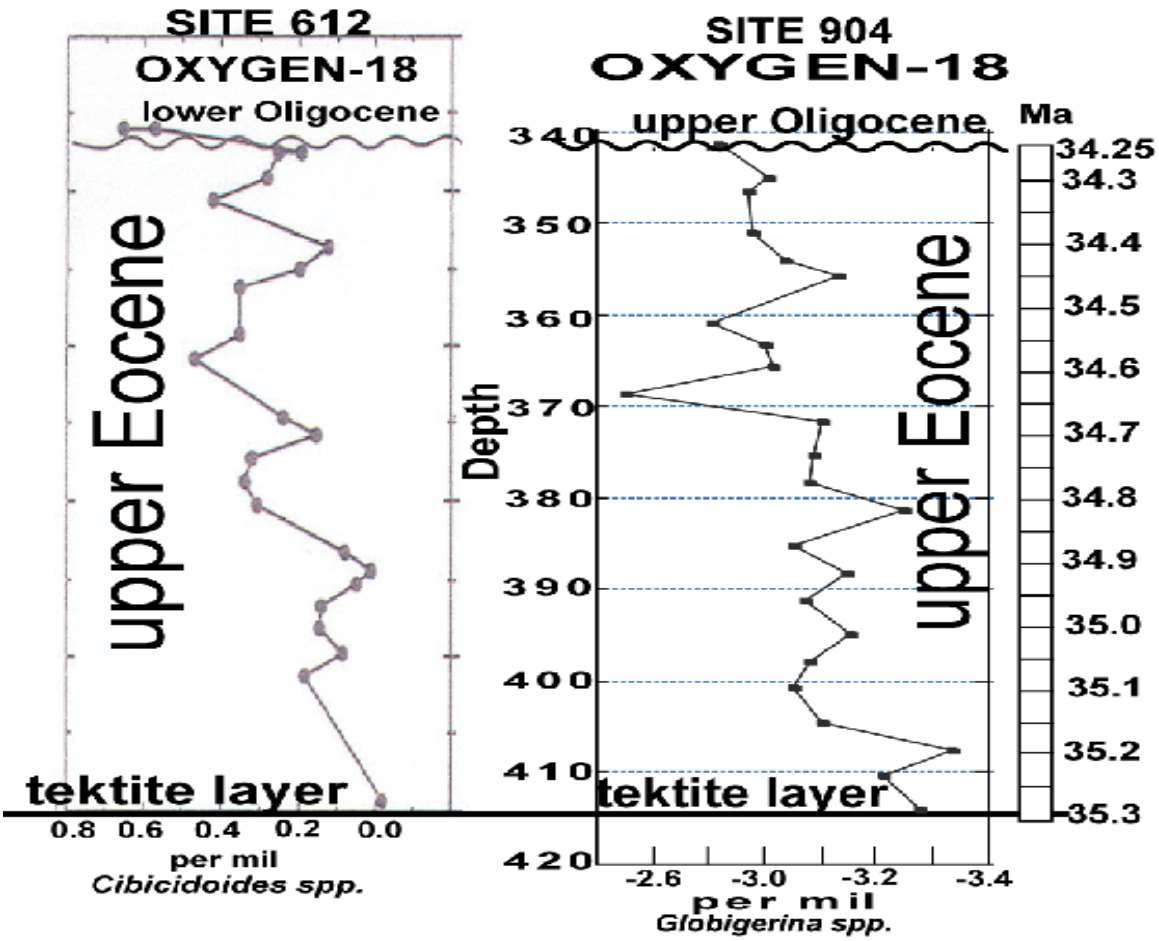

FIGURE 20: Oxygen Isotope Comparison of Sites 612 and 904. Both are New Jersey slope sites. Note $\delta^{18}O$ increase of 0.6 per mil (0.0 to 0.6) for benthonic *Cibicidoides spp.* from Site 612 (Miller et al., 1991). Note also $\delta^{18}O$ increase of 0.8 per mil (-3.6 to -2.8) for planktonic *Globigerina spp.* from Site 904. Both increases are approximately equal amounts. The tektite layer and the upper unconformity (3rd unconformity at 341 m. depth for Site 904) serve to correlate the two sections. Age control is from Site 904.

A global deep water cooling is manifested by a sharp jump up in $\delta^{18}O$ at the Eocene/Oligocene boundary (Figure 21a). This dramatic $\delta^{18}O$ increase attests to the presence of a significant ice sheet on Antarctica by this time (Global "Ice House"; Fig. 21a). Figure 21b presents the composite oxygen isotope record for the last 50 Ma. This significant global deep water cooling event designated ORi-1 by Abreu and Anderson (1998; see also Figure 3, page 35, this study) and documented globally (Zachos et al., 1996; Diester-Haass and Zahn,

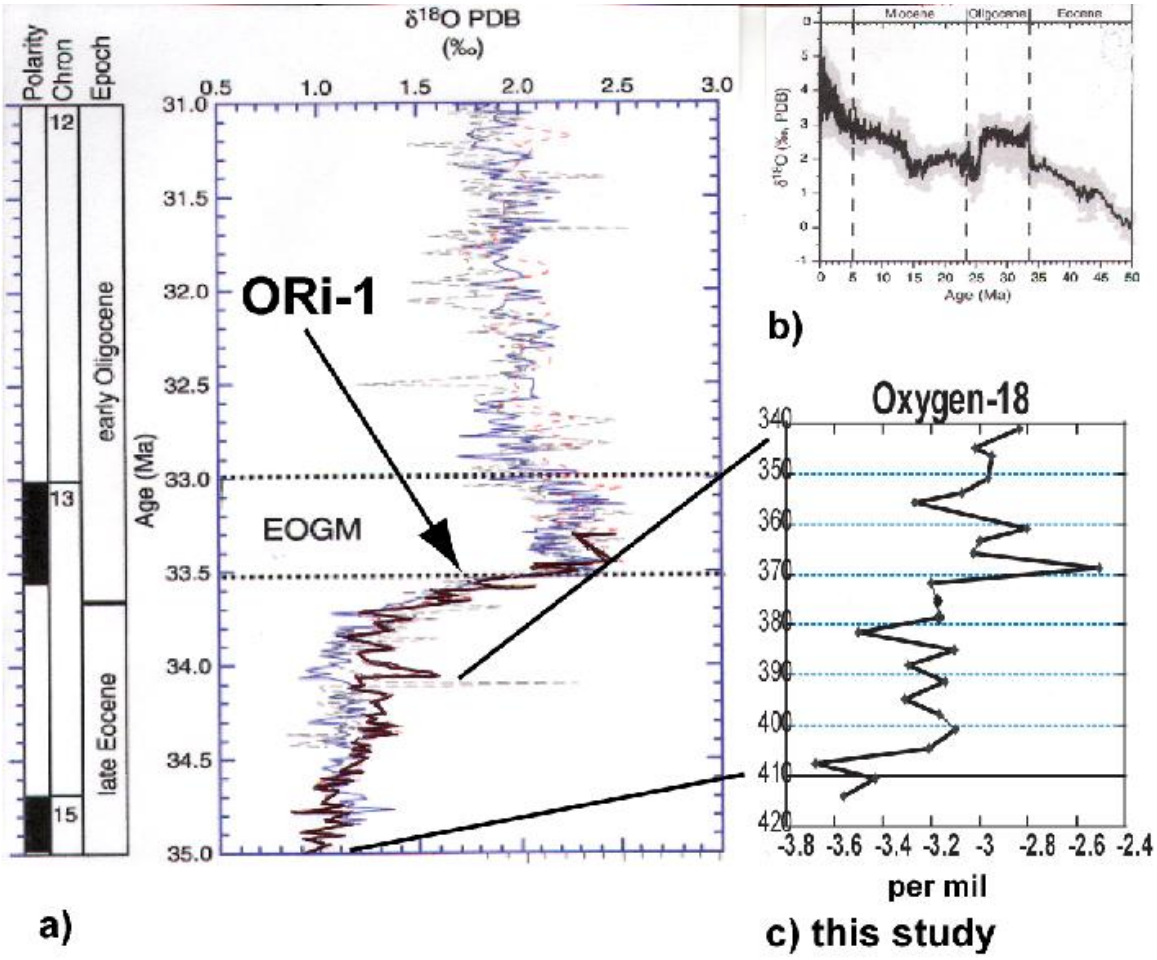

FIGURE 21: Comparison of Lower Resolution Oxygen Isotope Data to Global Record. **a).** Modified from Zachos et al., 2004. Composite of benthonic *Cibicidoides spp*. stable oxygen data for three ODP sites; 522 (central south Atlantic), 744 (Kergeulen Plateau, extreme southern Indian Ocean), and 689 (Maud Rise, extreme south Atlantic). A portion of the Site 689 record has been darkened for clarity. EOGM stands for early Oligocene Glacial Maximum. ORi-1 represents the dramatic global deep-water cooling event in the early Oligocene (see Figure 3, page 36 this study). Note the increase in $\delta^{18}O$ for site 689 from 1.0 to 1.5 per mil between 35.0 Ma and 34.2 Ma indicating slight cooling. Sites 522 and 744 do not show much of a shift for this interval. **b).** Composite oxygen isotope curve for the Cenozoic (part of Figure 3 from Pagani et al., 2005). **c).** Lower resolution oxygen isotope curve from this study based on the planktonic foram *Globigerina spp*. for the age interval from 35.3 Ma to 34.25 Ma. Compare the $\delta^{18}O$ increase from –3.7 to –2.8 per mil at New Jersey Site 904 to the Site 689 increase. Both increases are of similar magnitude.

1996; Diester-Haass and Zachos, 2003, and Zachos et al., 2004) is shown in Fig. 21a. Looking at Figure 21a the ORi-1 event begins about 33.7 Ma. The slight increase in $\delta^{18}O$ shown by the lower resolution oxygen isotope curve from this study (Figure 21c) takes place from 35.3 to 34.25 Ma or just before the beginning

of the ORi-1 event.

Placed in the temporal framework of early Oligocene Antarctic glaciation, the beginning of the $\delta^{18}O$ increase at New Jersey documented by this study (circa 35.3 Ma) comes some 1.5 Ma before the start of the ORi-1 event (33.7 Ma). The earliest glacial marine deposits from Seymour Island, Antarctic Peninsula, date to just at or very close to the Eocene / Oligocene boundary at 33.7 Ma and suggest the presence of a regionally extensive West Antarctica ice sheet by this time (Ivany et al., 2006). The question then is whether the slight $\delta^{18}O$ increase in surface waters detected at New Jersey between 35.3 and 34.25 Ma was indirectly related to the inception of Antarctic glaciation or to other regional factors. Several studies support the idea that the Antarctic ice sheet began to grow in the 2 million years or so before the ORi-1 event at 33.7 Ma. A drawdown in atmospheric carbon dioxide content (Hay et al., 2002; Barrett, 2003, and DeConto and Pollard, 2003), could have cooled the climate enough globally to slightly affect surface water temperatures off New Jersey in the late Eocene. Of course we still cannot say for sure what proportions of the $\delta^{18}O$ signal at New Jersey are due to ice volume, absolute temperature changes, or both.

Another important finding of the data shows a warmth towards the close of the late Eocene derived from the higher resolution oxygen isotope curve from this study (see Figure 9, page 55 and Figure 22 below). The period of warm surface waters off New Jersey comes between the two cooling events designated EPi-2 and ORi-1 by Abreu and Anderson (1998). This warm period must be looked at in relation to several important studies emphasizing the role of upper Eocene bolide

impacts (Poag et al., 2003, and Bodiselitsch et al. 2004). Poag et al. (2003) place the well known Chesapeake Bay impact structure at an age of 35.6 Ma based on magnetostratigraphic and biochronologic correlations. Poag et al. (2003) state that no radioisotopic date has yet been derived directly from the Chesapeake

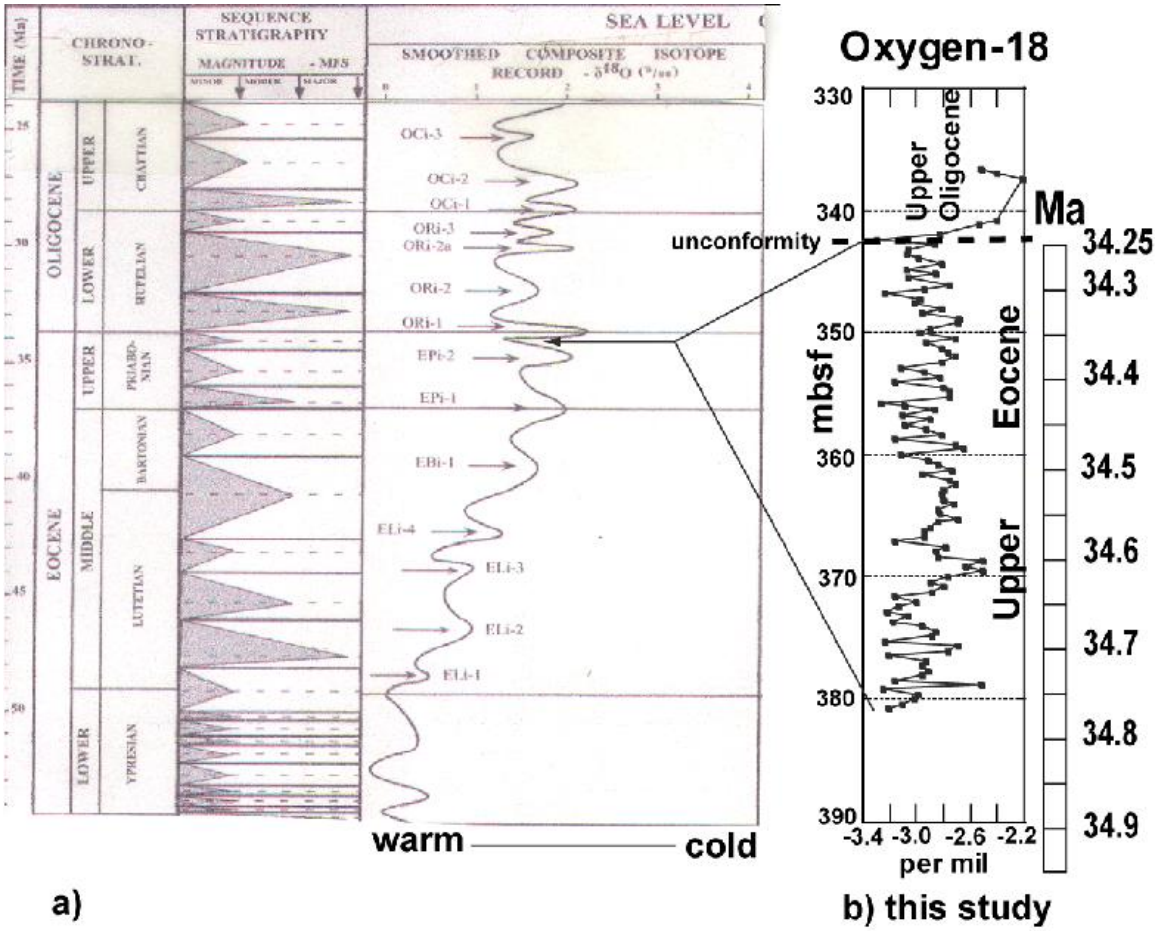

FIGURE 22: Comparison of High Resolution Oxygen Isotope Curve to Global Record. a). Modified view of Figure 4 from Abreu and Anderson (1998) showing composite oxygen isotope global record for the Eocene and Oligocene. Positive $\delta^{18}O$ excursions or cooling events are shown as peaks moving up to the right. Note the following two cooling events; at the very top of the upper Eocene (Priabonian) EPi-2 and at the beginning of the lower Oligocene (Rupelian) ORi-1. b). The higher resolution oxygen isotope record for this study coincides with the warm interval (peak to the left) between these two cooling events. Note the unconformity in the New Jersey record separating the upper Eocene from the upper Oligocene. Age control from Site 904 is included, with the higher resolution record spanning about a half a million years from 34.75 to 34.25 Ma.

Bay impact site. The Chesapeake Bay impact was along the continental shelf. The other well documented Late Eocene impact was at Popigai, Russia, which impacted land and is dated to 35.7 ± 0.8 Ma (Bottomley et al., 1997).

Poag et al. (2003) and Bodiselitsch et al. (2004) suggest that release of methane hydrates from shelf sediments may have initiated short periods of global warming that interrupted the long term Eocene – Oligocene cooling trend. As mentioned earlier in the literature review, the tektite layer at site 904 has been dated to 35.2 ± 0.1 Ma (McHugh et al., 1998) and is undoubtedly the result of the Chesapeake Bay impact. Pusz et. al. (2006) date correlative tektites from Alabama's Saint Stevens Quarry and ODP Site 1090 at 35.426 Ma based on magnetochronology. Could the impact event causing the tektite layer at Site 904 be responsible for the warm surface water conditions indicated by the oxygen isotope data from this study (Figure 22 above)? This is probably not the case, since there is a 0.45 Ma separation between the tektite layer at 35.3 Ma (average of 2 dates above; 35.2 and 35.426) and the beginning of the higher resolution oxygen isotope record at about 34.75 Ma (Figure 22). Any warming effects from the impact would probably not last 450,000 years. Additionally, the amount of warming effect of late Eocene bolide impacts remains uncertain.

A more likely explanation for the warmth recorded by the higher resolution oxygen isotope data is the presence of a modern-like western boundary current in the North Atlantic similar to the present day Gulf Stream. Iturralde-Vincent (2003) points out that shortly after the latest Eocene (37 Ma) during which there was an uplift along the axis of the Greater Antilles, a topographic barrier

developed during the Eocene-Oligocene transition (35-33 Ma). For a short time, this barrier (Figure 23 below) reduced water exchange between the Atlantic and the Caribbean-Pacific to a minimum, similar to the present day circulation pattern. This pattern would have enhanced the western boundary current passing by the New Jersey margin and kept surface waters there warm. Although the

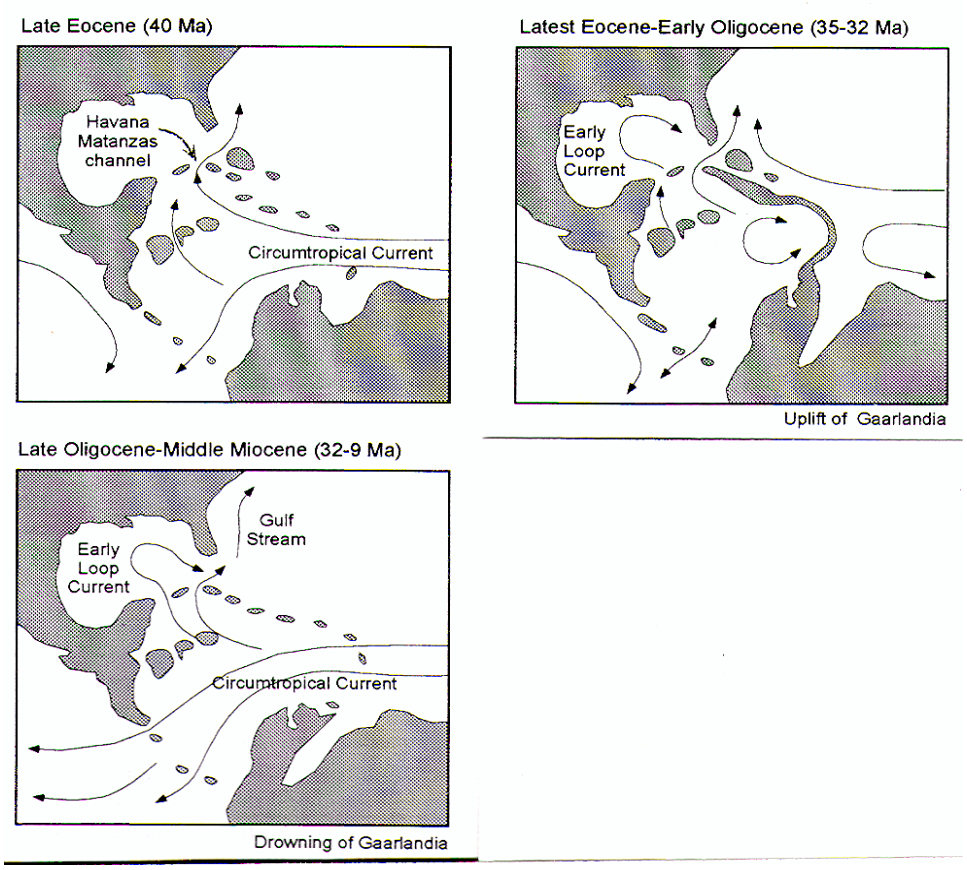

FIGURE 23: Paleogeographic Setting for the Caribbean Seaway During the Paleogene, after Figure 22.2 from Iturralde-Vincent (2003). Note Late Eocene time (40 Ma) when the Circumtropical Current (equatorial through-flow) is open between Atlantic and Pacific basins. By latest Eocene-Early Oligocene time (35-32 Ma), uplift of the landmass Gaarlandia has restricted equatorial through-flow and enhanced the Gulf Stream. By Late Oligocene-Middle Miocene time (32-9 Ma), the Circumtropical Current has commenced once again between North and South America.

timing of the uplift in the Caribbean is poorly constrained (35 – 33 Ma), it is still close enough in time to the stratigraphic record of Site 904 to be a plausible explanation. In addition, the warm surface waters above the continental slope where Globigerina were calcifying were not dramatically affected by cooling of deep water masses in the South Atlantic and Indian Ocean basins that was taking place in response to early ice sheet growth on Antarctica.

When looking at New Jersey, one also must consider the timing of the late Eocene cooling across the Atlantic in the Tethys region of central Europe. This important ocean gateway was also open during the late Eocene and served to allow deep-water current exchange between the Indian and Atlantic Oceans. Two important studies looked at benthic foraminiferal turnover rates and the relation of the Tethyan water mass to equatorial Atlantic and Indian Ocean water masses (Barbieri et al., 2003, and Nebelsick et al., 2003). In contrast to the over all cooling trend through the late Eocene recorded by data elsewhere, Nebelsick et al. (2003) conclude that an open Tethys seaway with low-latitude "tropical affinities" (benthic forams) persisted throughout the Eocene and Oligocene, which may have precluded any dramatic climate changes in their study area (central Europe and the Tethys Seaway). However, Coccioni and Galeotti (2003) examined benthic foraminiferal events from the Massignano Eocene/Oligocene boundary stratotype in central Italy and found that the extinction of a marker species, *Nuttalides truempyi*, is of global significance and the evolutionary pattern invokes a global event. In the sediments at Massignano, *Nuttalides truempyi* disappears well before deep water cooling in the Western

Tethys. Coccioni and Galeotti (2003) also note an important change in DOI (**dissolved oxygen index**) in the Italian sediments (planktonic foraminiferal Zone P16, upper Eocene) suggesting that following the major Nuttalides extinction event, the western Tethys was invaded by better oxygenated deep waters possibly from the Atlantic. The relationship of these regional changes in Europe and the Southern Ocean to bottom waters along the New Jersey slope in the upper Eocene remains an open question for future research.

SUMMARY OF CONCLUSIONS

1. A global cooling trend is manifested in the sediments of the NJ Continental Margin through the middle to the late Eocene. The general cooling trend is interrupted by warm and cool intervals manifested by an increase and decrease in the abundance of the *Globigerina spp*. foraminifera. These cycles are also manifested in the sand and clay fraction of the sediments that reflect increased terrigenous transport across the shelf to the slope in response to global cooling in the late Eocene. This cooling is documented globally.

2. The margin shows a shift from carbonate-dominated to siliciclastic-dominated sedimentation that began along the New Jersey slope at about 37 to 36 Ma. Clearly the data show a climate change was underway in the late Eocene with the mineralogy suggesting a cooling trend reflected by decreasing carbonate production and increased terrigenous transport to the slope.

3. A summary of the oxygen isotope data from this study did not unequivocally show a cooling trend in the late Eocene. Only the lower resolution $\delta^{18}O$ data (one sample per 40K yrs.) showed a slight cooling trend with values ranging from -3.67 per mil up to -2.83 per mil between 35.3 Ma and 34.25 Ma in the late Eocene. This trend agrees with a trend toward increased $\delta^{18}O$ in benthonic foraminifera from Site 612 that taken together with the Site 904 planktonic data strongly suggest an increase in Antarctic ice volume. The higher resolution (one sample per 5K yrs.) oxygen isotope data shows consistent

warmth during the period from 34.7 Ma to 34.25 Ma. This warmth was probably not related to late Eocene impact events recorded at Chesapeake Bay and Popigai, Russia. It is more likely related to a strong western boundary current flowing past New Jersey in response to tectonic events along the Caribbean Seaway.

4. Cyclicity was shown in the formation microscanner (FMS) logs and it was confirmed by spectral analysis that found a strong precessional signal in the conductivity data. For the late Eocene, strong spectral peaks were detected at frequencies of 23.8ka and 19.2ka, close to the Milankovitch precessional frequencies of 23ka and 19ka. The slight shift of both spectral peaks off the exact precessional frequencies is most likely related to slight uncertainty in the estimation of sedimentation rate for the late Eocene. For the middle Eocene, strong peaks were detected at frequencies of 23.4ka, and 18.7ka, also very close to the Milankovitch frequencies. Diagenesis in the middle Eocene has most likely clouded the signal somewhat.

5. The recording of Milankovitch cycles in the late Eocene of the New Jersey slope is the most significant finding of this study. The precessional signal in the conductivity data is due to orbitally driven climate cycles. Sedimentation responded directly to these climate cycles. Warm periods resulted in increased continental runoff and an increase in quartz silt and micas delivered to the slope. This caused a conductivity decrease to be measured on the FMS logs. During

cooler intervals, less silt and more clay is present in the slope sediments and the FMS measured higher conductivity for these intervals.

APPENDIX A

Grain Size Data

DEPTH	% 0.25- 0.5 mm. size
336.50	3.9
336.85	11.0
337.27	22.8
337.67	41.6
338.05	55.8
338.53	50.5
338.88	42.6
339.30	47.5
339.67	47.8
340.06	53.6
340.66	49.1
341.12	27.1
341.88	13.2
342.27	16.7
342.66	17.8
343.08	20.0
343.47	14.1
343.89	16.0
344.28	10.0
344.66	17.0
345.12	19.6
345.51	15.9
345.99	9.1
346.80	13.9
347.19	20.3
347.61	15.1
347.99	17.4
348.41	26.1
348.76	7.4
349.21	12.2
349.60	9.7
349.98	13.3
350.40	
350.74	22.2
351.18	14.3
351.53	17.2
351.93	18.2
352.40	14.7
352.78	20.0
353.17	14.9
353.58	10.0
353.99	12.8
354.38	6.9
354.78	10.6
355.17	18.2
355.85	22.2

356.30	22.4
356.65	22.4
357.10	20.6
357.47	12.5
357.93	19.3
358.29	21.8
358.71	19.4
359.07	27.6
359.49	17.9
359.87	20.8
360.41	20.0
360.80	22.0
361.20	23.2
361.59	25.0
361.99	20.6
362.41	21.4
362.80	17.6
363.20	18.3
363.62	26.2
363.99	28.6
364.41	17.6
364.83	20.9
365.19	20.4
365.45	17.6
365.86	17.7
366.26	17.7
366.70	24.6
367.10	18.0
367.50	18.0
367.93	14.6
368.40	12.8
369.16	8.3
369.54	14.3
369.95	15.2
370.36	8.3
370.76	15.1
371.22	16.7
371.60	13.9
372.01	16.3
372.42	12.9
372.82	10.8
373.20	12.1
373.60	7.3
374.01	9.4
374.40	17.6
374.79	16.4
375.16	15.8
375.60	13.8

375.97	10.0
376.40	9.1
376.82	4.8
377.19	9.1
377.57	8.7
378.01	16.7
378.80	16.0
379.19	8.0
379.56	8.7
380.03	7.7
380.44	7.7
380.80	6.4

APPENDIX B

Bulk Mineralogy Data

DEPTH	6 :Calcite	8 :Quartz	9 :OPAL-C	1 :Pyrite	5 :Albite	4 :Dolomit	7 :Microcli	2 :Siderite	3 :Amphibo
	3.04 •	3.34 •	4.31 •	2.71 •	3.19 •	2.89 •	3.24 •	2.79 •	8.45 •
	Intensity	Intensity	Intensity	Intensity	Intensity	Intensity	Intensity	Intensity	Intensity
341.22	1921	255		15		16	40		
345	1704	389	58	17					
346.4	1111	340	33	17					
350.9	2138	325		16					
353.9	1813	224	28	16		12			
360.9	2349	266	28						
363.2	2214	398		13		12			
365.7	2432	359		13			28	18	
368.7	1982	425		17					
371.7	2202	265	34					21	
375.4	1311	272	30	23	15		24	13	
378.4	1910	307		29	24				
381.4	2134	377	41	18				20	
385.1	2374	357	25	18			27		
388.1	1597	238		17		11			
391.2	1787	351		36					
394.8	2228	276		19					
397.8	2105	258		16					
400.8	2083	447		16					
404.54	1805	429		20					
407.5	1876	331		22	38				
410.5	1867	329							
414.1	1902	348		25	31	12	33		
416.85	1961	313	17	43				26	
417.15	2631	580		21	24				26
421.06	2457	147	26					20	
423.7	2604	103		24	9	8	11		
426.7	2175	146							
429.5	1994	146	27	19				21	
433.2	2613	124	26	14					
436.2	2349	106							
439.2	2288	152							
442.7	2606	150		13	11			16	
445.7	2636	162				6			
448.7	2627	177		22	16	6	21		
452.1	2550	231	16		14	7			
458.1	2894	105							
459.2	3132	114		9		9			21
467.9	2334	167	26	11					
469.1	2117	195		16	19	8	20		
471.6	2438	165				13			
474.6	2357	130							
477.6	2381	114		15			24		
482.7	2911	60		18					
485.7	2622	77					27	18	
490.4	2518	103							
495.6	3043	108		12		14			
503.4	2773	86							
510.2	2383	67				7			
516.2	2396	89				10	19		
519.5	2692	113	13	17		9	14	16	
522.5	2751	107		18		7		18	
525.5	2166	101		16	13				
533.1	2774	89	108	15		7	17	12	
536.1	2778	85	108			12	12	17	
538.7	2600	112	100	12				18	
544.9	2886	128	95	7		10	13		
546.3	2647	113	111	12	14	8	18	15	
559	2449	158	107	14	14	7		26	25
561	2514	130	143	11				23	
564	2030	95	220	14			20	18	

APPENDIX C

Stable Isotope Data

LOW RESOLUTION DATA SET

Depth (m.)	$\delta^{18}O$ (per mil)
341.22	-2.834
345.00	-3.02
346.40	-2.948
350.90	-2.962
353.90	-3.072
355.70	-3.267
360.90	-2.805
363.20	-2.998
365.70	-3.027
368.70	-2.506
371.70	-3.201
375.40	-3.175
378.40	-3.167
381.40	-3.501
385.10	-3.102
388.10	-3.294
391.20	-3.142
394.80	-3.31
397.80	-3.164
400.80	-3.099
404.50	-3.207
407.50	-3.678
410.50	-3.43
414.10	-3.561

HIGH RESOLUTION DATA SET

Depth (m.)	$\delta^{18}O$ (per mil)	Depth (m.)	$\delta^{18}O$ (per mil)	Depth (m.)	$\delta^{18}O$ (per mil)
336.50	-2.527	356.70	-3.117	373.60	-3.178
336.90	-2.402	357.10	-2.901	374.00	-2.967
337.30	-2.217	357.50	-3.096	374.40	-2.861
340.70	-2.406	357.90	-2.934	374.80	-2.891
341.10	-2.542	358.30	-2.809	375.20	-3.245
341.90	-2.828	358.70	-3.175	375.60	-2.696
342.30	-3.302	359.10	-2.709	376.00	-2.778
342.70	-2.876	359.50	-2.654	376.40	-3.22
343.10	-3.07	359.90	-3.119	376.80	-2.934
343.50	-3.083	360.40	-2.925	377.20	-2.957
343.90	-2.988	360.80	-2.844	377.60	-2.916
344.30	-2.809	361.20	-2.748	378.00	-2.956
344.70	-3.08	361.60	-2.96	378.40	-3.167
345.10	-2.853	362.00	-2.758	378.80	-2.516
345.50	-3.062	362.40	-2.715	379.20	-3.261
346.00	-2.755	362.80	-2.806	379.60	-2.995
346.40	-2.948	363.20	-2.821	380.00	-3.016
346.80	-3.249	363.60	-2.807	380.40	-3.117
347.20	-2.984	364.00	-2.731	380.80	-3.22
347.60	-3.017	364.40	-2.85		
348.00	-2.823	364.80	-2.834		
348.40	-2.965	365.20	-2.692		
348.80	-2.685	365.50	-2.848		
349.20	-2.692	365.90	-2.901		
349.60	-2.901	366.30	-2.946		
350.00	-2.973	366.70	-2.945		
350.40	-2.712	367.10	-3.166		
350.70	-2.933	367.50	-2.785		
351.20	-2.823	367.90	-2.857		
351.50	-2.765	368.40	-2.851		
351.90	-2.715	368.70	-2.506		
352.40	-2.81	369.20	-2.642		
352.80	-3.129	369.50	-2.512		
353.20	-2.941	370.00	-2.768		
353.60	-2.827	370.40	-2.9		
354.00	-3.175	370.80	-2.806		
354.40	-2.807	371.20	-2.891		
354.80	-2.754	371.60	-3.169		
355.20	-2.758	372.00	-3.007		
355.70	-3.267	372.40	-3.136		
355.90	-3.091	372.80	-3.23		
356.30	-2.873	373.20	-3.063		

APPENDIX D

Uncalibrated Conductivity Data (Dynamically Normalized)

NOTE : Each page contains 6 total columns of data, divided into 3 pairs of 2 columns each. The left column in each pair is depth below the sea bed in meters (m.). The right column in each pair is uncalibrated raw conductivity (no units). Going down-section the data should be read from the upper left to lower right corners of each page and from left to right across the 3 pairs of columns.

The entire data runs from a depth of 341.0026 m. to a maximum of 410.0017 m.

NOTE ALSO: Un-normalized data available upon request.

341.0026	27.6219	341.6122	18.9875	342.2218	26.6062
341.0153	25.4656	341.6249	19.6937	342.2345	28.2719
341.028	21.3625	341.6376	19.9062	342.2472	29.4031
341.0407	21.6375	341.6503	19.05	342.2599	26.7812
341.0534	24.1719	341.663	22.8875	342.2726	28.1375
341.0661	26.2313	341.6757	23.0187	342.2853	27.9156
341.0788	26.2687	341.6884	24.5469	342.298	26.4406
341.0915	32.225	341.7011	27.9281	342.3107	24.1
341.1042	36.55	341.7138	29.1188	342.3234	20.35
341.1169	34.6906	341.7265	26.1562	342.3361	20.6156
341.1296	30.7375	341.7392	25.1688	342.3488	21.4281
341.1423	29.4656	341.7519	25.5875	342.3615	21.2938
341.155	28.3656	341.7646	25.1125	342.3742	22.0625
341.1677	23.7969	341.7773	24.0531	342.3869	24.8531
341.1804	20.9562	341.79	21.1906	342.3996	25.6031
341.1931	21.8937	341.8027	20.2812	342.4123	24.2
341.2058	21.9156	341.8154	18.1187	342.425	25.35
341.2185	24.0781	341.8281	18.1813	342.4377	27.2875
341.2312	24.9813	341.8408	24.775	342.4504	28.6031
341.2439	26.8813	341.8535	25.4	342.4631	25.4937
341.2566	27.0344	341.8662	25.8938	342.4758	24.7594
341.2693	24.8375	341.8789	26.3375	342.4885	23.1875
341.282	22.9219	341.8916	23.6062	342.5012	25.5031
341.2947	22.3375	341.9043	27.0312	342.5139	27.1531
341.3074	24.95	341.917	25.3062	342.5266	27.2125
341.3201	29.7812	341.9297	23.3063	342.5393	30.7812
341.3328	30.8094	341.9424	26.2531	342.552	28.4031
341.3455	27.5438	341.9551	28.45	342.5647	26.2688
341.3582	25.475	341.9678	26.5531	342.5774	26.8563
341.3709	22.8	341.9805	22.5281	342.5901	28.6719
341.3836	20.6	341.9932	27.2969	342.6028	28.8125
341.3963	22.0875	342.0059	33.2594	342.6155	31.85
341.409	24.1781	342.0186	30.7063	342.6282	32.6906
341.4217	21.4875	342.0313	25.8875	342.6409	32.6
341.4344	18.0594	342.044	20.6313	342.6536	33.6469
341.4471	21.6781	342.0567	18.5594	342.6663	35.4313
341.4598	25.1656	342.0694	21.0781	342.679	34.4562
341.4725	24.4156	342.0821	23.2313	342.6917	34.9156
341.4852	22.1625	342.0948	22.8438	342.7044	37.2156
341.4979	18.1531	342.1075	21.1031	342.7171	45.6719
341.5106	16.4781	342.1202	22.6469	342.7298	41.3719
341.5233	19.9813	342.1329	24.225	342.7425	37.3281
341.536	25.4969	342.1456	23.7281	342.7552	36.65
341.5487	24.1031	342.1583	24.3281	342.7679	34.9875
341.5614	23.1531	342.171	26.3781	342.7806	33.75
341.5741	20.6781	342.1837	27.5	342.7933	31.8844
341.5868	22.2062	342.1964	24.4844	342.806	31.1313
341.5995	22.9469	342.2091	26.1469	342.8187	29.775

342.8314	28.8281	343.441	29.75	344.0506	31.9156
342.8441	30.4594	343.4537	31.0375	344.0633	29.6344
342.8568	37.7156	343.4664	31.0938	344.076	25.7562
342.8695	37.9469	343.4791	29.9219	344.0887	26.4594
342.8822	33.5625	343.4918	31.7063	344.1014	31.9875
342.8949	31.7313	343.5045	38.8406	344.1141	29.3438
342.9076	31.6625	343.5172	42.7625	344.1268	27.9656
342.9203	31.8344	343.5299	42.6594	344.1395	31.175
342.933	33.3219	343.5426	44.2469	344.1522	30.0656
342.9457	37.5156	343.5553	45.8219	344.1649	25.7031
342.9584	38.8219	343.568	44.3219	344.1776	24.8656
342.9711	35.8531	343.5807	46.8781	344.1903	25.9594
342.9838	37.5719	343.5934	48.6094	344.203	30.9344
342.9965	38.5594	343.6061	46.1156	344.2157	28.25
343.0092	32.1875	343.6188	47.2906	344.2284	27.2344
343.0219	34.125	343.6315	47.4469	344.2411	30.0375
343.0346	37.2094	343.6442	46.95	344.2538	31.5531
343.0473	38.3312	343.6569	47.125	344.2665	24.8938
343.06	39.7906	343.6696	47.4062	344.2792	22.7812
343.0727	39.6437	343.6823	47.7406	344.2919	21.9406
343.0854	41.15	343.695	47.1406	344.3046	21.8375
343.0981	43.4375	343.7077	45.8375	344.3173	23.0469
343.1108	44.3656	343.7204	44.3531	344.33	20.6344
343.1235	45.4906	343.7331	43.5	344.3427	17.9812
343.1362	44.475	343.7458	44.1656	344.3554	18.4375
343.1489	43.4625	343.7585	40.9844	344.3681	22.7125
343.1616	42.4844	343.7712	41.7063	344.3808	27.9188
343.1743	40.6125	343.7839	43.25	344.3935	27.5875
343.187	40.2812	343.7966	43.95	344.4062	20.3125
343.1997	40.0312	343.8093	40.4844	344.4189	15.2125
343.2124	37.8094	343.822	40.9875	344.4316	16.0625
343.2251	35.7531	343.8347	41.6	344.4443	19.7281
343.2378	36.1656	343.8474	38.2188	344.457	19.3563
343.2505	35.2344	343.8601	38.3219	344.4697	22.775
343.2632	33.5312	343.8728	38.5094	344.4824	33.175
343.2759	33.7344	343.8855	33.7438	344.4951	27.0719
343.2886	35.1094	343.8982	35.3625	344.5078	21.8281
343.3013	32.8844	343.9109	34.95	344.5205	22.775
343.314	30.1688	343.9236	33.275	344.5332	22.7938
343.3267	32.2406	343.9363	27.9188	344.5459	22.55
343.3394	29.7438	343.949	32.1188	344.5586	19.2313
343.3521	25.0875	343.9617	32.7344	344.5713	19.875
343.3648	29.1906	343.9744	28.9781	344.584	20.7812
343.3775	26.2344	343.9871	29.45	344.5967	22.7062
343.3902	25.0812	343.9998	31.0562	344.6094	20.3375
343.4029	29.5344	344.0125	29.6812	344.6221	23.0688
343.4156	29.5938	344.0252	35.4219	344.6348	22.0312
343.4283	28.5563	344.0379	31.2781	344.6475	30.8219

344.6602	29.7	345.2698	38.7188	345.8794	41.35
344.6729	26.8688	345.2825	40.5563	345.8921	43.575
344.6856	27.6844	345.2952	41.8906	345.9048	46.0719
344.6983	23.0781	345.3079	43.1469	345.9175	45.6094
344.711	25.4937	345.3206	45.9344	345.9302	44.4344
344.7237	33.0906	345.3333	48.7219	345.9429	45.3187
344.7364	32.9125	345.346	49.6406	345.9556	45.3969
344.7491	34.9844	345.3587	47.25	345.9683	45.3563
344.7618	30.525	345.3714	49.2969	345.981	45.3281
344.7745	37.5875	345.3841	49.2812	345.9937	42.7031
344.7872	39.6844	345.3968	49.7125	346.0064	41.1656
344.7999	36.8469	345.4095	49.5812	346.0191	42.7844
344.8126	32.875	345.4222	45.4156	346.0318	37.5312
344.8253	34.0812	345.4349	43.7844	346.0445	39.3094
344.838	34.0687	345.4476	38.9344	346.0572	39.3344
344.8507	37.3187	345.4603	38.8937	346.0699	39.6344
344.8634	35.5344	345.473	42.1969	346.0826	38.3625
344.8761	33.0062	345.4857	44.0312	346.0953	37.7812
344.8888	32.5687	345.4984	39.7094	346.108	39.5938
344.9015	34.7156	345.5111	33.5594	346.1207	35.5906
344.9142	33.7062	345.5238	38.35	346.1334	34.4844
344.9269	36.2406	345.5365	33.525	346.1461	36.6813
344.9396	37.5156	345.5492	36.5688	346.1588	36.3156
344.9523	38.8688	345.5619	37.6375	346.1715	34.3281
344.965	37.2875	345.5746	36.5719	346.1842	33.5656
344.9777	33.5	345.5873	36.1781	346.1969	33.2469
344.9904	29.7375	345.6	36.7875	346.2096	33.0375
345.0031	29.4594	345.6127	36.075	346.2223	31.5938
345.0158	31.7438	345.6254	33.7469	346.235	30.525
345.0285	33.9469	345.6381	34.3187	346.2477	30.4438
345.0412	32.3625	345.6508	33.6969	346.2604	32.3313
345.0539	33.0281	345.6635	35.2188	346.2731	34.6094
345.0666	33.5312	345.6762	34.1344	346.2858	30.8937
345.0793	29.1	345.6889	33.8125	346.2985	32.0781
345.092	30.3438	345.7016	34.2188	346.3112	32.6875
345.1047	28.1031	345.7143	32.1156	346.3239	29.7437
345.1174	28.5531	345.727	40.5938	346.3366	32.4531
345.1301	25.1469	345.7397	41.1906	346.3493	31.0344
345.1428	24.8937	345.7524	41.6125	346.362	28.9625
345.1555	28.4156	345.7651	42.3781	346.3747	29.2344
345.1682	25.775	345.7778	42.475	346.3874	28.7844
345.1809	27.5719	345.7905	42.8562	346.4001	27.0875
345.1936	31.8469	345.8032	45.9719	346.4128	26.6813
345.2063	29.975	345.8159	44.0031	346.4255	27.2219
345.219	34.0187	345.8286	44.9344	346.4382	30.3656
345.2317	34.0812	345.8413	42.2062	346.4509	30.0062
345.2444	31.1	345.854	42.5438	346.4636	29.6469
345.2571	34.5312	345.8667	41.2812	346.4763	30.4594

346.489	29.0656	347.0986	25.1406	347.7082	30.475
346.5017	31.4313	347.1113	19.3438	347.7209	35.3406
346.5144	29.4531	347.124	21.8531	347.7336	34.7531
346.5271	30.6063	347.1367	19.8719	347.7463	38.1937
346.5398	32.1313	347.1494	21.525	347.759	37.4813
346.5525	32.1437	347.1621	22.9156	347.7717	39.3344
346.5652	32.9969	347.1748	25.0812	347.7844	33.0875
346.5779	33.2375	347.1875	22.1031	347.7971	37.5156
346.5906	32.4062	347.2002	17.9844	347.8098	39.1625
346.6033	32.7781	347.2129	20.9781	347.8225	35.75
346.616	31.8094	347.2256	15.6	347.8352	43.925
346.6287	32.0906	347.2383	13.9625	347.8479	39.9344
346.6414	30.7344	347.251	15.5938	347.8606	42.2344
346.6541	30.125	347.2637	13.2188	347.8733	40.6531
346.6668	30.7406	347.2764	11.5312	347.886	44.725
346.6795	27.9281	347.2891	13.1781	347.8987	38.9
346.6922	30.4406	347.3018	12.4875	347.9114	39.5781
346.7049	30.1281	347.3145	8.7688	347.9241	43.9125
346.7176	27.775	347.3272	11.4125	347.9368	33.9156
346.7303	26.2562	347.3399	6.6969	347.9495	40.15
346.743	28.6656	347.3526	9.1625	347.9622	34.0875
346.7557	26.2281	347.3653	7.275	347.9749	38.6594
346.7684	25.1594	347.378	6.3313	347.9876	34.2531
346.7811	30.0625	347.3907	4.7781	348.0003	38.825
346.7938	36.65	347.4034	4.8719	348.013	40.7188
346.8065	37.7406	347.4161	9.2281	348.0257	37.1625
346.8192	33.4937	347.4288	14.5219	348.0384	42.2094
346.8319	32.0219	347.4415	22.5281	348.0511	36.5406
346.8446	33.9906	347.4542	25.8063	348.0638	43.2312
346.8573	31.4937	347.4669	28.5531	348.0765	36.4344
346.87	30.6875	347.4796	31.0344	348.0892	43.8312
346.8827	26.5219	347.4923	32.6125	348.1019	40.9313
346.8954	27.7531	347.505	32.9813	348.1146	38.3063
346.9081	27.5688	347.5177	33.4156	348.1273	38.1344
346.9208	33.1344	347.5304	28.9344	348.14	40.1656
346.9335	32.7313	347.5431	27.9469	348.1527	42.6094
346.9462	33.7156	347.5558	24.45	348.1654	32.5687
346.9589	26.3094	347.5685	21.0094	348.1781	35.15
346.9716	28.3906	347.5812	21.1937	348.1908	29.3563
346.9843	30.5125	347.5939	19.2938	348.2035	28.6469
346.997	26.0938	347.6066	20.2031	348.2162	26.9813
347.0097	26.1531	347.6193	24.7219	348.2289	25.7375
347.0224	28.6063	347.632	30.3656	348.2416	20.6219
347.0351	24.6594	347.6447	27.8281	348.2543	28.0531
347.0478	23.5406	347.6574	30.5031	348.267	19.3687
347.0605	20.7063	347.6701	31.8375	348.2797	18.3469
347.0732	20.7875	347.6828	33.9094	348.2924	24.5875
347.0859	23.1937	347.6955	29.8969	348.3051	24.8937

348.3178	21.6344	348.9274	30.5625	349.537	43.225
348.3305	23.9688	348.9401	31.0969	349.5497	40.5312
348.3432	23.5719	348.9528	31.5063	349.5624	39.4281
348.3559	21.2687	348.9655	37.3625	349.5751	33.575
348.3686	24.2094	348.9782	32.525	349.5878	39.0812
348.3813	20.6562	348.9909	36.225	349.6005	41.3
348.394	25.8406	349.0036	34.8469	349.6132	40.5719
348.4067	22.4844	349.0163	37.7844	349.6259	40.9875
348.4194	22.8531	349.029	33.4906	349.6386	42.325
348.4321	21.8031	349.0417	41.3812	349.6513	38.3187
348.4448	23.8969	349.0544	37.8906	349.664	37.575
348.4575	20.6312	349.0671	34.8156	349.6767	37.1562
348.4702	21.5125	349.0798	30.1344	349.6894	41.9938
348.4829	21.0125	349.0925	34.9937	349.7021	41.675
348.4956	23.5656	349.1052	37.4562	349.7148	41.4875
348.5083	18.7344	349.1179	38.875	349.7275	42.4875
348.521	22.1687	349.1306	44.1781	349.7402	37.775
348.5337	19.8906	349.1433	40.9031	349.7529	34.1125
348.5464	20.1656	349.156	39.1375	349.7656	35.1437
348.5591	23.6875	349.1687	41.5469	349.7783	35.7437
348.5718	23.9	349.1814	38.2375	349.791	35.0531
348.5845	23.4	349.1941	34.4281	349.8037	38.0594
348.5972	25.8563	349.2068	29.4469	349.8164	36.8188
348.6099	23.4156	349.2195	36.1125	349.8291	35.7438
348.6226	29.3594	349.2322	27.7281	349.8418	41.2375
348.6353	28.5125	349.2449	32.5094	349.8545	33.2625
348.648	25.9969	349.2576	30.8844	349.8672	31.7
348.6607	24.2969	349.2703	33.1781	349.8799	30.0063
348.6734	23.6937	349.283	31.7125	349.8926	32.5406
348.6861	31.6969	349.2957	33.4969	349.9053	36.0125
348.6988	28.7969	349.3084	35.2438	349.918	36.0156
348.7115	30.9	349.3211	29.8187	349.9307	33.55
348.7242	29.5281	349.3338	34.7469	349.9434	31.9969
348.7369	31.0063	349.3465	39.7594	349.9561	32.8906
348.7496	27.0562	349.3592	34.0406	349.9688	32.6562
348.7623	28.925	349.3719	38.3281	349.9815	33.1625
348.775	28.5781	349.3846	43.0938	349.9942	32.6656
348.7877	30.7812	349.3973	41.3906	350.0069	29.2031
348.8004	33.0437	349.41	44.0094	350.0196	28.1344
348.8131	30.6156	349.4227	41.6531	350.0323	30.6781
348.8258	27.5594	349.4354	44.5219	350.045	30.0781
348.8385	30.7	349.4481	43.8812	350.0577	28.5781
348.8512	27.0844	349.4608	43.8187	350.0704	27.2094
348.8639	26.7031	349.4735	40.9625	350.0831	28.8156
348.8766	26.6656	349.4862	40.75	350.0958	27.7344
348.8893	24.1812	349.4989	38.6531	350.1085	28.8
348.902	27.4938	349.5116	36.25	350.1212	29.3563
348.9147	24.3406	349.5243	40.8688	350.1339	30.6594

350.1466	30.4719	350.7562	28.9656	351.3658	25.9469
350.1593	34.8156	350.7689	26.2844	351.3785	23.25
350.172	36.4656	350.7816	23.9594	351.3912	23.7906
350.1847	38.6063	350.7943	22.9688	351.4039	24.0312
350.1974	39.9219	350.807	22.5469	351.4166	22.8937
350.2101	33.825	350.8197	21.6312	351.4293	22.2031
350.2228	34.6188	350.8324	20.775	351.442	21.9313
350.2355	36.7125	350.8451	21.6094	351.4547	23.225
350.2482	33.9375	350.8578	23.5687	351.4674	21.1094
350.2609	39.7969	350.8705	24.375	351.4801	25.3
350.2736	43.45	350.8832	27.5469	351.4928	20.3375
350.2863	40.4906	350.8959	30.0406	351.5055	21.4656
350.299	39.5438	350.9086	30.3062	351.5182	20.325
350.3117	41.1313	350.9213	30.0312	351.5309	19.6531
350.3244	42.8281	350.934	28.5312	351.5436	20.95
350.3371	43.8438	350.9467	30.5344	351.5563	20.5563
350.3498	44.975	350.9594	29.4375	351.569	23.5312
350.3625	45.1375	350.9721	30.5406	351.5817	21.6562
350.3752	43.4563	350.9848	30.3344	351.5944	20.9625
350.3879	39.425	350.9975	30.6063	351.6071	21.3813
350.4006	41.2719	351.0102	31.0719	351.6198	22.5625
350.4133	45.0969	351.0229	31.5594	351.6325	24.9375
350.426	45.6813	351.0356	32.4188	351.6452	25.3031
350.4387	48.9094	351.0483	32.6	351.6579	25.5063
350.4514	48.9187	351.061	31.3406	351.6706	23.0062
350.4641	50.1375	351.0737	32.2313	351.6833	23.4625
350.4768	48.6844	351.0864	29.1375	351.696	19.5344
350.4895	47.9844	351.0991	27.3156	351.7087	19.1688
350.5022	45.8313	351.1118	27.9469	351.7214	23.0656
350.5149	44.5625	351.1245	28.9031	351.7341	19.7125
350.5276	43.0094	351.1372	24.625	351.7468	19.3375
350.5403	42.8938	351.1499	24.8531	351.7595	20.4031
350.553	38.2094	351.1626	25.2969	351.7722	18.1
350.5657	37.2906	351.1753	22.2219	351.7849	20.9438
350.5784	35.3281	351.188	20.0125	351.7976	18.9
350.5911	35.9781	351.2007	22.4906	351.8103	21.5344
350.6038	35.7469	351.2134	17.3125	351.823	18.5219
350.6165	36.0687	351.2261	16.4	351.8357	21.0969
350.6292	36.4938	351.2388	18.9781	351.8484	23.2875
350.6419	35.4969	351.2515	19.6594	351.8611	23.4844
350.6546	35.4094	351.2642	18.7062	351.8738	21.2344
350.6673	35.05	351.2769	20.6344	351.8865	19.8156
350.68	34.4125	351.2896	21.4125	351.8992	21.1375
350.6927	32.9688	351.3023	23.4188	351.9119	18.0812
350.7054	33.0156	351.315	26.7031	351.9246	20.0969
350.7181	33.7062	351.3277	23.6406	351.9373	18.7781
350.7308	31.3469	351.3404	22.9313	351.95	24.3031
350.7435	29.5219	351.3531	24.1156	351.9627	19.075

351.9754	18.2844	352.585	32.9281	353.1946	31.8781
351.9881	16.1094	352.5977	34.425	353.2073	33.4188
352.0008	17.6562	352.6104	36.5	353.22	34.7875
352.0135	23.9688	352.6231	36.2594	353.2327	31.3406
352.0262	25.3906	352.6358	33.8188	353.2454	34.8063
352.0389	25.0094	352.6485	32.5406	353.2581	34.2031
352.0516	25.9562	352.6612	33.175	353.2708	37.2875
352.0643	32.7031	352.6739	30.4125	353.2835	39.0688
352.077	32.75	352.6866	33.675	353.2962	42.0812
352.0897	18.0969	352.6993	29.0687	353.3089	42.3031
352.1024	5	352.712	26.4844	353.3216	40.7281
352.1151	3.1844	352.7247	26.625	353.3343	41.55
352.1278	5.3438	352.7374	27.0688	353.347	48.0656
352.1405	9.2094	352.7501	26.8594	353.3597	50.9406
352.1532	10.6812	352.7628	29.5344	353.3724	49.325
352.1659	14.3	352.7755	24.35	353.3851	48.4188
352.1786	18.5531	352.7882	26.8219	353.3978	52.2906
352.1913	18.9688	352.8009	27.1	353.4105	54.725
352.204	24.8781	352.8136	26.4781	353.4232	53.7156
352.2167	30.6688	352.8263	23.9094	353.4359	52.6438
352.2294	35.8875	352.839	25.3719	353.4486	51.9656
352.2421	36.9031	352.8517	24.3656	353.4613	51.1813
352.2548	32.0031	352.8644	24.4031	353.474	51.3406
352.2675	37.025	352.8771	22.7313	353.4867	51.3313
352.2802	40.1969	352.8898	22.675	353.4994	51.3063
352.2929	40.0344	352.9025	22.4531	353.5121	52.6156
352.3056	41.8531	352.9152	28.6031	353.5248	48.1375
352.3183	42.4906	352.9279	29.3312	353.5375	44.6906
352.331	43.1219	352.9406	33.1875	353.5502	44.1562
352.3437	43.3219	352.9533	29.4188	353.5629	44.9187
352.3564	41.1156	352.966	30.0969	353.5756	44.5812
352.3691	40.9469	352.9787	28.1281	353.5883	44.275
352.3818	38.9531	352.9914	23.7844	353.601	46.8188
352.3945	39.1312	353.0041	26.7906	353.6137	45.7781
352.4072	37.3906	353.0168	27.7656	353.6264	43.9219
352.4199	42.3969	353.0295	28.3031	353.6391	45.5969
352.4326	43.2125	353.0422	27.025	353.6518	44.1531
352.4453	39.6406	353.0549	28.5562	353.6645	42.4375
352.458	35.5406	353.0676	26.0031	353.6772	43.9094
352.4707	34.8438	353.0803	28.65	353.6899	43.4656
352.4834	35.4469	353.093	27.0719	353.7026	45.9094
352.4961	36.7563	353.1057	29.9469	353.7153	48.7344
352.5088	35.6813	353.1184	35.2219	353.728	49.9719
352.5215	34.3812	353.1311	33.7125	353.7407	48.1719
352.5342	31.5406	353.1438	29.5781	353.7534	46.6437
352.5469	33.0469	353.1565	28.1312	353.7661	39.4094
352.5596	34.7375	353.1692	28.1219	353.7788	37.2594
352.5723	30.4438	353.1819	30.6844	353.7915	33.6062

353.8042	24.6594	354.4138	44.7281	355.0234	32.3063
353.8169	23.9781	354.4265	44.0687	355.0361	29.3094
353.8296	20.7594	354.4392	43.225	355.0488	27.7531
353.8423	21.6375	354.4519	43.7625	355.0615	30.975
353.855	28.3875	354.4646	41.5156	355.0742	33.7656
353.8677	31.6813	354.4773	38.7906	355.0869	31.8969
353.8804	26.2469	354.49	38.2938	355.0996	34.3094
353.8931	23.7594	354.5027	37.1938	355.1123	39.1688
353.9058	20.0531	354.5154	39.125	355.125	36.9188
353.9185	20.9625	354.5281	39.4781	355.1377	40.6344
353.9312	20.1625	354.5408	39.2781	355.1504	38.6187
353.9439	18.5594	354.5535	37.1031	355.1631	37.5062
353.9566	22.6906	354.5662	39.175	355.1758	41.3094
353.9693	21.4344	354.5789	37.8656	355.1885	41.2781
353.982	16.3281	354.5916	38.2125	355.2012	41.7188
353.9947	16.7313	354.6043	38.6031	355.2139	38.85
354.0074	17.7625	354.617	38.5	355.2266	40.5719
354.0201	18.7406	354.6297	39.1219	355.2393	38.925
354.0328	16.0594	354.6424	38.9344	355.252	37
354.0455	16.2156	354.6551	40.3438	355.2647	34.95
354.0582	19.0594	354.6678	39.7469	355.2774	31.3875
354.0709	21.4594	354.6805	38.6531	355.2901	33.8219
354.0836	21.7906	354.6932	39.7219	355.3028	26.4062
354.0963	21.4969	354.7059	37.3875	355.3155	28.0031
354.109	22.7625	354.7186	35.7656	355.3282	23.1344
354.1217	26.3125	354.7313	36.4813	355.3409	19.9688
354.1344	23.05	354.744	31.4156	355.3536	25.0375
354.1471	22.8094	354.7567	30.0469	355.3663	23.2125
354.1598	24.3375	354.7694	29.6281	355.379	23.1594
354.1725	28.0531	354.7821	29.6594	355.3917	18.2125
354.1852	28.9438	354.7948	27.2156	355.4044	16.675
354.1979	29.1281	354.8075	27.3969	355.4171	13.7938
354.2106	29.3062	354.8202	32.3281	355.4298	14.1313
354.2233	33.1031	354.8329	35.6469	355.4425	10.6406
354.236	37.025	354.8456	35.1219	355.4552	10.9
354.2487	36.5969	354.8583	31.0469	355.4679	10.4344
354.2614	38.0938	354.871	33.5781	355.4806	10.625
354.2741	34	354.8837	35.3719	355.4933	8.0625
354.2868	33.5781	354.8964	33.3187	355.506	5.5531
354.2995	36.3969	354.9091	29.3188	355.5187	8.4594
354.3122	36.6906	354.9218	27.5187	355.5314	8.8094
354.3249	35.5125	354.9345	28.6844	355.5441	17.6531
354.3376	38.925	354.9472	30.4594	355.5568	26.1844
354.3503	42.2937	354.9599	25.3844	355.5695	28.0156
354.363	44.5125	354.9726	27.8937	355.5822	16.6688
354.3757	48.2437	354.9853	31.2313	355.5949	18.0562
354.3884	48.3125	354.998	35.475	355.6076	19.5969
354.4011	47.075	355.0107	32.5	355.6203	21.75

355.633	28.4969	356.2426	41.2156	356.8522	17.9906
355.6457	28.7656	356.2553	44.875	356.8649	16.9812
355.6584	23.1906	356.268	47.5375	356.8776	21.3062
355.6711	27.7719	356.2807	44.1313	356.8903	17.8094
355.6838	23.3938	356.2934	44.2219	356.903	14.0531
355.6965	27.3687	356.3061	47.8969	356.9157	16.5656
355.7092	30.4812	356.3188	44.6344	356.9284	19.0719
355.7219	23.3844	356.3315	40.6906	356.9411	16.5312
355.7346	22.8375	356.3442	35.2031	356.9538	19.5719
355.7473	24.6438	356.3569	32.1344	356.9665	21.9531
355.76	21.7094	356.3696	31.9969	356.9792	18.8219
355.7727	19.1	356.3823	35.0844	356.9919	16.8594
355.7854	20.6156	356.395	33.5219	357.0046	14.4719
355.7981	20.5063	356.4077	29.6625	357.0173	13.1344
355.8108	21.8563	356.4204	28.7469	357.03	18.7563
355.8235	22.2313	356.4331	37.2687	357.0427	17.2687
355.8362	28.4938	356.4458	38.2188	357.0554	21.2875
355.8489	30.9938	356.4585	37.3344	357.0681	19.8563
355.8616	28.6344	356.4712	34.45	357.0808	19.7344
355.8743	30.1656	356.4839	31.3406	357.0935	21.4875
355.887	29.8844	356.4966	28.9	357.1062	20.1437
355.8997	32.0656	356.5093	28.5781	357.1189	20.3406
355.9124	38.4281	356.522	26.6656	357.1316	25.75
355.9251	39.5938	356.5347	26.6219	357.1443	22.9031
355.9378	42.8031	356.5474	27.6969	357.157	24.3125
355.9505	46.2125	356.5601	24.1156	357.1697	27.9844
355.9632	49.1688	356.5728	19.5781	357.1824	28.45
355.9759	48.1594	356.5855	21.9906	357.1951	30.8563
355.9886	49.4	356.5982	25.0438	357.2078	32.3875
356.0013	49.6469	356.6109	19.75	357.2205	31.5906
356.014	50.4344	356.6236	25.8031	357.2332	29.7563
356.0267	48.775	356.6363	28.9031	357.2459	28.8875
356.0394	48.9531	356.649	20.9469	357.2586	27.7469
356.0521	49.3531	356.6617	16.4344	357.2713	30.4906
356.0648	48.3031	356.6744	18.275	357.284	29.9281
356.0775	48.0187	356.6871	18.7844	357.2967	30.3406
356.0902	45.5719	356.6998	23.9438	357.3094	30.5594
356.1029	48.35	356.7125	25.6437	357.3221	34.4281
356.1156	48.7938	356.7252	22.1281	357.3348	40.4313
356.1283	44.6625	356.7379	17.7906	357.3475	39.575
356.141	41.4313	356.7506	19.3312	357.3602	32.0812
356.1537	38.1813	356.7633	25.8469	357.3729	28.2937
356.1664	36.1344	356.776	23.875	357.3856	42.0469
356.1791	39.2125	356.7887	23.5656	357.3983	41.6469
356.1918	36.275	356.8014	21.0906	357.411	42.2125
356.2045	39.2438	356.8141	19.0563	357.4237	42.3781
356.2172	40.1937	356.8268	20.1812	357.4364	39.0719
356.2299	40.1844	356.8395	19.3625	357.4491	40.0156

357.4618	41.3438	358.0714	30.825	358.681	45.3188
357.4745	37.6625	358.0841	31.5125	358.6937	42.7719
357.4872	37.6594	358.0968	31.65	358.7064	46.9469
357.4999	38.1219	358.1095	31.4656	358.7191	46.125
357.5126	36.9469	358.1222	31.5406	358.7318	40.4781
357.5253	34.7906	358.1349	30.1281	358.7445	41.0406
357.538	33.9875	358.1476	27.3781	358.7572	40.8719
357.5507	32.5312	358.1603	28.7563	358.7699	40.0531
357.5634	32.8406	358.173	29.7375	358.7826	39.9625
357.5761	31.4094	358.1857	25.2875	358.7953	34.7031
357.5888	32.5	358.1984	20.4094	358.808	36.3156
357.6015	35.625	358.2111	17.0438	358.8207	35.5188
357.6142	32.8969	358.2238	16.3531	358.8334	34.2844
357.6269	30.0969	358.2365	20.5687	358.8461	40.4219
357.6396	29.8375	358.2492	23.8625	358.8588	42.0031
357.6523	32.3688	358.2619	21.4188	358.8715	38.6562
357.665	32.0344	358.2746	15.525	358.8842	29.6719
357.6777	27.65	358.2873	17.7062	358.8969	23.1219
357.6904	26.4	358.3	18.2156	358.9096	24.7938
357.7031	27.0844	358.3127	16.7688	358.9223	25.825
357.7158	33.3656	358.3254	19.4219	358.935	28.1719
357.7285	30.1781	358.3381	18.3062	358.9477	26.9469
357.7412	31.4281	358.3508	17.45	358.9604	31.8938
357.7539	30.1063	358.3635	16.1375	358.9731	23.9094
357.7666	29.9281	358.3762	17.6938	358.9858	30.3125
357.7793	38.7094	358.3889	17.2656	358.9985	34.5719
357.792	36.9875	358.4016	20.3156	359.0112	37.2875
357.8047	32.2062	358.4143	19.6281	359.0239	39.0656
357.8174	33.9219	358.427	17.2219	359.0366	41.2938
357.8301	35.2937	358.4397	16.2281	359.0493	43.6062
357.8428	40.2156	358.4524	20.3344	359.062	39.55
357.8555	38.2406	358.4651	19.7594	359.0747	30.6625
357.8682	37.1687	358.4778	27.2781	359.0874	23.3063
357.8809	41.7906	358.4905	27.4594	359.1001	26.1125
357.8936	38.1656	358.5032	24.125	359.1128	27.35
357.9063	37.7594	358.5159	24.1688	359.1255	22.5062
357.919	36.075	358.5286	26.4844	359.1382	24.0844
357.9317	38.8	358.5413	28.9	359.1509	31.5406
357.9444	42.2812	358.554	28.0719	359.1636	31.4531
357.9571	43.1562	358.5667	31.6531	359.1763	27.3531
357.9698	41.8875	358.5794	28.6406	359.189	30.3625
357.9825	45.6719	358.5921	33.925	359.2017	21.3406
357.9952	45.125	358.6048	33.7281	359.2144	18.0875
358.0079	42.325	358.6175	39.2656	359.2271	15.4344
358.0206	41.9406	358.6302	38.8875	359.2398	16.6313
358.0333	38.8969	358.6429	39.5063	359.2525	16.1781
358.046	42.2875	358.6556	39.9906	359.2652	17.8281
358.0587	39.05	358.6683	43.2625	359.2779	19.0281

359.2906	15.3063	359.9002	30.0094	360.5098	14.1063
359.3033	19.1406	359.9129	34.4344	360.5225	11.3938
359.316	21.7031	359.9256	30.5719	360.5352	12.7875
359.3287	22.5406	359.9383	34.1969	360.5479	14.0688
359.3414	29.05	359.951	32.7594	360.5606	12.6938
359.3541	36.7094	359.9637	44.1281	360.5733	15.4812
359.3668	38.2625	359.9764	45.7938	360.586	16.0969
359.3795	36.775	359.9891	41.0969	360.5987	10.9625
359.3922	40.35	360.0018	43.1281	360.6114	14.9969
359.4049	41.0781	360.0145	45.1375	360.6241	12.2281
359.4176	44.4844	360.0272	43.3438	360.6368	13.2656
359.4303	44.0094	360.0399	41.6875	360.6495	15.0813
359.443	45.1813	360.0526	40.6438	360.6622	15.1969
359.4557	45.2344	360.0653	38.9344	360.6749	16.1844
359.4684	44.5188	360.078	41.2969	360.6876	16.0312
359.4811	45.4563	360.0907	40.9156	360.7003	22.5969
359.4938	43.4094	360.1034	41.1156	360.713	22.4469
359.5065	39.8281	360.1161	42.6656	360.7257	25.1312
359.5192	40.5875	360.1288	44.4	360.7384	22.4594
359.5319	34.4688	360.1415	43.1719	360.7511	23.9844
359.5446	37.7375	360.1542	42.6188	360.7638	25.7719
359.5573	39.35	360.1669	45.4062	360.7765	20.9344
359.57	39.9469	360.1796	45.275	360.7892	16.8219
359.5827	37.4844	360.1923	45.2406	360.8019	16.7875
359.5954	37.4875	360.205	42.4406	360.8146	15.5312
359.6081	36.5781	360.2177	45.0094	360.8273	19.525
359.6208	37.45	360.2304	43.6938	360.84	21.4219
359.6335	39.6688	360.2431	42.0781	360.8527	14.0562
359.6462	40.4031	360.2558	45.0406	360.8654	14.8719
359.6589	41.9688	360.2685	45.125	360.8781	20.4156
359.6716	42.1375	360.2812	44.8375	360.8908	17.75
359.6843	43.9594	360.2939	46.825	360.9035	11.2781
359.697	43.6812	360.3066	47.8781	360.9162	13.4969
359.7097	43.4281	360.3193	46.2188	360.9289	13.3438
359.7224	37.3344	360.332	46.4437	360.9416	18.5156
359.7351	39.0156	360.3447	42.2906	360.9543	17.7969
359.7478	36.9094	360.3574	41.1781	360.967	17.0875
359.7605	27.8875	360.3701	39.9219	360.9797	16.5469
359.7732	24.8406	360.3828	40.5938	360.9924	17.6812
359.7859	25.7375	360.3955	35.0312	361.0051	18.2781
359.7986	26.7875	360.4082	33.1	361.0178	18.1
359.8113	24.9969	360.4209	25.8875	361.0305	18.2625
359.824	23.1219	360.4336	27.2719	361.0432	19.4688
359.8367	23.2625	360.4463	17.5656	361.0559	17.5375
359.8494	28.8594	360.459	17.3406	361.0686	20.9875
359.8621	26.2094	360.4717	16.7969	361.0813	25.5187
359.8748	24.0219	360.4844	20.2437	361.094	27.2531
359.8875	30.125	360.4971	13.675	361.1067	26.2375

361.1194	22.0875	361.729	32.4156	362.3386	35.9406
361.1321	21.0656	361.7417	32.9469	362.3513	39.9562
361.1448	26.0594	361.7544	38.1469	362.364	28.0406
361.1575	30.1375	361.7671	32.1031	362.3767	32.9062
361.1702	30.2906	361.7798	34.6188	362.3894	30.5469
361.1829	29.5375	361.7925	35.6688	362.4021	32.8469
361.1956	28.8469	361.8052	31.2781	362.4148	34.9813
361.2083	29.2	361.8179	34.7312	362.4275	31.9406
361.221	29.2406	361.8306	33.3031	362.4402	35.8313
361.2337	30.5406	361.8433	32.8	362.4529	27.2125
361.2464	30.9437	361.856	30.0438	362.4656	24.8719
361.2591	39.3531	361.8687	27.7219	362.4783	21.4125
361.2718	27.5062	361.8814	30.6	362.491	24.8344
361.2845	25.1562	361.8941	26.875	362.5037	19.6719
361.2972	29.175	361.9068	30.9937	362.5164	24.4688
361.3099	28.9094	361.9195	30.3219	362.5291	22.425
361.3226	36.5812	361.9322	35.8906	362.5418	24.1156
361.3353	38.1687	361.9449	30.0219	362.5545	20.6812
361.348	35.7219	361.9576	34.375	362.5672	18.0469
361.3607	35.9875	361.9703	33.6031	362.5799	17.9031
361.3734	40.5	361.983	32.3375	362.5926	18.8156
361.3861	46.9906	361.9957	34.45	362.6053	17.3313
361.3988	46.4437	362.0084	26.8438	362.618	14.2
361.4115	44.6688	362.0211	21.2	362.6307	15.7281
361.4242	47.3344	362.0338	22.0312	362.6434	20.4313
361.4369	51.9844	362.0465	27.8937	362.6561	20.2594
361.4496	51.0219	362.0592	31.3219	362.6688	26.3594
361.4623	51.9219	362.0719	37.1781	362.6815	26.2406
361.475	52.6438	362.0846	32.4	362.6942	27.7094
361.4877	52.5219	362.0973	32.3781	362.7069	27.7625
361.5004	56.8406	362.11	28.6	362.7196	28.6594
361.5131	57.2906	362.1227	33.7	362.7323	25.5906
361.5258	57.2063	362.1354	37.3469	362.745	22.625
361.5385	55.9688	362.1481	31.1906	362.7577	19.8063
361.5512	53.8375	362.1608	34.1125	362.7704	23.3375
361.5639	54.2906	362.1735	34.6312	362.7831	24.0094
361.5766	52.4781	362.1862	26.6938	362.7958	31
361.5893	54.5938	362.1989	18.4656	362.8085	31.9781
361.602	52.7781	362.2116	23.3625	362.8212	36.3969
361.6147	46.1	362.2243	20.2125	362.8339	42.8969
361.6274	43.8094	362.237	16.8938	362.8466	42.0125
361.6401	42.9875	362.2497	19.2969	362.8593	34.7438
361.6528	39.7062	362.2624	23.8281	362.872	36.5063
361.6655	42.825	362.2751	20.7656	362.8847	37.4313
361.6782	39.1906	362.2878	26.1812	362.8974	39.9594
361.6909	38.9281	362.3005	26.7875	362.9101	38.5094
361.7036	37.0687	362.3132	31.9344	362.9228	37.5531
361.7163	38.0438	362.3259	38.9656	362.9355	42.2687

362.9482	44.6531	363.5578	30.8031	364.1674	48.3781
362.9609	37.8906	363.5705	30.9719	364.1801	45.9656
362.9736	35.8219	363.5832	29.8063	364.1928	43.4375
362.9863	35.0563	363.5959	25.1625	364.2055	41.4531
362.999	35.075	363.6086	27.7219	364.2182	39.5031
363.0117	35.6531	363.6213	30.4875	364.2309	38.2844
363.0244	37.2063	363.634	28.1	364.2436	35.9094
363.0371	38.875	363.6467	26.4625	364.2563	36.3031
363.0498	29.8031	363.6594	32.5656	364.269	36.9813
363.0625	29.6094	363.6721	31.525	364.2817	31.875
363.0752	32.1719	363.6848	30.4156	364.2944	28.8563
363.0879	32.4219	363.6975	29.475	364.3071	28.6281
363.1006	29.6906	363.7102	34.4719	364.3198	30.7969
363.1133	34.3781	363.7229	38.3312	364.3325	26.9344
363.126	25.3563	363.7356	39.9062	364.3452	25.325
363.1387	28.7562	363.7483	35.4938	364.3579	22.3094
363.1514	27.0344	363.761	38.7594	364.3706	25.0781
363.1641	25.7156	363.7737	38.9031	364.3833	29.4688
363.1768	27.5562	363.7864	40.0594	364.396	26.4031
363.1895	28.8375	363.7991	38.9344	364.4087	25.45
363.2022	29.8719	363.8118	34.8906	364.4214	26.4813
363.2149	29.7437	363.8245	36.2094	364.4341	27.3375
363.2276	21.1156	363.8372	36.1719	364.4468	26.45
363.2403	21.9375	363.8499	36.6281	364.4595	27.7844
363.253	22.375	363.8626	38.8906	364.4722	27.4
363.2657	24.6031	363.8753	36.3906	364.4849	27.7313
363.2784	24.7	363.888	34.7062	364.4976	26.4969
363.2911	23.5563	363.9007	36.2375	364.5103	24.0281
363.3038	23.0531	363.9134	38.3563	364.523	23.925
363.3165	21.9125	363.9261	35.7625	364.5357	25.575
363.3292	25.0562	363.9388	33.6344	364.5484	31.4281
363.3419	22.9156	363.9515	33.2719	364.5611	35.4219
363.3546	21.6875	363.9642	38.4563	364.5738	28.6656
363.3673	15.4812	363.9769	37.5594	364.5865	29.9031
363.38	15.9375	363.9896	34.2656	364.5992	29.4125
363.3927	16.9625	364.0023	34.9531	364.6119	27.8188
363.4054	21.4656	364.015	40.0312	364.6246	29.5719
363.4181	20.7812	364.0277	44.9406	364.6373	25.7094
363.4308	20.5	364.0404	47.0281	364.65	26.7437
363.4435	22.6125	364.0531	45.4594	364.6627	28.0469
363.4562	26.4281	364.0658	45.1219	364.6754	27.8875
363.4689	30.5156	364.0785	45.2	364.6881	23.7031
363.4816	34.7063	364.0912	44.7094	364.7008	17.9375
363.4943	31.2094	364.1039	41.1375	364.7135	19.0156
363.507	27.875	364.1166	39.8719	364.7262	23.4469
363.5197	33.0375	364.1293	45.3969	364.7389	23.5781
363.5324	33.6687	364.142	47.6844	364.7516	22.4156
363.5451	34.2781	364.1547	50.4	364.7643	17.4813

364.777	15.125	365.3866	46.2	365.9962	32.9844
364.7897	12.7656	365.3993	49.1594	366.0089	32.5438
364.8024	13.7625	365.412	47.7969	366.0216	31.0844
364.8151	11.3656	365.4247	46.2687	366.0343	28.3969
364.8278	11.0031	365.4374	45.5656	366.047	34.0469
364.8405	13.8125	365.4501	47.5969	366.0597	33.0844
364.8532	15.6156	365.4628	49.1281	366.0724	30.2625
364.8659	14.425	365.4755	51.0812	366.0851	34.3031
364.8786	14.8281	365.4882	53.0094	366.0978	33.7281
364.8913	16.0656	365.5009	52.4	366.1105	30.5719
364.904	20.7344	365.5136	53.9156	366.1232	35.775
364.9167	24.5094	365.5263	54.4781	366.1359	34.2719
364.9294	26.6688	365.539	55.6156	366.1486	33.9469
364.9421	27.8563	365.5517	55.1938	366.1613	37.025
364.9548	30.2531	365.5644	57.3531	366.174	34.2375
364.9675	30.7094	365.5771	56.5469	366.1867	35.8844
364.9802	32.3844	365.5898	55.5437	366.1994	33.7344
364.9929	31.5187	365.6025	55.8187	366.2121	33.9562
365.0056	30.7094	365.6152	51.1438	366.2248	34.7438
365.0183	35.1094	365.6279	48.9812	366.2375	33.4688
365.031	31.9625	365.6406	47.2437	366.2502	31.6125
365.0437	30.3375	365.6533	46.0125	366.2629	29.0281
365.0564	30.9156	365.666	42.9562	366.2756	31.9312
365.0691	36.8625	365.6787	39.2969	366.2883	33.1281
365.0818	36.4781	365.6914	36.2875	366.301	28.6875
365.0945	40.0844	365.7041	32.8719	366.3137	32.6281
365.1072	34.6031	365.7168	34.4719	366.3264	34.525
365.1199	33.5281	365.7295	34.775	366.3391	29.7375
365.1326	34.6406	365.7422	33.4156	366.3518	30.4594
365.1453	34.5938	365.7549	31.5125	366.3645	28.475
365.158	35.0375	365.7676	30.1781	366.3772	30.2469
365.1707	37.1688	365.7803	29.0906	366.3899	22.15
365.1834	36.3781	365.793	28.7	366.4026	23.2906
365.1961	39.6906	365.8057	29.2938	366.4153	25.2219
365.2088	39.0063	365.8184	33.8688	366.428	25.1875
365.2215	39.6562	365.8311	28.925	366.4407	22.975
365.2342	42.7125	365.8438	31.0344	366.4534	23.7781
365.2469	41.7687	365.8565	26.0125	366.4661	23.1281
365.2596	43.9875	365.8692	30.5875	366.4788	23.7406
365.2723	42.7687	365.8819	30.2	366.4915	18.8594
365.285	42.9625	365.8946	32.7062	366.5042	24.8563
365.2977	37.2625	365.9073	30.4562	366.5169	28.7437
365.3104	34.5	365.92	29.1344	366.5296	24.9688
365.3231	37.7344	365.9327	32.4031	366.5423	29.3719
365.3358	42.6844	365.9454	29.5063	366.555	29.45
365.3485	43.1406	365.9581	30.7938	366.5677	26.6094
365.3612	40.8844	365.9708	30.6187	366.5804	23.5063
365.3739	41.6906	365.9835	29.275	366.5931	24.7906

366.6058	31.8875	367.2154	34.6656	367.825	17.9281
366.6185	30.3969	367.2281	35.3063	367.8377	19.8625
366.6312	28.7437	367.2408	35.5844	367.8504	22.0469
366.6439	28.7063	367.2535	37.5	367.8631	19.375
366.6566	31.9156	367.2662	35.8125	367.8758	17.25
366.6693	30.8906	367.2789	38.7531	367.8885	22.8219
366.682	27.8344	367.2916	39.9219	367.9012	27.3719
366.6947	35.5812	367.3043	37.7531	367.9139	24.55
366.7074	31.1313	367.317	38.2656	367.9266	29.0125
366.7201	34.4062	367.3297	33.2906	367.9393	32.3719
366.7328	31.4531	367.3424	30.5719	367.952	32.8719
366.7455	30.6	367.3551	25.6406	367.9647	37.2469
366.7582	33.2062	367.3678	23.6562	367.9774	28.2969
366.7709	35.3937	367.3805	25.4594	367.9901	26.5469
366.7836	36.3813	367.3932	27.2625	368.0028	28.4344
366.7963	30.0812	367.4059	29.9906	368.0155	23.8281
366.809	23.4625	367.4186	27.6812	368.0282	21.4625
366.8217	19.6313	367.4313	23.4969	368.0409	28.7969
366.8344	23.575	367.444	25.6031	368.0536	28.575
366.8471	21.3531	367.4567	22.8406	368.0663	28.9
366.8598	20.9406	367.4694	27.1781	368.079	29.6187
366.8725	25.9656	367.4821	27.1281	368.0917	30.2219
366.8852	21.8969	367.4948	28.0187	368.1044	26.25
366.8979	24.1625	367.5075	25.0719	368.1171	25.4906
366.9106	30.1687	367.5202	24.25	368.1298	23.8312
366.9233	29.4688	367.5329	18.3844	368.1425	27.8219
366.936	30.6687	367.5456	21.8594	368.1552	29.7125
366.9487	31.65	367.5583	18.9438	368.1679	31.125
366.9614	31.2719	367.571	24.175	368.1806	30.3219
366.9741	33.8187	367.5837	31.9625	368.1933	29.2094
366.9868	33.8219	367.5964	28.0531	368.206	26.1156
366.9995	40.1406	367.6091	29.6281	368.2187	26.3656
367.0122	39.3937	367.6218	26.5906	368.2314	28.4281
367.0249	35.7188	367.6345	27.5	368.2441	37.5625
367.0376	37.5156	367.6472	24.6	368.2568	38.2344
367.0503	35.475	367.6599	23.0188	368.2695	42.6625
367.063	35.5094	367.6726	25.3562	368.2822	45.1094
367.0757	36.3063	367.6853	24.1063	368.2949	45.8094
367.0884	38.225	367.698	23.8406	368.3076	42.8187
367.1011	39.4844	367.7107	25.9094	368.3203	42.7031
367.1138	38.4719	367.7234	29.5406	368.333	43.3062
367.1265	37.3	367.7361	30.4688	368.3457	45.9313
367.1392	39.1438	367.7488	28.3125	368.3584	47.6625
367.1519	37.2687	367.7615	24.9219	368.3711	50.4188
367.1646	34.9313	367.7742	27.0531	368.3838	46.8031
367.1773	35.225	367.7869	25.5781	368.3965	37.1281
367.19	34.6094	367.7996	22.9438	368.4092	42.5781
367.2027	34.7781	367.8123	22.2562	368.4219	42.8

368.4346	37.9406	369.0442	25.3375	369.6538	43.3375
368.4473	36.6656	369.0569	29.375	369.6665	46.5813
368.46	34.9688	369.0696	31.8687	369.6792	46.1906
368.4727	33.4219	369.0823	28.05	369.6919	49.8312
368.4854	29.9406	369.095	25.5969	369.7046	48.6
368.4981	28.3	369.1077	31.3594	369.7173	50.4375
368.5108	25.1	369.1204	28.4688	369.73	49.95
368.5235	27.6031	369.1331	31.4	369.7427	48.7938
368.5362	22.8563	369.1458	29.3625	369.7554	49.1875
368.5489	26.8	369.1585	27.275	369.7681	47.7469
368.5616	28.9125	369.1712	22.9781	369.7808	47.4688
368.5743	33.1719	369.1839	23.2187	369.7935	46.0031
368.587	34.4906	369.1966	21.25	369.8062	45.0875
368.5997	34.2156	369.2093	21.4406	369.8189	41.7469
368.6124	24.6969	369.222	20.1969	369.8316	42.1281
368.6251	21.6313	369.2347	16.7125	369.8443	34.6344
368.6378	17.5406	369.2474	15.9312	369.857	32.2719
368.6505	17.4469	369.2601	17.6031	369.8697	29.1437
368.6632	22.3781	369.2728	11.1531	369.8824	29.6188
368.6759	23.075	369.2855	15.7	369.8951	30.9781
368.6886	28.4937	369.2982	14.7375	369.9078	29.2969
368.7013	27.9781	369.3109	14.7375	369.9205	26.7781
368.714	29.9656	369.3236	14.0906	369.9332	23.2281
368.7267	27.9406	369.3363	15.6094	369.9459	24.275
368.7394	29.1531	369.349	15.4469	369.9586	32.4062
368.7521	30.3656	369.3617	17.7188	369.9713	30.175
368.7648	32.5187	369.3744	18.5531	369.984	34.7781
368.7775	32.85	369.3871	19.1437	369.9967	36.4406
368.7902	35.7469	369.3998	23.7281	370.0094	35.7812
368.8029	33.6281	369.4125	26.9406	370.0221	30.8594
368.8156	36.3281	369.4252	18.6469	370.0348	31.1375
368.8283	42.4781	369.4379	20.2188	370.0475	35.4781
368.841	43.7062	369.4506	25.3062	370.0602	41.4281
368.8537	46.6562	369.4633	24.7844	370.0729	39.8188
368.8664	42.4406	369.476	21.9625	370.0856	33.175
368.8791	38.2344	369.4887	24.3937	370.0983	34.3156
368.8918	38.7094	369.5014	22.6156	370.111	36.3281
368.9045	37.3125	369.5141	23.5062	370.1237	39.5438
368.9172	35.4187	369.5268	24.3125	370.1364	44.2156
368.9299	35.0094	369.5395	23.4188	370.1491	44.4813
368.9426	37.0219	369.5522	26.5688	370.1618	43.8656
368.9553	33.9906	369.5649	26.1594	370.1745	46.4125
368.968	32.2406	369.5776	28.0656	370.1872	49.9312
368.9807	35.5563	369.5903	33.3219	370.1999	49.8906
368.9934	39.1094	369.603	37.3531	370.2126	44.1156
369.0061	32.5875	369.6157	30.9719	370.2253	45.8875
369.0188	26.8281	369.6284	35.4562	370.238	42.5594
369.0315	22.0812	369.6411	38.9875	370.2507	40.75

370.2634	41.575	370.873	27.9688	371.4826	42.325
370.2761	44.3469	370.8857	33.0719	371.4953	40.1531
370.2888	42.2188	370.8984	24.8031	371.508	34.8969
370.3015	37.225	370.9111	21.8125	371.5207	34.2969
370.3142	36.5062	370.9238	22.3531	371.5334	34.9875
370.3269	34.6969	370.9365	22.775	371.5461	33.5719
370.3396	35.0625	370.9492	21.3563	371.5588	35.3469
370.3523	25.9938	370.9619	24.7344	371.5715	39.0687
370.365	30.45	370.9746	30.5844	371.5842	38.4656
370.3777	27.2375	370.9873	33.5594	371.5969	38.2812
370.3904	25.7031	371	31.1156	371.6096	35.9688
370.4031	23.6562	371.0127	28.1844	371.6223	35.4125
370.4158	20.6125	371.0254	31.7719	371.635	34.175
370.4285	19.5531	371.0381	36.3844	371.6477	37.0438
370.4412	20.2656	371.0508	36.3312	371.6604	35.4156
370.4539	22.5469	371.0635	38.5719	371.6731	32.0844
370.4666	19.7031	371.0762	36.3625	371.6858	26.7469
370.4793	24.6969	371.0889	36.575	371.6985	26.4844
370.492	32.6781	371.1016	36.6375	371.7112	26.7031
370.5047	31.2844	371.1143	38.425	371.7239	31.8687
370.5174	25.275	371.127	34.2719	371.7366	35.0281
370.5301	19.175	371.1397	33.7094	371.7493	34.7781
370.5428	21.4438	371.1524	33.2031	371.762	34.0438
370.5555	18.0188	371.1651	35.5219	371.7747	32.2625
370.5682	19.1812	371.1778	40.2062	371.7874	33.4875
370.5809	16.6031	371.1905	43.4688	371.8001	31.9312
370.5936	17.5531	371.2032	44.8937	371.8128	35.0187
370.6063	19.0156	371.2159	37.3187	371.8255	33.6844
370.619	19.3281	371.2286	43.875	371.8382	39.1031
370.6317	19.2844	371.2413	44.7156	371.8509	42.7375
370.6444	18.7062	371.254	47.2062	371.8636	41.2563
370.6571	18.4719	371.2667	49.4469	371.8763	37.6312
370.6698	16.7594	371.2794	50.3687	371.889	28.575
370.6825	20.9844	371.2921	47.0969	371.9017	27.1188
370.6952	21.25	371.3048	49.5406	371.9144	28.6156
370.7079	22.7281	371.3175	48.825	371.9271	30.9719
370.7206	19.5969	371.3302	47.1969	371.9398	30.0531
370.7333	22.375	371.3429	44.6562	371.9525	28.4156
370.746	23.8937	371.3556	44.5844	371.9652	25.6937
370.7587	23.2219	371.3683	47.6313	371.9779	24.5656
370.7714	18.7188	371.381	41.4469	371.9906	26.5688
370.7841	19.4375	371.3937	41.5156	372.0033	25.2813
370.7968	16.6688	371.4064	39.7406	372.016	26.6156
370.8095	16.1531	371.4191	40.1125	372.0287	29.7719
370.8222	17.1125	371.4318	39.8312	372.0414	33.9375
370.8349	22.5281	371.4445	41.5031	372.0541	32.0719
370.8476	26.5344	371.4572	37.9219	372.0668	24.9469
370.8603	26.3125	371.4699	39.6719	372.0795	26.1187

372.0922	27.3312	372.7018	26.7031	373.3114	30.3281
372.1049	28.0969	372.7145	26.6688	373.3241	27.6969
372.1176	30.225	372.7272	31.0531	373.3368	29.3656
372.1303	29.3031	372.7399	32.2375	373.3495	29.3344
372.143	32.1375	372.7526	35.5125	373.3622	31.1094
372.1557	31.5875	372.7653	36.3375	373.3749	30.2562
372.1684	29.4406	372.778	40.2531	373.3876	32.8813
372.1811	31.4781	372.7907	42.0563	373.4003	33.4437
372.1938	30.8937	372.8034	40.9813	373.413	33.325
372.2065	28.8469	372.8161	41.5688	373.4257	36.35
372.2192	25.7437	372.8288	41.0844	373.4384	32.6844
372.2319	24.9313	372.8415	44.6813	373.4511	29.8625
372.2446	19.3344	372.8542	47.0344	373.4638	32.0406
372.2573	19.7469	372.8669	45.6719	373.4765	32.7375
372.27	21.8094	372.8796	42.7344	373.4892	37.6062
372.2827	21.5312	372.8923	42.1937	373.5019	40.3594
372.2954	17.1844	372.905	40.3937	373.5146	39.4125
372.3081	17.7375	372.9177	39.9406	373.5273	42.7375
372.3208	22.7281	372.9304	39.8156	373.54	44.8656
372.3335	21.9438	372.9431	42.8469	373.5527	44.7
372.3462	15.5375	372.9558	46.8187	373.5654	46.6937
372.3589	15.075	372.9685	45.2406	373.5781	43.425
372.3716	16.3813	372.9812	45.2188	373.5908	41.8219
372.3843	16.7469	372.9939	46.1562	373.6035	42.8781
372.397	16.6156	373.0066	43.8719	373.6162	42.6219
372.4097	18.3438	373.0193	47.35	373.6289	42.7719
372.4224	17.2563	373.032	48.3188	373.6416	42.9187
372.4351	16.5	373.0447	47.5781	373.6543	41.4344
372.4478	17.425	373.0574	47.0094	373.667	43.3844
372.4605	17.1844	373.0701	39.6531	373.6797	43.45
372.4732	20.4875	373.0828	41.1406	373.6924	45.175
372.4859	18.8094	373.0955	36.6781	373.7051	46.4281
372.4986	17.8188	373.1082	36.9969	373.7178	45.9531
372.5113	15.2625	373.1209	36.075	373.7305	47.1812
372.524	18.1406	373.1336	35.2656	373.7432	45.7188
372.5367	19.4438	373.1463	37.1594	373.7559	45.7687
372.5494	19.6969	373.159	35.8344	373.7686	45.075
372.5621	18.6031	373.1717	33.3406	373.7813	45.5875
372.5748	19.3656	373.1844	34.875	373.794	48.1719
372.5875	21.2188	373.1971	33.4156	373.8067	47.1781
372.6002	21.4812	373.2098	32.5438	373.8194	44.5781
372.6129	20.1406	373.2225	31.9656	373.8321	43.4062
372.6256	18.55	373.2352	31.2969	373.8448	43.2875
372.6383	27.1	373.2479	31.4219	373.8575	40.4312
372.651	28.5906	373.2606	32.225	373.8702	37.1656
372.6637	27.9719	373.2733	31.525	373.8829	37.75
372.6764	29.675	373.286	31.7906	373.8956	37.6094
372.6891	28.475	373.2987	30.8406	373.9083	39.6781

373.921	37.4906	374.5306	20.0687	375.1402	43.5594
373.9337	39.525	374.5433	20.5844	375.1529	42.9844
373.9464	35.7688	374.556	21.7094	375.1656	40.9375
373.9591	36.1344	374.5687	19.8156	375.1783	43.0594
373.9718	36.2781	374.5814	21.7375	375.191	47.8906
373.9845	34.9938	374.5941	25.5625	375.2037	48.7562
373.9972	33.0438	374.6068	25.6125	375.2164	43.8156
374.0099	29.025	374.6195	24.0562	375.2291	44.8719
374.0226	30.8406	374.6322	21.9031	375.2418	40.1469
374.0353	29.1406	374.6449	23.5125	375.2545	37.1719
374.048	28.975	374.6576	21.975	375.2672	36.775
374.0607	29.3312	374.6703	24.1	375.2799	32.1625
374.0734	29.4625	374.683	26.2	375.2926	32.3844
374.0861	29.7937	374.6957	31.2406	375.3053	29.3188
374.0988	28.8812	374.7084	32.9469	375.318	25.1562
374.1115	32.7375	374.7211	31.7812	375.3307	26.1781
374.1242	34.35	374.7338	34.7469	375.3434	22.7438
374.1369	29.4938	374.7465	37.7969	375.3561	23.8375
374.1496	34.0625	374.7592	39.3312	375.3688	22.95
374.1623	33.1781	374.7719	34.9062	375.3815	24.1625
374.175	32.7094	374.7846	35.7625	375.3942	22.2938
374.1877	33.5125	374.7973	40.0844	375.4069	20.9406
374.2004	34.4062	374.81	40.1406	375.4196	16.7281
374.2131	34.0125	374.8227	41.3687	375.4323	15.3875
374.2258	33.8719	374.8354	43.2531	375.445	12.675
374.2385	29.7812	374.8481	42.3531	375.4577	12.5656
374.2512	25.3156	374.8608	37.9313	375.4704	14.5437
374.2639	30.4937	374.8735	37.1437	375.4831	13.1375
374.2766	29.4969	374.8862	35.8875	375.4958	15.1969
374.2893	29.7938	374.8989	36.1125	375.5085	18.0219
374.302	32.4	374.9116	35.5781	375.5212	19.3969
374.3147	30.2969	374.9243	39.3844	375.5339	18.3156
374.3274	23.1156	374.937	42.1844	375.5466	23.1594
374.3401	24.7719	374.9497	42.3063	375.5593	18.1969
374.3528	21.8875	374.9624	39.1156	375.572	19.1906
374.3655	23.3594	374.9751	39.1063	375.5847	19.5375
374.3782	25.125	374.9878	39.6188	375.5974	19.0531
374.3909	27.5687	375.0005	39.7594	375.6101	21.8281
374.4036	23.7656	375.0132	43.8156	375.6228	19.3531
374.4163	27.7125	375.0259	41.2375	375.6355	20.0844
374.429	30.4906	375.0386	36.7	375.6482	21.6938
374.4417	26.8781	375.0513	41.2812	375.6609	21.4812
374.4544	21.5469	375.064	41.1375	375.6736	18.7188
374.4671	20.7906	375.0767	40.5125	375.6863	21.7969
374.4798	21.2875	375.0894	41.7844	375.699	23.8781
374.4925	22.4	375.1021	46.5156	375.7117	21.9
374.5052	24.2875	375.1148	45.5031	375.7244	18.9406
374.5179	22.6594	375.1275	40.7594	375.7371	21.225

375.7498	20.1906	376.3594	47.4469	376.969	30.6687
375.7625	22.7594	376.3721	43	376.9817	27.6219
375.7752	21.4375	376.3848	40.6094	376.9944	25.3937
375.7879	25.6562	376.3975	37.0438	377.0071	24.1719
375.8006	15.7875	376.4102	41.7219	377.0198	22.0687
375.8133	22.0344	376.4229	45.6312	377.0325	21.9
375.826	28.3219	376.4356	44.5594	377.0452	24.0219
375.8387	21.0469	376.4483	44.3	377.0579	23.7625
375.8514	18.7	376.461	40.5469	377.0706	21.1125
375.8641	22.1313	376.4737	37.0594	377.0833	12.9656
375.8768	26.2156	376.4864	40.1719	377.096	14.4187
375.8895	27.6906	376.4991	38.05	377.1087	17.5969
375.9022	22.9594	376.5118	37.2625	377.1214	13.2781
375.9149	21.5969	376.5245	36.8719	377.1341	11.7531
375.9276	24.6469	376.5372	40.1063	377.1468	9.8313
375.9403	25.2969	376.5499	37.2156	377.1595	10.4594
375.953	21.0469	376.5626	39.8312	377.1722	12.275
375.9657	25.9594	376.5753	35	377.1849	11.3719
375.9784	27.0531	376.588	36.8313	377.1976	9.9969
375.9911	29.7625	376.6007	35.4062	377.2103	10.1469
376.0038	32.7406	376.6134	39.8344	377.223	13.0688
376.0165	32.3031	376.6261	42.85	377.2357	13.8969
376.0292	26.2625	376.6388	41.4969	377.2484	14.3719
376.0419	22.5875	376.6515	37.1781	377.2611	16.2219
376.0546	25.6	376.6642	36.9062	377.2738	19.9344
376.0673	28.0156	376.6769	39.1437	377.2865	20.0438
376.08	31.4	376.6896	32.3937	377.2992	20.8938
376.0927	30.7219	376.7023	32.3469	377.3119	17.225
376.1054	32.775	376.715	35.825	377.3246	15.0594
376.1181	37.9219	376.7277	32.95	377.3373	17.9375
376.1308	34.9906	376.7404	34.9062	377.35	24.4469
376.1435	35.6406	376.7531	32.825	377.3627	20.3031
376.1562	37.1875	376.7658	34.8594	377.3754	17.5344
376.1689	36.5219	376.7785	32.5594	377.3881	22.0906
376.1816	42.9969	376.7912	33.0875	377.4008	18.2375
376.1943	41.5938	376.8039	30.475	377.4135	19.0781
376.207	42.1844	376.8166	29.8844	377.4262	17.8625
376.2197	38.4406	376.8293	34.8344	377.4389	22.6375
376.2324	42.8656	376.842	31.9281	377.4516	24.0469
376.2451	44.5781	376.8547	30.9125	377.4643	21.9406
376.2578	46.8688	376.8674	28.4781	377.477	19.5625
376.2705	47.3312	376.8801	30.8	377.4897	21.425
376.2832	43.4813	376.8928	32.0562	377.5024	19.85
376.2959	43.1531	376.9055	28.1531	377.5151	19.825
376.3086	42.3	376.9182	26.3531	377.5278	19.2344
376.3213	41.275	376.9309	23.8688	377.5405	20.6406
376.334	45.8687	376.9436	30.8156	377.5532	22.1156
376.3467	43.7344	376.9563	30.0094	377.5659	20.3375

377.5786	22.8781	378.1882	42.5062	378.7978	42.475
377.5913	23.9281	378.2009	45.4062	378.8105	39.4469
377.604	21.9656	378.2136	43.1594	378.8232	37.225
377.6167	21.8688	378.2263	41.425	378.8359	39.4313
377.6294	20.9875	378.239	40.0531	378.8486	40.5719
377.6421	28.45	378.2517	43.3688	378.8613	40.6156
377.6548	21.2625	378.2644	41.3281	378.874	37.4312
377.6675	24.7437	378.2771	41.5219	378.8867	35.4094
377.6802	23.0781	378.2898	43.4656	378.8994	36.8406
377.6929	25.4625	378.3025	40.9281	378.9121	36.2938
377.7056	19.5125	378.3152	43.1375	378.9248	41.9219
377.7183	20.3625	378.3279	44.9375	378.9375	35.5312
377.731	21.1937	378.3406	51.0687	378.9502	34.0406
377.7437	26.6906	378.3533	52.2625	378.9629	31.8844
377.7564	23.7344	378.366	51.5531	378.9756	26.6781
377.7691	22.1406	378.3787	52.0813	378.9883	30.175
377.7818	25.3813	378.3914	48.6469	379.001	30.7094
377.7945	27.7313	378.4041	46.725	379.0137	26.8594
377.8072	25.3062	378.4168	43.1875	379.0264	22.3125
377.8199	27.1813	378.4295	45.5875	379.0391	24.4563
377.8326	29.8906	378.4422	41.0062	379.0518	24.8125
377.8453	31.9312	378.4549	43.1281	379.0645	18.5938
377.858	33.85	378.4676	43.4	379.0772	18.825
377.8707	28.3906	378.4803	41.1688	379.0899	21.4344
377.8834	30.1156	378.493	32.9125	379.1026	25.4188
377.8961	27.9063	378.5057	31.5156	379.1153	21.0125
377.9088	28.5219	378.5184	31.3	379.128	20.5406
377.9215	26.1469	378.5311	31.9188	379.1407	31.7375
377.9342	25.95	378.5438	29.8719	379.1534	22.8687
377.9469	32.4938	378.5565	31.0844	379.1661	23.1406
377.9596	31.5781	378.5692	34.3469	379.1788	25.2188
377.9723	27.6594	378.5819	31.7719	379.1915	21.0187
377.985	27.6719	378.5946	25.7937	379.2042	20.1
377.9977	30.2437	378.6073	26.8594	379.2169	19.275
378.0104	26.825	378.62	29.1406	379.2296	22.2219
378.0231	30.6187	378.6327	27.5781	379.2423	22.5875
378.0358	31.5344	378.6454	24.9688	379.255	22.825
378.0485	38.5531	378.6581	25.3687	379.2677	21.3125
378.0612	40.2406	378.6708	27.0031	379.2804	23.2594
378.0739	44.4969	378.6835	30.4062	379.2931	22.3438
378.0866	42.1469	378.6962	32.3812	379.3058	16.2313
378.0993	42.2156	378.7089	33.7531	379.3185	13.6719
378.112	44.1781	378.7216	37.6344	379.3312	15.7781
378.1247	42.3344	378.7343	43.4281	379.3439	15.775
378.1374	38.2969	378.747	40.5688	379.3566	18.5938
378.1501	37.3625	378.7597	33.9844	379.3693	16.2219
378.1628	37.9219	378.7724	38.4	379.382	19.5
378.1755	36.7531	378.7851	43.1688	379.3947	20.0875

379.4074	17.8187	380.017	47.0469	380.6266	29.2687
379.4201	24.9125	380.0297	48.1312	380.6393	32.8156
379.4328	17.4406	380.0424	48.7125	380.652	29.5125
379.4455	13.7781	380.0551	52.2562	380.6647	32.4094
379.4582	15.2625	380.0678	53.9906	380.6774	32.2375
379.4709	17.6281	380.0805	55.8625	380.6901	30.1281
379.4836	13.9875	380.0932	55.1156	380.7028	31.75
379.4963	20.5063	380.1059	55.7344	380.7155	33.6281
379.509	18.675	380.1186	56.1437	380.7282	30.9562
379.5217	22.9469	380.1313	54.9656	380.7409	33.15
379.5344	14.0344	380.144	54.5125	380.7536	31.5469
379.5471	19.7719	380.1567	53.8687	380.7663	31.8938
379.5598	20.1719	380.1694	52.2969	380.779	30.2281
379.5725	23.0281	380.1821	51.1313	380.7917	27.575
379.5852	28.1156	380.1948	51.3969	380.8044	31.4937
379.5979	31.3469	380.2075	51.7906	380.8171	30.35
379.6106	29.7563	380.2202	51.7594	380.8298	29.4312
379.6233	31.7812	380.2329	53.2125	380.8425	23.2781
379.636	24.8906	380.2456	51.5625	380.8552	21.4594
379.6487	27.1031	380.2583	50.4219	380.8679	19.1188
379.6614	23.7031	380.271	48.6156	380.8806	18.4688
379.6741	26.4594	380.2837	49.2	380.8933	20.0312
379.6868	24.0344	380.2964	47.6875	380.906	21.8594
379.6995	23.8812	380.3091	47.3344	380.9187	20.5844
379.7122	22.6031	380.3218	46.4625	380.9314	16.8625
379.7249	24.6094	380.3345	48.7844	380.9441	22.2687
379.7376	32.8406	380.3472	47.35	380.9568	18.1719
379.7503	25.6531	380.3599	47.0813	380.9695	18.4594
379.763	28.8281	380.3726	46.3406	380.9822	18.1156
379.7757	30.0156	380.3853	45.5469	380.9949	18.0375
379.7884	28.3156	380.398	49.0719	381.0076	15.9469
379.8011	29.9125	380.4107	48.3906	381.0203	16.8062
379.8138	30.2188	380.4234	44.9531	381.033	14.2
379.8265	33.5187	380.4361	46.7031	381.0457	12.3312
379.8392	35.85	380.4488	46.1906	381.0584	13.2594
379.8519	37.0563	380.4615	46.925	381.0711	11.5031
379.8646	38	380.4742	47.6281	381.0838	11.325
379.8773	37.7938	380.4869	43.4094	381.0965	16.7531
379.89	39.5438	380.4996	42.3906	381.1092	16.6531
379.9027	41.5594	380.5123	38.6625	381.1219	13.6031
379.9154	41.5062	380.525	37.8969	381.1346	14.9969
379.9281	40.2188	380.5377	35.8531	381.1473	12.975
379.9408	44.2875	380.5504	34.3781	381.16	10.9906
379.9535	41.8844	380.5631	36.25	381.1727	12.5875
379.9662	43.7156	380.5758	32.2531	381.1854	9.8125
379.9789	44.3063	380.5885	32.8406	381.1981	13.2687
379.9916	45.5969	380.6012	31.9156	381.2108	13.5688
380.0043	43.7156	380.6139	29.5469	381.2235	11.5437

381.2362	13.8563	381.8458	46.6594	382.4554	25.9438
381.2489	11.2188	381.8585	45.6406	382.4681	24.0625
381.2616	10.5562	381.8712	46.95	382.4808	27.7281
381.2743	8.2375	381.8839	46.3094	382.4935	31.0437
381.287	9.675	381.8966	47.1969	382.5062	23.7344
381.2997	10.5813	381.9093	43.775	382.5189	23.7031
381.3124	16.2906	381.922	44.8125	382.5316	22.3687
381.3251	18.5063	381.9347	46.9969	382.5443	27.3875
381.3378	20.0031	381.9474	45.7781	382.557	24.7906
381.3505	22.7531	381.9601	44.4844	382.5697	20.6406
381.3632	20.1938	381.9728	46.15	382.5824	22.7875
381.3759	24.475	381.9855	43.5312	382.5951	19.2906
381.3886	23.7437	381.9982	43.4375	382.6078	19.775
381.4013	25.2969	382.0109	43.55	382.6205	21.2719
381.414	25.3312	382.0236	44.7719	382.6332	22.0531
381.4267	26.0906	382.0363	42.2812	382.6459	20.1219
381.4394	28.525	382.049	40.3688	382.6586	19.1281
381.4521	30.2375	382.0617	41.2281	382.6713	15.1
381.4648	26.7531	382.0744	41.8719	382.684	17.6031
381.4775	28.2938	382.0871	42.0031	382.6967	19.7937
381.4902	34.8875	382.0998	40.6188	382.7094	21.6469
381.5029	31.5406	382.1125	38.7938	382.7221	19.8125
381.5156	29.9625	382.1252	37.4781	382.7348	19.1094
381.5283	28.3875	382.1379	39.6656	382.7475	25.3656
381.541	29.8406	382.1506	38.3281	382.7602	20.5656
381.5537	32.3031	382.1633	37.7031	382.7729	23.8969
381.5664	31.0438	382.176	34.55	382.7856	21.1969
381.5791	27.75	382.1887	31.2563	382.7983	20.2
381.5918	35.6406	382.2014	34.7719	382.811	19.2
381.6045	35.9813	382.2141	32.8625	382.8237	18.7031
381.6172	30.7	382.2268	30.5219	382.8364	23.2188
381.6299	34.7094	382.2395	34.3063	382.8491	25.0031
381.6426	41.1469	382.2522	31.1094	382.8618	25.4906
381.6553	41.7938	382.2649	29.7125	382.8745	24.0281
381.668	46.5812	382.2776	31.175	382.8872	21.1406
381.6807	41.9781	382.2903	27.0188	382.8999	22.7062
381.6934	41.0563	382.303	31.5906	382.9126	27.9188
381.7061	45.4031	382.3157	31.6781	382.9253	32.0031
381.7188	41.1063	382.3284	33.6375	382.938	25.4219
381.7315	44.3531	382.3411	27.5406	382.9507	25.8875
381.7442	44.3125	382.3538	21.4031	382.9634	31.7562
381.7569	40.1969	382.3665	26.1937	382.9761	29.5906
381.7696	41.3813	382.3792	26.9156	382.9888	26.8219
381.7823	40.1719	382.3919	34.7313	383.0015	29.6094
381.795	45.9594	382.4046	33.0781	383.0142	37.6094
381.8077	44.2031	382.4173	25.5844	383.0269	37.125
381.8204	44.4437	382.43	18.4656	383.0396	33.825
381.8331	44.1594	382.4427	21.8875	383.0523	34.9781

383.065	36.6625	383.6746	30.1344	384.2842	25.8906
383.0777	28.4938	383.6873	31.4469	384.2969	24.5781
383.0904	28.2469	383.7	27.6344	384.3096	25.0094
383.1031	29.5031	383.7127	29.225	384.3223	21.2188
383.1158	34.0531	383.7254	28.3906	384.335	23.2156
383.1285	38.6531	383.7381	24.9688	384.3477	26.5406
383.1412	39.1937	383.7508	29.1031	384.3604	25.5375
383.1539	40.2344	383.7635	28.6437	384.3731	26.0875
383.1666	38.8937	383.7762	30.2438	384.3858	22.9313
383.1793	40.8312	383.7889	34.9875	384.3985	24.3375
383.192	45.2281	383.8016	29.2094	384.4112	21.4188
383.2047	45.475	383.8143	22.65	384.4239	27.1562
383.2174	48.3281	383.827	26.9375	384.4366	25.3906
383.2301	46.3156	383.8397	27.0656	384.4493	22.9438
383.2428	42.5031	383.8524	31.2656	384.462	21.9406
383.2555	37.8812	383.8651	25.6875	384.4747	20.8031
383.2682	44.7281	383.8778	28.3813	384.4874	23.0437
383.2809	47.8375	383.8905	28.3844	384.5001	26.4438
383.2936	47.1844	383.9032	27.9781	384.5128	25.6469
383.3063	45.6938	383.9159	26.2656	384.5255	29.2719
383.319	47.4625	383.9286	22.4656	384.5382	27.3344
383.3317	43.475	383.9413	25.6094	384.5509	29.9688
383.3444	44.3187	383.954	21.7063	384.5636	25.7312
383.3571	46.0219	383.9667	25.0187	384.5763	30.2188
383.3698	50.3062	383.9794	27.8094	384.589	28.8219
383.3825	51.3531	383.9921	24.475	384.6017	25.8187
383.3952	51.1	384.0048	23.8281	384.6144	29.6688
383.4079	48.5781	384.0175	20.675	384.6271	25.1875
383.4206	45.6125	384.0302	23.6063	384.6398	27.2
383.4333	47.0344	384.0429	23.3406	384.6525	31.7313
383.446	48.6344	384.0556	30.9094	384.6652	30.275
383.4587	48.3219	384.0683	20.5375	384.6779	27.7875
383.4714	47.1219	384.081	23.7844	384.6906	27.4313
383.4841	47.3938	384.0937	19.4406	384.7033	32.0656
383.4968	46.1219	384.1064	20.1656	384.716	32.4062
383.5095	46.2	384.1191	20.4125	384.7287	31.3812
383.5222	41.1813	384.1318	26.7625	384.7414	31.2219
383.5349	47.6719	384.1445	17.2531	384.7541	32.9969
383.5476	34.7844	384.1572	20.7094	384.7668	32.1156
383.5603	42.6875	384.1699	24.7	384.7795	34.225
383.573	38.825	384.1826	18.7313	384.7922	33.2062
383.5857	39.7469	384.1953	18.8312	384.8049	34.8563
383.5984	33.2937	384.208	21.3406	384.8176	38.2875
383.6111	32.7	384.2207	21.1781	384.8303	35.9688
383.6238	24.5219	384.2334	24.3406	384.843	34.4531
383.6365	28.6313	384.2461	22.9094	384.8557	37.4562
383.6492	34.4813	384.2588	20.3187	384.8684	39.3188
383.6619	34.9313	384.2715	24.975	384.8811	39.0687

384.8938	32.5219	385.5034	33.8406	386.113	31.5781
384.9065	38.7812	385.5161	35.3969	386.1257	22.7625
384.9192	36.4281	385.5288	30.025	386.1384	24.6281
384.9319	38.8219	385.5415	29.4469	386.1511	25.4219
384.9446	38.7125	385.5542	26.5969	386.1638	29.4156
384.9573	38.8406	385.5669	31.9312	386.1765	29.1094
384.97	39.9437	385.5796	33.8594	386.1892	22.7906
384.9827	42.8625	385.5923	33.0375	386.2019	24.5063
384.9954	44.8438	385.605	35.4969	386.2146	24.3937
385.0081	42.7281	385.6177	40.2031	386.2273	22.9719
385.0208	37.6719	385.6304	42.2469	386.24	22.3438
385.0335	39.6813	385.6431	40.9781	386.2527	25.1688
385.0462	42.5094	385.6558	36.4156	386.2654	22.0437
385.0589	42.5437	385.6685	36.5625	386.2781	24.6656
385.0716	45.5125	385.6812	33.8937	386.2908	23.2625
385.0843	44.5094	385.6939	39.7219	386.3035	20.9844
385.097	42.0344	385.7066	37.8719	386.3162	20.4344
385.1097	46.0969	385.7193	39.6531	386.3289	17.2375
385.1224	44.1875	385.732	33.1375	386.3416	20.7219
385.1351	41.55	385.7447	31.7031	386.3543	25.7094
385.1478	42.5438	385.7574	27.0094	386.367	27.6906
385.1605	38.9375	385.7701	33.6969	386.3797	26.6625
385.1732	40.4188	385.7828	31.1531	386.3924	26.6312
385.1859	41.5219	385.7955	26.8188	386.4051	26.2188
385.1986	41.4344	385.8082	29.0031	386.4178	29.9875
385.2113	40.8781	385.8209	26.125	386.4305	29.8219
385.224	42.5812	385.8336	24.2031	386.4432	31.7406
385.2367	42.0719	385.8463	28.8312	386.4559	34.7031
385.2494	45.3406	385.859	24.9969	386.4686	33.9156
385.2621	44.7594	385.8717	28.7031	386.4813	29.6938
385.2748	45.3094	385.8844	31.9781	386.494	26.6344
385.2875	41.7281	385.8971	28.8844	386.5067	29.2125
385.3002	41.0062	385.9098	32.6875	386.5194	30.3
385.3129	37.4188	385.9225	29.2094	386.5321	34.5562
385.3256	39.1937	385.9352	29.4875	386.5448	34.3469
385.3383	43.1063	385.9479	22.7094	386.5575	27.1813
385.351	44.2625	385.9606	30.7094	386.5702	21.3656
385.3637	47.4844	385.9733	32.3531	386.5829	21.7156
385.3764	48.0719	385.986	24.1094	386.5956	23.4469
385.3891	42.7375	385.9987	20.5156	386.6083	21.7656
385.4018	43.7188	386.0114	22.2531	386.621	24.4219
385.4145	41.3719	386.0241	25.2812	386.6337	23.6469
385.4272	42.6812	386.0368	26.1812	386.6464	22.7844
385.4399	42.9656	386.0495	24.0844	386.6591	26.0125
385.4526	43.4344	386.0622	30.7781	386.6718	30.8438
385.4653	38.6312	386.0749	28.6094	386.6845	35.5812
385.478	35.6719	386.0876	29.0594	386.6972	31.9625
385.4907	33.8594	386.1003	34.3031	386.7099	29.7812

386.7226	25.7188	387.3322	31.0219	387.9418	37.75
386.7353	22.9875	387.3449	27.1969	387.9545	37.0656
386.748	26.125	387.3576	29.0938	387.9672	37.2594
386.7607	29.1562	387.3703	29.9	387.9799	34.3281
386.7734	27.5	387.383	28.2875	387.9926	35.7938
386.7861	27.1219	387.3957	27.8969	388.0053	36.5281
386.7988	20.9875	387.4084	35.05	388.018	37.825
386.8115	28.5031	387.4211	36.2281	388.0307	41.225
386.8242	29.5344	387.4338	32.7594	388.0434	40.4688
386.8369	30.9156	387.4465	32.9719	388.0561	40.2313
386.8496	31.7469	387.4592	33.1781	388.0688	39.8156
386.8623	31.9188	387.4719	36.5594	388.0815	37.175
386.875	38.9375	387.4846	33.8375	388.0942	25.6344
386.8877	39.5	387.4973	28.0094	388.1069	31.6906
386.9004	32.7094	387.51	29.3406	388.1196	30.0031
386.9131	29.425	387.5227	36.4969	388.1323	29.1094
386.9258	30.3969	387.5354	36.925	388.145	32.3844
386.9385	35.7313	387.5481	31.4344	388.1577	31.4688
386.9512	36.4469	387.5608	34.325	388.1704	25.5906
386.9639	34.4875	387.5735	39.2062	388.1831	23.7156
386.9766	35.5281	387.5862	26.2938	388.1958	25.6937
386.9893	36.6094	387.5989	31.1187	388.2085	27.7094
387.002	34.9375	387.6116	33.8	388.2212	33.025
387.0147	33.1031	387.6243	33.4188	388.2339	31.325
387.0274	33.6562	387.637	33.7437	388.2466	29.1
387.0401	33.9313	387.6497	29.7313	388.2593	33.2094
387.0528	33.3719	387.6624	29.8281	388.272	30.6938
387.0655	30.7125	387.6751	30.9813	388.2847	34.0156
387.0782	33.3969	387.6878	30.5531	388.2974	32.8719
387.0909	35.95	387.7005	30.7062	388.3101	34.0156
387.1036	31.9438	387.7132	29.1031	388.3228	34.1094
387.1163	33.2937	387.7259	34.3063	388.3355	31.4281
387.129	38.2594	387.7386	36.3219	388.3482	34.4969
387.1417	40.9344	387.7513	33.6094	388.3609	27.3812
387.1544	35.2844	387.764	36.7	388.3736	25.3844
387.1671	36.7406	387.7767	32.5969	388.3863	22.525
387.1798	36.7438	387.7894	32.625	388.399	27.4875
387.1925	30.6	387.8021	41.8438	388.4117	29.675
387.2052	30.175	387.8148	38.5094	388.4244	26.0188
387.2179	27.4594	387.8275	40.1156	388.4371	24.8344
387.2306	27.9469	387.8402	39.4594	388.4498	26.1906
387.2433	32.1188	387.8529	39.9094	388.4625	26.8531
387.256	28.6438	387.8656	39.3438	388.4752	27.4344
387.2687	22.1875	387.8783	36.6688	388.4879	28.5562
387.2814	24.1781	387.891	37.7719	388.5006	29.2281
387.2941	25.75	387.9037	37.6969	388.5133	21.3312
387.3068	29.5187	387.9164	37.0812	388.526	20.2156
387.3195	29.9375	387.9291	37.3031	388.5387	18.5625

388.5514	19.1906	389.161	33.3562	389.7706	32.7156
388.5641	25.7531	389.1737	34.4969	389.7833	27.3625
388.5768	21.3625	389.1864	28.0656	389.796	24.7438
388.5895	22.5094	389.1991	27.3563	389.8087	26.7687
388.6022	24.3469	389.2118	33.6094	389.8214	24.5438
388.6149	24.9875	389.2245	27.7812	389.8341	23.1281
388.6276	25.4562	389.2372	28.225	389.8468	21.675
388.6403	21.8531	389.2499	28.8812	389.8595	19.5125
388.653	20.9469	389.2626	32.2375	389.8722	33.625
388.6657	20.4	389.2753	28.2313	389.8849	37.1562
388.6784	18.8938	389.288	27.2062	389.8976	42.4531
388.6911	23.8937	389.3007	23.1906	389.9103	43.6781
388.7038	28.5906	389.3134	21.6156	389.923	44.2781
388.7165	30.0156	389.3261	24.4937	389.9357	44.4938
388.7292	21.5781	389.3388	27.6562	389.9484	43.3906
388.7419	21.3344	389.3515	21.3969	389.9611	40.5531
388.7546	22.1031	389.3642	22.1094	389.9738	41.6063
388.7673	23.1625	389.3769	25.7469	389.9865	40.2438
388.78	24.8188	389.3896	25.0906	389.9992	35.8063
388.7927	30.3094	389.4023	28.2781	390.0119	30.4313
388.8054	24.6031	389.415	33.4125	390.0246	28.2969
388.8181	22.3875	389.4277	29.4	390.0373	30.4156
388.8308	23.4438	389.4404	28.1281	390.05	28.6375
388.8435	26.9344	389.4531	31.1344	390.0627	28.2781
388.8562	32.3875	389.4658	31.8969	390.0754	28.7781
388.8689	37.4406	389.4785	32.9344	390.0881	28.8875
388.8816	36.9656	389.4912	33.2031	390.1008	25.6656
388.8943	38.6406	389.5039	32.9688	390.1135	23.225
388.907	37.5719	389.5166	34.4594	390.1262	23.5312
388.9197	37.2781	389.5293	32.0656	390.1389	24.5875
388.9324	40.1219	389.542	30.0094	390.1516	24.9594
388.9451	36.7406	389.5547	30.5094	390.1643	28.1
388.9578	30.8031	389.5674	30.8469	390.177	28.5312
388.9705	30.0094	389.5801	33.9656	390.1897	30.1562
388.9832	39.7625	389.5928	32.6344	390.2024	29.6812
388.9959	34.0844	389.6055	33.8844	390.2151	27.1687
389.0086	36.7313	389.6182	35.5125	390.2278	27.0906
389.0213	35.5563	389.6309	33.9938	390.2405	25.5875
389.034	33.5438	389.6436	34.6094	390.2532	25.9562
389.0467	37.5	389.6563	33.9031	390.2659	27.2375
389.0594	41.2031	389.669	30.8844	390.2786	28.4406
389.0721	39.1406	389.6817	34.2781	390.2913	28.8656
389.0848	40.7812	389.6944	33.1156	390.304	31.6156
389.0975	37.2156	389.7071	30.4688	390.3167	36.3812
389.1102	35.125	389.7198	31.1719	390.3294	37.425
389.1229	38.1437	389.7325	30.2094	390.3421	38.8
389.1356	35.9594	389.7452	31.2812	390.3548	39.2562
389.1483	32.7937	389.7579	36.0344	390.3675	37.3719

390.3802	37.7	390.9898	31.7812	391.5994	35.5687
390.3929	36.8719	391.0025	30.9969	391.6121	37.4375
390.4056	36.7625	391.0152	26.75	391.6248	32.8563
390.4183	36.4562	391.0279	24.5344	391.6375	29.6906
390.431	36.8812	391.0406	22.8781	391.6502	26.6156
390.4437	36.525	391.0533	21.7719	391.6629	23.6219
390.4564	35.525	391.066	23.3781	391.6756	28.3188
390.4691	36.4188	391.0787	19.6031	391.6883	24.4375
390.4818	36.1469	391.0914	16.9438	391.701	29.7344
390.4945	36.7875	391.1041	18.9625	391.7137	29.5563
390.5072	38.025	391.1168	15.6469	391.7264	32.3875
390.5199	38.2656	391.1295	13.5906	391.7391	32.5
390.5326	37.5156	391.1422	14.0781	391.7518	36.4969
390.5453	37.5406	391.1549	15.7625	391.7645	29.7
390.558	36.7406	391.1676	18.4781	391.7772	28.7437
390.5707	34.9469	391.1803	13.4656	391.7899	39.1438
390.5834	34.8344	391.193	17.2531	391.8026	41.5219
390.5961	33.2625	391.2057	22.2844	391.8153	31.1219
390.6088	32.6469	391.2184	17.4562	391.828	42.8781
390.6215	31.0563	391.2311	15.2062	391.8407	46.1875
390.6342	31.3094	391.2438	19.5594	391.8534	40.9125
390.6469	33.2406	391.2565	21.4969	391.8661	36.4938
390.6596	34.5062	391.2692	14.9688	391.8788	37.6281
390.6723	34.6406	391.2819	15.7625	391.8915	40.1219
390.685	34.125	391.2946	18.5813	391.9042	36.4375
390.6977	35.35	391.3073	21.1844	391.9169	35.2688
390.7104	37.05	391.32	23.8719	391.9296	45.0563
390.7231	38.5219	391.3327	29.5656	391.9423	45.1437
390.7358	38.3594	391.3454	30.3594	391.955	42.9281
390.7485	38.4844	391.3581	19.7406	391.9677	43.8312
390.7612	41.2594	391.3708	23.4344	391.9804	38.5625
390.7739	43.0844	391.3835	30.8344	391.9931	33.1531
390.7866	44.5781	391.3962	21.7594	392.0058	31.0687
390.7993	44.5719	391.4089	22.9438	392.0185	38.8844
390.812	45.4531	391.4216	25.5906	392.0312	39.025
390.8247	46.3063	391.4343	28.6781	392.0439	41.2156
390.8374	46.5375	391.447	33.5844	392.0566	43.825
390.8501	42.4781	391.4597	37.575	392.0693	42.8063
390.8628	40.1594	391.4724	36.6094	392.082	39.1781
390.8755	36.6844	391.4851	35.1875	392.0947	41.4906
390.8882	35.25	391.4978	35.0906	392.1074	36.5812
390.9009	37.1906	391.5105	40.1688	392.1201	33.7438
390.9136	38.5875	391.5232	37.6625	392.1328	33.0375
390.9263	37.7156	391.5359	43.2406	392.1455	34.3031
390.939	33.7313	391.5486	36.5625	392.1582	35.0562
390.9517	32.5563	391.5613	40.2469	392.1709	32.0406
390.9644	31.2469	391.574	37.7062	392.1836	35.6437
390.9771	30.0438	391.5867	35.7562	392.1963	33.6437

392.209	30.7281	392.8186	19.725	393.4282	40.2
392.2217	28.4062	392.8313	20.8969	393.4409	45.1781
392.2344	26.9375	392.844	20.3406	393.4536	45.475
392.2471	25.3406	392.8567	18.0844	393.4663	47.075
392.2598	22.5375	392.8694	17.1469	393.479	45.5531
392.2725	20.3625	392.8821	17.9219	393.4917	46.0781
392.2852	21.3219	392.8948	19.475	393.5044	45.5906
392.2979	23.5219	392.9075	21.3844	393.5171	46.0563
392.3106	22.6594	392.9202	21.4781	393.5298	46.9844
392.3233	20.1594	392.9329	21.0312	393.5425	43.7812
392.336	21.975	392.9456	25.5031	393.5552	44.2344
392.3487	29.2781	392.9583	21.5625	393.5679	47.4625
392.3614	27.5969	392.971	20.8469	393.5806	46.5625
392.3741	26.9844	392.9837	20.6219	393.5933	47.6094
392.3868	27.9656	392.9964	23.7719	393.606	45.0563
392.3995	30.5219	393.0091	25.6125	393.6187	42.9656
392.4122	30.6469	393.0218	24.9094	393.6314	41.6031
392.4249	30.8031	393.0345	22.55	393.6441	43.2844
392.4376	30.75	393.0472	23.0906	393.6568	40.7688
392.4503	30.8	393.0599	22.475	393.6695	40.5031
392.463	30.9281	393.0726	28.45	393.6822	37.0125
392.4757	30.6594	393.0853	25.7375	393.6949	39.3094
392.4884	30.225	393.098	28.7594	393.7076	38.8375
392.5011	32.5563	393.1107	26.1219	393.7203	31.25
392.5138	35.8812	393.1234	27.4406	393.733	36.2156
392.5265	30.6719	393.1361	27.4688	393.7457	35.1312
392.5392	31.5125	393.1488	32.8813	393.7584	34.1
392.5519	28.9906	393.1615	32.625	393.7711	34.7594
392.5646	27.8063	393.1742	34.7094	393.7838	34.5938
392.5773	29.1875	393.1869	34.0656	393.7965	33.2875
392.59	26.1219	393.1996	40.4406	393.8092	33.0531
392.6027	24.9344	393.2123	41.8094	393.8219	33.9094
392.6154	23.2	393.225	41.0687	393.8346	34.75
392.6281	23.7875	393.2377	41.3219	393.8473	32.725
392.6408	25.7344	393.2504	36.4562	393.86	38.0219
392.6535	24.0406	393.2631	35.4563	393.8727	34.6969
392.6662	20.6437	393.2758	37.6344	393.8854	32.7812
392.6789	21.2781	393.2885	38.8063	393.8981	31.375
392.6916	19.6594	393.3012	38.525	393.9108	29.3969
392.7043	16.3625	393.3139	38.4281	393.9235	26.1313
392.717	15.0531	393.3266	41.625	393.9362	26.8281
392.7297	17.5594	393.3393	41.35	393.9489	26.7094
392.7424	19.9281	393.352	39.95	393.9616	26.85
392.7551	18.1844	393.3647	37.2188	393.9743	27.2031
392.7678	13.9688	393.3774	37.7531	393.987	31.0062
392.7805	15.1719	393.3901	41.6125	393.9997	33.4437
392.7932	16.3719	393.4028	43.2063	394.0124	29.5156
392.8059	19.3125	393.4155	40.1438	394.0251	26.775

394.0378	30.5281	394.6474	32.8094	395.257	12.7875
394.0505	34.5563	394.6601	31.2562	395.2697	15.2031
394.0632	32.0813	394.6728	28.4219	395.2824	20.4719
394.0759	34.3438	394.6855	31.6344	395.2951	24.5312
394.0886	34.7344	394.6982	32.7719	395.3078	29.8281
394.1013	37.0187	394.7109	29.5719	395.3205	28.85
394.114	40.5656	394.7236	26.4375	395.3332	26.2094
394.1267	37.3688	394.7363	26.2625	395.3459	28.0375
394.1394	37.2781	394.749	25.9812	395.3586	28.1094
394.1521	35.7875	394.7617	26.1	395.3713	35.6813
394.1648	34.0563	394.7744	35.1375	395.384	26.8594
394.1775	36.4	394.7871	36.4531	395.3967	27.4594
394.1902	38.4219	394.7998	34.8125	395.4094	26.825
394.2029	36.5875	394.8125	34.3281	395.4221	28.6188
394.2156	32.8219	394.8252	36.3812	395.4348	35.4656
394.2283	31.65	394.8379	37.3063	395.4475	36.7344
394.241	30.875	394.8506	32.9344	395.4602	29.9156
394.2537	34.25	394.8633	32.5281	395.4729	30.525
394.2664	38.8406	394.876	28.1438	395.4856	25.9594
394.2791	37.0406	394.8887	31.1906	395.4983	29.0625
394.2918	33.9156	394.9014	32.6344	395.511	27.2406
394.3045	39.1375	394.9141	32.9188	395.5237	32.2125
394.3172	42.0031	394.9268	28.9969	395.5364	30.7875
394.3299	45.7312	394.9395	30.6	395.5491	40.975
394.3426	45.9531	394.9522	30.4531	395.5618	45.5281
394.3553	47.7219	394.9649	37.4938	395.5745	40.5594
394.368	46.825	394.9776	30.2938	395.5872	39.65
394.3807	45.5812	394.9903	32.5594	395.5999	37.7562
394.3934	44.3094	395.003	31.7625	395.6126	35.6031
394.4061	40.6656	395.0157	34.2219	395.6253	39.7
394.4188	43.1688	395.0284	33.9469	395.638	39.6938
394.4315	43.4719	395.0411	32.0844	395.6507	42.6094
394.4442	40.075	395.0538	34.5094	395.6634	44.4281
394.4569	34.8625	395.0665	35.7375	395.6761	47.25
394.4696	30.7094	395.0792	38.2812	395.6888	46.0844
394.4823	33.3281	395.0919	34.2219	395.7015	50.3687
394.495	31.1094	395.1046	32.2406	395.7142	43.8781
394.5077	31.5312	395.1173	26.025	395.7269	39.5594
394.5204	30.7062	395.13	29.3969	395.7396	36.6281
394.5331	29.8406	395.1427	25.5906	395.7523	36.5938
394.5458	33.1156	395.1554	25.2906	395.765	40.7
394.5585	37.2687	395.1681	27.4625	395.7777	40.4844
394.5712	35.0375	395.1808	23.8375	395.7904	38.075
394.5839	34.0875	395.1935	22.1938	395.8031	35.1687
394.5966	27.6281	395.2062	19.0969	395.8158	30.7188
394.6093	25.9219	395.2189	21.8906	395.8285	34.4781
394.622	30.6625	395.2316	22.2969	395.8412	29.1969
394.6347	31.9344	395.2443	17.9594	395.8539	28.3313

395.8666	26.9594	396.4762	26.6031	397.0858	36.1062
395.8793	31.4625	396.4889	24.3031	397.0985	37.6156
395.892	28.6156	396.5016	22.9156	397.1112	44.1437
395.9047	36.1875	396.5143	24.4844	397.1239	47.4625
395.9174	26.3406	396.527	23.1844	397.1366	48.6281
395.9301	27.8844	396.5397	21.8344	397.1493	48.3094
395.9428	23.1094	396.5524	21.8094	397.162	47.85
395.9555	18.8094	396.5651	22.7219	397.1747	48.8906
395.9682	18.2469	396.5778	20.6656	397.1874	49.725
395.9809	18.6469	396.5905	17.7906	397.2001	50.7938
395.9936	19.9875	396.6032	17.4219	397.2128	50.0344
396.0063	22.375	396.6159	17.8281	397.2255	47.7312
396.019	18.05	396.6286	18.9031	397.2382	45.6031
396.0317	16.7594	396.6413	25.1531	397.2509	48.4781
396.0444	21.2812	396.654	23.8531	397.2636	47.4344
396.0571	32.3344	396.6667	15.2844	397.2763	44.0375
396.0698	34.4813	396.6794	17.3344	397.289	36.6562
396.0825	17.85	396.6921	25.5469	397.3017	31.2594
396.0952	20.5187	396.7048	23.2719	397.3144	29.4469
396.1079	16.3125	396.7175	15.7875	397.3271	33.2313
396.1206	21.6562	396.7302	20.0094	397.3398	36.6687
396.1333	17.9406	396.7429	22.0094	397.3525	32.0656
396.146	19.1281	396.7556	26.6375	397.3652	28.1781
396.1587	21.7563	396.7683	33.1063	397.3779	31.5
396.1714	23.2469	396.781	39.6875	397.3906	27.6219
396.1841	25.225	396.7937	39.7312	397.4033	38.2656
396.1968	22.3031	396.8064	36.425	397.416	28.7969
396.2095	31.1125	396.8191	39.7875	397.4287	26.4813
396.2222	38.2281	396.8318	31.9688	397.4414	25.0469
396.2349	30.9781	396.8445	34.4094	397.4541	17.8125
396.2476	30.3	396.8572	33.6844	397.4668	22.3813
396.2603	24.9375	396.8699	29.8375	397.4795	24.9031
396.273	31.0844	396.8826	26.9531	397.4922	26.2844
396.2857	23.0938	396.8953	33.9844	397.5049	25.4656
396.2984	26.1813	396.908	29.1062	397.5176	27.7969
396.3111	27.3687	396.9207	29.5625	397.5303	35.8406
396.3238	22.6313	396.9334	32.8375	397.543	30.4094
396.3365	21.3813	396.9461	30.2219	397.5557	25.8844
396.3492	20.9	396.9588	30.2844	397.5684	27.7125
396.3619	19.8813	396.9715	31.1594	397.5811	33.2688
396.3746	21.7281	396.9842	32.5812	397.5938	38.0781
396.3873	23.6125	396.9969	34.8875	397.6065	41.9
396.4	30.5594	397.0096	37.0156	397.6192	41.5875
396.4127	27.8875	397.0223	40.325	397.6319	38.7906
396.4254	26.3781	397.035	42.6437	397.6446	40.7344
396.4381	22.8188	397.0477	32.5063	397.6573	42.7812
396.4508	20.9438	397.0604	34.3563	397.67	42.0719
396.4635	26.1812	397.0731	35.9625	397.6827	41.1781

397.6954	41.3906	398.305	47.0531	398.9146	18.8281
397.7081	39.8094	398.3177	45.6625	398.9273	24.5312
397.7208	40.8594	398.3304	49.4844	398.94	20.2
397.7335	45.45	398.3431	46.4906	398.9527	21.275
397.7462	45.2406	398.3558	43.3656	398.9654	19.9156
397.7589	41.6375	398.3685	40.3937	398.9781	20.5969
397.7716	40.3219	398.3812	39.3906	398.9908	16.9188
397.7843	37.1125	398.3939	34.0625	399.0035	15.4094
397.797	43.9437	398.4066	32.2687	399.0162	20.6406
397.8097	45.4	398.4193	24.95	399.0289	22.8781
397.8224	47.5875	398.432	29.9094	399.0416	24.2062
397.8351	42.675	398.4447	25.2	399.0543	21.8094
397.8478	37.6156	398.4574	28.8094	399.067	20.7687
397.8605	40.0656	398.4701	21.275	399.0797	28.1813
397.8732	37.7562	398.4828	17.6375	399.0924	26.7188
397.8859	35.5344	398.4955	16.6406	399.1051	31.9844
397.8986	31.2219	398.5082	18.275	399.1178	27.4656
397.9113	25.0187	398.5209	19.0969	399.1305	22.6594
397.924	24.3375	398.5336	11.7125	399.1432	22.5406
397.9367	23.2625	398.5463	11.3344	399.1559	26.4844
397.9494	28.4625	398.559	13.7781	399.1686	24.8312
397.9621	27.3125	398.5717	15.8	399.1813	22.0656
397.9748	33.1625	398.5844	14.0531	399.194	28.9625
397.9875	37.7188	398.5971	12.6906	399.2067	28.6437
398.0002	33.5406	398.6098	15.7906	399.2194	28.15
398.0129	28.6531	398.6225	13.2937	399.2321	27.8625
398.0256	26.8969	398.6352	18.4781	399.2448	35.9531
398.0383	33.7344	398.6479	18.7313	399.2575	30.0906
398.051	28.2531	398.6606	19.7281	399.2702	31.4656
398.0637	26.8438	398.6733	18.6687	399.2829	29.3625
398.0764	29.1031	398.686	19.9844	399.2956	31.9062
398.0891	25.8344	398.6987	18.4531	399.3083	38.125
398.1018	32.225	398.7114	15.9281	399.321	37.4094
398.1145	30.3688	398.7241	14.9406	399.3337	37.1438
398.1272	30.7781	398.7368	17.3188	399.3464	34.875
398.1399	34.7219	398.7495	20.5844	399.3591	30.5
398.1526	34.6281	398.7622	19.1438	399.3718	30.8062
398.1653	35.7406	398.7749	16.8031	399.3845	27.925
398.178	36.3312	398.7876	20.1781	399.3972	29.3438
398.1907	35.1281	398.8003	22.0938	399.4099	28.2719
398.2034	35.7188	398.813	28.6938	399.4226	39.8469
398.2161	37.5687	398.8257	23.8875	399.4353	36.2625
398.2288	40.1656	398.8384	21.8062	399.448	33.7719
398.2415	37.8062	398.8511	19.075	399.4607	32.8688
398.2542	43.4156	398.8638	19.0406	399.4734	30.7625
398.2669	46	398.8765	17.4344	399.4861	36.3563
398.2796	45.2063	398.8892	23.1844	399.4988	38.4031
398.2923	45.3563	398.9019	20.1156	399.5115	35.9437

399.5242	33.1437	400.1338	25.5156	400.7434	39.2562
399.5369	28.3375	400.1465	26.0125	400.7561	40.8156
399.5496	30.4562	400.1592	28.9875	400.7688	39.6094
399.5623	31.1969	400.1719	29.2875	400.7815	39.275
399.575	30.7906	400.1846	28.6812	400.7942	39.3
399.5877	33.5563	400.1973	18.8719	400.8069	39.75
399.6004	36.6406	400.21	19.6781	400.8196	35.7594
399.6131	40.6688	400.2227	20.1406	400.8323	39.2094
399.6258	42.5687	400.2354	18.9281	400.845	38.8625
399.6385	40.525	400.2481	19.525	400.8577	39.9
399.6512	32.0563	400.2608	25.2875	400.8704	33.1969
399.6639	34.1313	400.2735	24.3438	400.8831	36.4906
399.6766	33.4188	400.2862	30.8687	400.8958	39.2156
399.6893	36.8531	400.2989	29.0594	400.9085	31.6938
399.702	38.7812	400.3116	27.9844	400.9212	31.125
399.7147	38.0094	400.3243	25.25	400.9339	35.6406
399.7274	32.3469	400.337	31.9094	400.9466	36.7688
399.7401	30.075	400.3497	26.5312	400.9593	39.6469
399.7528	36.9531	400.3624	25.8688	400.972	39.2594
399.7655	36.4	400.3751	23.4938	400.9847	34.4062
399.7782	29.325	400.3878	27.2906	400.9974	39.1906
399.7909	34.3187	400.4005	31.9187	401.0101	41.1469
399.8036	33.3688	400.4132	24.7219	401.0228	40.3563
399.8163	32.6656	400.4259	20.4937	401.0355	44.075
399.829	33.6781	400.4386	20.5031	401.0482	44.1156
399.8417	33.4938	400.4513	27.1781	401.0609	40.1469
399.8544	30.1562	400.464	30.6219	401.0736	37.0312
399.8671	32.7438	400.4767	32.075	401.0863	37.125
399.8798	32.4938	400.4894	34.9781	401.099	36.7938
399.8925	28.1125	400.5021	33.8969	401.1117	35.8094
399.9052	26.8062	400.5148	36.0875	401.1244	35.8
399.9179	30.4906	400.5275	38.8281	401.1371	38.7094
399.9306	25.15	400.5402	38.9375	401.1498	38.5531
399.9433	26.3656	400.5529	36.6063	401.1625	33.5813
399.956	21.2313	400.5656	33.4344	401.1752	39.15
399.9687	24.5688	400.5783	32.1219	401.1879	39.1344
399.9814	23.4406	400.591	33.2281	401.2006	37.2344
399.9941	22.375	400.6037	37.2875	401.2133	35.225
400.0068	25.9937	400.6164	39.4188	401.226	39.7906
400.0195	26.9469	400.6291	43.8687	401.2387	38.4625
400.0322	30.7688	400.6418	42.7344	401.2514	38.9594
400.0449	28.1594	400.6545	42.3156	401.2641	41.0062
400.0576	27.7188	400.6672	42.125	401.2768	37.3438
400.0703	27.6281	400.6799	43.3375	401.2895	38.8531
400.083	27.1594	400.6926	40.3313	401.3022	42.8469
400.0957	32.3344	400.7053	43.5562	401.3149	41.2844
400.1084	27.3531	400.718	37.1969	401.3276	40.2937
400.1211	25.3188	400.7307	39.5031	401.3403	43.3656

401.353	44.2781	401.9626	13.4469	402.5722	45.425
401.3657	42.7156	401.9753	17.7281	402.5849	45.7313
401.3784	43.2812	401.988	18.575	402.5976	47.1781
401.3911	40.6812	402.0007	17.9312	402.6103	39.9813
401.4038	45.45	402.0134	20.4563	402.623	41.3563
401.4165	41.85	402.0261	21.3656	402.6357	40.7281
401.4292	41.2	402.0388	19.7562	402.6484	42.0375
401.4419	44.0844	402.0515	17.8	402.6611	41.0656
401.4546	38.5219	402.0642	16.925	402.6738	40.7937
401.4673	36.8594	402.0769	19.2781	402.6865	42.4375
401.48	35.6219	402.0896	22.4094	402.6992	43.375
401.4927	29.1594	402.1023	21.5375	402.7119	41.0594
401.5054	34.0344	402.115	22.7844	402.7246	40.2156
401.5181	33.7594	402.1277	31.3625	402.7373	40.3937
401.5308	37.1094	402.1404	28.8656	402.75	39.9438
401.5435	38.8688	402.1531	31.5188	402.7627	40.4313
401.5562	33.9906	402.1658	30.1344	402.7754	42.1937
401.5689	33.8844	402.1785	30.6406	402.7881	39.6562
401.5816	32.7625	402.1912	29.9719	402.8008	38.0062
401.5943	31.55	402.2039	27.7125	402.8135	38.3281
401.607	29.7094	402.2166	24.325	402.8262	37.5187
401.6197	29.7125	402.2293	26.3969	402.8389	42.4906
401.6324	30.1656	402.242	26.5656	402.8516	40.8406
401.6451	31.3875	402.2547	29.6625	402.8643	46.2344
401.6578	31.5219	402.2674	32.0625	402.877	46.0469
401.6705	25.825	402.2801	31.3844	402.8897	43.0687
401.6832	24.9906	402.2928	31.3406	402.9024	44.3469
401.6959	25.625	402.3055	33.6469	402.9151	45.3031
401.7086	23.1656	402.3182	34.0938	402.9278	47.4875
401.7213	25.6188	402.3309	36.7875	402.9405	46.1219
401.734	24.875	402.3436	36.7844	402.9532	47.1688
401.7467	23.3594	402.3563	33.4688	402.9659	48.4531
401.7594	22.5094	402.369	36.5656	402.9786	47.7375
401.7721	23.9406	402.3817	39.3312	402.9913	49.2562
401.7848	21.2125	402.3944	36.95	403.004	52.3688
401.7975	19.0844	402.4071	32.8063	403.0167	50.2094
401.8102	15.9031	402.4198	37.6281	403.0294	51.6
401.8229	18.3656	402.4325	37.0375	403.0421	52.1031
401.8356	14.575	402.4452	34.4594	403.0548	48.7594
401.8483	12.9625	402.4579	34.3375	403.0675	47.1594
401.861	10.6906	402.4706	41.4844	403.0802	41.4969
401.8737	11.2906	402.4833	41.2281	403.0929	46.3094
401.8864	10.9375	402.496	45.2156	403.1056	47.1813
401.8991	14.1125	402.5087	41.1625	403.1183	47.5469
401.9118	13	402.5214	44.3094	403.131	48.0344
401.9245	13.4219	402.5341	42.3094	403.1437	46.5906
401.9372	13.1156	402.5468	45.9594	403.1564	45.5062
401.9499	14.6125	402.5595	46.1906	403.1691	44.1125

403.1818	46.0906	403.7914	33.2562	404.401	12.7375
403.1945	47.7812	403.8041	32.2438	404.4137	13.1344
403.2072	46.6656	403.8168	25.4156	404.4264	13.0906
403.2199	45.0875	403.8295	22.3406	404.4391	11.8313
403.2326	45.1219	403.8422	28.5031	404.4518	11.7437
403.2453	43.6687	403.8549	27.9656	404.4645	12.7156
403.258	43.2625	403.8676	27.6156	404.4772	11.6156
403.2707	41.8906	403.8803	31.2156	404.4899	12.2313
403.2834	41.6875	403.893	33.6063	404.5026	15.95
403.2961	41.1125	403.9057	35.3125	404.5153	17.7281
403.3088	41.0688	403.9184	30.5094	404.528	13.8937
403.3215	36.1031	403.9311	29.3	404.5407	17.0344
403.3342	37.6813	403.9438	27.0188	404.5534	21.5594
403.3469	35.8937	403.9565	23.4438	404.5661	21.925
403.3596	35.075	403.9692	22.3875	404.5788	18.9438
403.3723	33.2313	403.9819	26.1594	404.5915	17.4375
403.385	29.1563	403.9946	25.975	404.6042	16.0406
403.3977	27.9406	404.0073	28.3844	404.6169	17.1656
403.4104	28.2094	404.02	29.4031	404.6296	18.1156
403.4231	31.4156	404.0327	30.1844	404.6423	14.8531
403.4358	32.425	404.0454	31.1281	404.655	16.4813
403.4485	30.1031	404.0581	28.1906	404.6677	17.0844
403.4612	31.0125	404.0708	29.2531	404.6804	16.9219
403.4739	28.95	404.0835	32.6781	404.6931	21.4656
403.4866	26.7375	404.0962	31.375	404.7058	25.8063
403.4993	29.7531	404.1089	31.7281	404.7185	20.1875
403.512	30.4813	404.1216	27.85	404.7312	19.2469
403.5247	32.1406	404.1343	27.8563	404.7439	18.6781
403.5374	26.85	404.147	28.1344	404.7566	26.2406
403.5501	31.7844	404.1597	26.9375	404.7693	23.6281
403.5628	29.7125	404.1724	22.3656	404.782	25.5031
403.5755	30.0063	404.1851	19.9188	404.7947	32.4344
403.5882	31.675	404.1978	22.6031	404.8074	31.1437
403.6009	32.425	404.2105	15.6781	404.8201	37.3156
403.6136	26.075	404.2232	17.7781	404.8328	38.1
403.6263	25.0344	404.2359	22.4094	404.8455	32.0813
403.639	29.1937	404.2486	19.6187	404.8582	32.5531
403.6517	29.2563	404.2613	18.0188	404.8709	32.2219
403.6644	27.4187	404.274	14.05	404.8836	30.1219
403.6771	25.9625	404.2867	19.3813	404.8963	28.1281
403.6898	26.9563	404.2994	21.05	404.909	27.9813
403.7025	27.9437	404.3121	20.125	404.9217	27.1125
403.7152	29.7	404.3248	22.0406	404.9344	32.5344
403.7279	29.9375	404.3375	21.1187	404.9471	29.8875
403.7406	30.8437	404.3502	18.6625	404.9598	34.3031
403.7533	33.0062	404.3629	15.6375	404.9725	32.9813
403.766	26.3531	404.3756	15.2844	404.9852	36.1188
403.7787	31.8344	404.3883	14.6281	404.9979	39.1094

405.0106	37.0906	405.6202	38.9656	406.2298	23.3844
405.0233	37.1125	405.6329	29.3531	406.2425	22.4094
405.036	34.5875	405.6456	33.6781	406.2552	15.175
405.0487	33.2375	405.6583	29.2219	406.2679	18.4469
405.0614	31.6656	405.671	31.6094	406.2806	13.3812
405.0741	30.1313	405.6837	27.0562	406.2933	18.475
405.0868	28.9625	405.6964	27.55	406.306	17.1031
405.0995	34.2156	405.7091	30.9969	406.3187	20.7781
405.1122	32.2594	405.7218	28.0625	406.3314	17.0625
405.1249	38.1906	405.7345	31.7563	406.3441	22.975
405.1376	33.7156	405.7472	29.5688	406.3568	16.6688
405.1503	34.6625	405.7599	34.55	406.3695	17.8188
405.163	33.275	405.7726	27.9906	406.3822	20.625
405.1757	34.4062	405.7853	31.3094	406.3949	21.7281
405.1884	37.2188	405.798	37.5781	406.4076	23.4531
405.2011	39.4562	405.8107	25.3781	406.4203	24.025
405.2138	26.5469	405.8234	31.7906	406.433	28.1969
405.2265	33.2625	405.8361	34.3875	406.4457	27.0812
405.2392	31.3875	405.8488	31.5656	406.4584	31.9312
405.2519	34.8625	405.8615	30.2063	406.4711	28.6625
405.2646	35.8906	405.8742	31.5594	406.4838	34.8937
405.2773	32.8187	405.8869	32.8156	406.4965	28.1031
405.29	31.4469	405.8996	34.2875	406.5092	32.9406
405.3027	32.4188	405.9123	30.3656	406.5219	23.8219
405.3154	30.2406	405.925	37.9812	406.5346	31.825
405.3281	27.3375	405.9377	33.0406	406.5473	25.575
405.3408	32.4594	405.9504	39.1031	406.56	28.0688
405.3535	31.6594	405.9631	33.1719	406.5727	30.3156
405.3662	29.3187	405.9758	35.2438	406.5854	39.475
405.3789	31.45	405.9885	33.25	406.5981	35.6937
405.3916	32.3312	406.0012	31.2125	406.6108	33.4344
405.4043	35.0312	406.0139	29.4937	406.6235	33.8562
405.417	38.6469	406.0266	30.5281	406.6362	41.7625
405.4297	36.9406	406.0393	32.2656	406.6489	37.3656
405.4424	32.3812	406.052	32.9125	406.6616	40.5812
405.4551	36.1156	406.0647	27.4969	406.6743	34.05
405.4678	33.9375	406.0774	30.1844	406.687	31.4
405.4805	32.4594	406.0901	29.6906	406.6997	37.1656
405.4932	33.6281	406.1028	29.3062	406.7124	40.1281
405.5059	32.7375	406.1155	27.125	406.7251	43.2063
405.5186	34.0156	406.1282	25.6937	406.7378	40.1625
405.5313	39.3312	406.1409	29.15	406.7505	40.9094
405.544	37.2469	406.1536	26.7938	406.7632	44.6406
405.5567	36.5219	406.1663	28.3563	406.7759	42.5156
405.5694	32.9281	406.179	25.1094	406.7886	40.5625
405.5821	37.1594	406.1917	25.9281	406.8013	41.7656
405.5948	39.8719	406.2044	24.9406	406.814	41.075
405.6075	38.2719	406.2171	25.2594	406.8267	36.6844

406.8394	36.0312	407.449	37.1094	408.0586	42.1219
406.8521	40.1	407.4617	34.5063	408.0713	45.3937
406.8648	38.9688	407.4744	35.7938	408.084	42.5969
406.8775	35.7188	407.4871	29.1562	408.0967	44.1906
406.8902	37.5938	407.4998	40.9531	408.1094	43.6031
406.9029	37.6063	407.5125	33.5156	408.1221	40.5281
406.9156	39.0844	407.5252	30.3312	408.1348	40.1
406.9283	34.8375	407.5379	22.3656	408.1475	42.9125
406.941	41.8219	407.5506	20.2625	408.1602	38.65
406.9537	40.9688	407.5633	31.6094	408.1729	42.1219
406.9664	41.825	407.576	30.1313	408.1856	47.8781
406.9791	36.7437	407.5887	29.1	408.1983	47.0125
406.9918	39.0719	407.6014	24.0438	408.211	44.1031
407.0045	45.0875	407.6141	32.3594	408.2237	45.7
407.0172	40.6719	407.6268	31.5656	408.2364	40.45
407.0299	36.9125	407.6395	31.975	408.2491	37.4313
407.0426	37.0344	407.6522	37.9437	408.2618	41.9656
407.0553	33.8781	407.6649	39.8469	408.2745	39.0219
407.068	30.475	407.6776	38.9781	408.2872	38.8344
407.0807	28.6562	407.6903	43.3406	408.2999	35.7438
407.0934	34.3688	407.703	45.1	408.3126	40.9656
407.1061	28.6156	407.7157	30.95	408.3253	39.7125
407.1188	37.6438	407.7284	22.05	408.338	33.0719
407.1315	35.6781	407.7411	28.975	408.3507	36.9719
407.1442	39.7594	407.7538	34.7156	408.3634	44.5
407.1569	39.0125	407.7665	31.625	408.3761	35.225
407.1696	43.7562	407.7792	21.7156	408.3888	40.4781
407.1823	42.3625	407.7919	31.2531	408.4015	37.0344
407.195	38.6312	407.8046	30.7219	408.4142	31.2094
407.2077	41.5531	407.8173	37.15	408.4269	34.7281
407.2204	46.4938	407.83	40.25	408.4396	31.7625
407.2331	42.45	407.8427	44.5938	408.4523	36.1625
407.2458	40.175	407.8554	42.2687	408.465	38.9594
407.2585	34.9313	407.8681	32.2531	408.4777	42.4938
407.2712	34.8906	407.8808	28.2625	408.4904	36.8438
407.2839	34.1312	407.8935	37.4469	408.5031	32.625
407.2966	35.6219	407.9062	33.8531	408.5158	30.3312
407.3093	35.4562	407.9189	37.2875	408.5285	37.1437
407.322	37.45	407.9316	34.8187	408.5412	34.8219
407.3347	31.3531	407.9443	45.6437	408.5539	38.3719
407.3474	23.8062	407.957	38.2781	408.5666	34.8219
407.3601	29.65	407.9697	40.7156	408.5793	44.4125
407.3728	38.0406	407.9824	33.8344	408.592	32.2
407.3855	43.8094	407.9951	37.2	408.6047	35.3063
407.3982	39.2594	408.0078	26.9281	408.6174	32.8219
407.4109	39.25	408.0205	26.0563	408.6301	33.7188
407.4236	41.3125	408.0332	42.0813	408.6428	36.775
407.4363	41.85	408.0459	34.7219	408.6555	33.2125

408.6682	30.1688	409.2778	26.1844	409.8874	32.6781
408.6809	24.0687	409.2905	25.4437	409.9001	27.0813
408.6936	23.9656	409.3032	26.0875	409.9128	31.2094
408.7063	24.6938	409.3159	18.9156	409.9255	22.9125
408.719	30.575	409.3286	28.4625	409.9382	30.8344
408.7317	25.5562	409.3413	23.6063	409.9509	24.8406
408.7444	25.6312	409.354	21.1375	409.9636	22.5531
408.7571	25.6125	409.3667	24.8594	409.9763	24.9438
408.7698	27.575	409.3794	21.1781	409.989	29.125
408.7825	26.7812	409.3921	27.3594	410.0017	24.8094
408.7952	24.2844	409.4048	23.8375		
408.8079	23.0531	409.4175	34.8625		
408.8206	25.0531	409.4302	27.4281		
408.8333	25.375	409.4429	24.9156		
408.846	26.2938	409.4556	29.7062		
408.8587	26.3438	409.4683	28.3313		
408.8714	31.3188	409.481	31.7		
408.8841	30.6219	409.4937	23.5719		
408.8968	32.525	409.5064	27.0969		
408.9095	33.2562	409.5191	30.0813		
408.9222	27.1656	409.5318	30.9219		
408.9349	31.0844	409.5445	32.7531		
408.9476	34.1188	409.5572	27.2062		
408.9603	35.2156	409.5699	28.8531		
408.973	34.6937	409.5826	24.6562		
408.9857	38.4437	409.5953	24.5969		
408.9984	36.2656	409.608	25.675		
409.0111	34.4875	409.6207	23.9688		
409.0238	33.6375	409.6334	27.1656		
409.0365	39.4313	409.6461	21.7563		
409.0492	30.0031	409.6588	22.1219		
409.0619	34.9156	409.6715	24.8656		
409.0746	34.6125	409.6842	26.5281		
409.0873	31.6063	409.6969	20.9		
409.1	33.3937	409.7096	19.8781		
409.1127	28.4313	409.7223	16.3969		
409.1254	28.3688	409.735	22.2469		
409.1381	26.8719	409.7477	14.9656		
409.1508	25.4656	409.7604	20.15		
409.1635	26.7531	409.7731	18.4219		
409.1762	28.3625	409.7858	30.2469		
409.1889	23.25	409.7985	27.0531		
409.2016	27.9344	409.8112	29.9937		
409.2143	32.175	409.8239	36.2625		
409.227	31.8563	409.8366	38.2		
409.2397	26.8531	409.8493	29.4094		
409.2524	22.1031	409.862	35.6688		
409.2651	21.4938	409.8747	27.2531		

BIBLIOGRAPHY

Abreu, V.S. and Anderson, J.B. (1998) Glacial eustacy during the Cenozoic: sequence stratigraphic implications, AAPG Bulletin, V. 82, No. 7, 1385-1400.

Akgun, F., Akay, E., and Erdogan, B. (2002) Tertiary terrestrial to shallow marine deposition in central Anatolia; a palynological approach: Turkish Journal of Earth Sciences: 11, no.2, 127-160.

Aubry, Marie-Pierre (1996) Data Report: Eocene to Upper Miocene calcareous nannofossil stratigraphy: IN Mountain,G.S., Miller, K.G., and Blum, P., Poag, C.W., and Twichell, D.C. (Eds.), Proc. ODP, Sci. Results, 150: College Station, TX., 435-437.

Aubry, M., Snyder, S.W., Van Fossen, M.C., Urbat, M., Miller, K.G., and McHugh, C.M.G. (1996) Stratigraphy of the Eocene chalks recovered from the New Jersey margin, Leg 150: synthesis: IN Mountain, G.S., Miller, K.G., and Blum, P., Poag, C.W., and Twichell, D.C. (Eds.), Proc. ODP, Sci. Results, 150: College Station, TX., 429-432.

Austin, J.A., Jr., Christie-Blick, N., Malone, M.J., et al., (1998) Proceedings of the Ocean Drilling Program, Initial Reports, Vol. 174A.

Barbieri, R., Benjamini, C., Monechi, S., and Reale, V. (2003) Stratigraphy and benthic foraminiferal events across the Middle-Late Eocene transition in Western Negev, Israel: IN Prothero, D.R., Ivany, L.C., and Nesbitt, E.A., Eds., From Greenhouse to Icehouse: The Marine Eocene-Oligocene Transition. Columbia Univ. Press, N.Y., p. 453-470.

Barrett, P. (2003) Cooling a climate: Nature, 421, 221-223.

Beniamovski, V., Alekseev-Alexander, A., Ovechkina, M.N., and Oberhaensli, H. (2003) Middle to upper Eocene dysoxic-anoxic Kuma Formation (Northeast Peri-Tethys); biostratigraphy and paleoenvironments: G.S.A. Special Paper No. 369, 95-112.

Berggren, W.A. and Miller, K.G. (1989) Cenozoic bathyal and abyssal calcareous benthic foraminiferal zonations: Micropaleontology, 35: 308-320.

Berggren, W.A., Kent, D.V., Swisher, C.C., III, and Aubry, M.-P. (1995) A revised Cenozoic geochronology and chronostratigraphy : IN Berggren, W.A., Kent, D.V., and Hardenbol, J. (Eds.), Geochronology, Time Scales, and Global Stratigraphic Correlations: A Unified Temporal Framework for an Historical Geology: Soc. Econ. Paleon. Miner. Spec. Publ., 54: 129-212.

Bestland, E.A. (2000) Weathering flux and CO_2 consumption determined from paleosol sequences across the Eocene-Oligocene transition: Palaeogeog., Palaeoclim., Palaeoecol., 156, no.3-4, 301-326.

Blackman, R. B., and J. W. Tukey (1958) The Measurement of Power Spectra From the Point of View of Communication Engineering. Dover Publications, New York, 190 pp.

Bodiselitsch, B., Montanari, A., Koeberl, C., and Coccioni, R. (2004) Delayed climate cooling in the Late Eocene caused by multiple impacts: high-resolution geochemical studies at Massignano, Italy: Earth and Plan. Sci. Letters, 223, 283-302.

Bohaty, S.M., Harwood, D.M., and Zachos, J.C. (2000) Eocene "jump starting" of thermohaline upwelling in the Southern Ocean: G.S.A. Abstracts with Programs, 32, no. 7, 146.

Bohaty, S. M. and Zachos, J.C. (2003) Significant Southern Ocean warming event in the late middle Eocene: Geology, 31, no. 11: 1017-1020.

Bolli, H.M., Beckmann, J.P., and Saunders, J.B. (1994) Benthic Foraminiferal Biostratigraphy of the South Caribbean Region. Cambridge Univ. Press.

Bottomley, R.J., Grieve, R.A., York, D., and Masaitis, V. (1997) The age of the Popagai impact event and its relation to events at the Eocene / Oligocene boundary: Nature, 388, 365-388.

Browning, J.V., Miller, K.G., and Bybell, L.M. (1997) Upper Eocene sequence stratigraphy and the Absecon Inlet Formation, New Jersey coastal plain: IN Miller, K.G. and Snyder, S.W. (Eds.), Proc. ODP, Sci. Results, 150X: College Station, TX., 243-265.

Browning, J.V., Miller, K.G., and Olsson, R.K. (1997) Lower to Middle Eocene benthic foraminiferal biofacies and lithostratigraphic units and their relationship to sequences, New Jersey coastal plain: IN Miller, K.G. and Snyder, S.W. (Eds.), Proc. ODP, Sci. Results, 150X: College Station, TX, 207-228.

Browning, J.V., Miller, K.G., and Pak, D.K. (1996) Global implications of lower to middle Eocene sequence boundaries on the New Jersey coastal plain: The icehouse cometh: Geol., v. 24, no. 7, 639-642.

Browning, J.V., Miller, K.G., and Pak, D.K. (1996) Global implications of lower to middle Eocene sequence boundaries on the New Jersey coastal plain: The icehouse cometh, Geology, v. 24, no. 7, 639-642.

Browning, J.V., Miller, K.G., Van Fossen, M., Liu, C., Pak, D.K., Aubry, M., and Bybell, L.M. (1997) Lower to middle Eocene sequences of the New Jersey coastal plain and their significance for global climate change: IN Miller, K.G. and Snyder, S.W. (Eds.), Proc. ODP, Sci. Results, 150X: College Station, TX.,229-242.

Campbell, D.C. and Campbell, M.R. (2003) Biotic patterns in Eocene-Oligocene mollusks of the Atlantic coastal plain, U.S.A.: IN Prothero, D.R., Ivany, L.C., and Nesbitt, E.A., Eds., From Greenhouse to Icehouse: The Marine Eocene-Oligocene Transition. Columbia Univ. Press, N.Y., p. 341-353.

Coccioni, R. and Galeotti, S. (2003) Deep-water benthic foraminiferal events from the Massignano Eocene/Oligocene boundary stratotype, Central Italy: IN Prothero, D.R., Ivany, L.C., and Nesbitt, E.A., Eds., From Greenhouse to Icehouse: The Marine Eocene-Oligocene Transition. Columbia Univ. Press, N.Y., p. 438-452.

Coxall, H.K., Pearson, P.N., Shackleton, N.J., and Hall, M.A. (2000) Hantkeninid depth adaptation; an evolving life strategy in a changing ocean: Geology, 28, no. 1, 87-90.

Curry, W.B., Thunell, R.C., and Honjo, S. (1983) Seasonal changes in the isotopic composition of planktonic foraminifera collected in Panama Basin sediment traps: Earth & Planetary Sci. Letters, 64, 33-43.

DeConto, R. and Pollard, D. (2001) The early glacial history of Antarctica; a new modeling perspective: Quaderni di Geofisica, 16, 45-47.

DeConto, R. and Pollard, D. (2003) Rapid Cenozoic glaciation of Antarctica induced by declining atmospheric CO_2: Nature, 421, 245-249.

Diekmann, B., Kuhn, G., Gersonde, R., and Mackensen, A. (2004) Middle Eocene to early Miocene environmental changes in the sub-Antarctic Southern Ocean; evidence from biogenic and terrigenous depositional patterns at ODP Site 1090: Global and Planetary Change, 40, no. 3-4, 295-313.

Diester-Haass, L. and Zahn, R. (1996) Eocene-Oligocene transition in the Southern Ocean: history of water mass circulation and biological productivity: Geology, 24, 163-166.

Diester-Haass, L. and Zachos, J. (2003) The Eocene-Oligocene transition in the equatorial Atlantic (ODP Site 925): paleoproductivity increase and positive $\delta^{13}C$ excursion: IN Prothero, D.R., Ivany, L.C., and Nesbitt, E.A., Eds., From Greenhouse to Icehouse: The Marine Eocene-Oligocene Transition. Columbia Univ. Press, N.Y., p. 397-416.

Dockery III, D.T., and Lozouet, P. (2003) Molluscan faunas across the Eocene/Oligocene boundary in the North American Gulf Coastal Plain, with comparisons to those of the Eocene and Oligocene of France: IN Prothero, D.R., Ivany, L.C., and Nesbitt, E.A., Eds., From Greenhouse to Icehouse: The Marine Eocene-Oligocene Transition. Columbia Univ. Press, N.Y., p. 303-340.

Ermann, W. (1998) Implications of late Eocene to early Miocene clay mineral assemblages in McMurdo Sound (Ross Sea, Antarctica) on paleoclimate and ice dynamics: Palaeogeog., Palaeoclim., Palaeoecol., 139, no. 3-4, 213-231.

Elsik, W.C. and Yancey, T.E. (2000) Palynomorph assemblage zones in the context of changing paleoclimate, middle Eocene to lower Oligocene of East Texas: AAPG Bulletin, 84, no. 10, p. 1676.

Fairbanks, R.G., Wiebe, P.H., and Be, A.W.H. (1980) Vertical distribution and isotopic composition of living planktonic foraminifera in the Western North Atlantic: Science, v. 207, 61-63.

Fluegeman, R.H. (2003) Late-Eocene early-Oligocene benthic foraminifera in the Gulf Coastal Plain: regional vs. global influences: IN Prothero, D.R., Ivany, L.C., and Nesbitt, E.A., Eds., From Greenhouse to Icehouse: The Marine Eocene-Oligocene Transition. Columbia Univ. Press, N.Y., p. 283-293.

Gammon, P.R., James, N.P., and Pisera, A. (2000) Eocene spiculites and spongolites in southwestern Australia; not deep, not polar, but shallow and warm: Geology, 28, no. 9, 855-858.

Haq, B.U., Hardenbol, J., and Vail, P.R. (1987) Chronology of Fluctuating Sea Levels Since the Triassic, Science, v. 235, 1156-1166.

Hay, W.W., Soeding, E., and DeConto, R.M. (2002) The late Cenozoic uplift - climate change paradox: Int. J. Earth Sci., 91, 746-774.

Hickman, C.S. (2003) Evidence for abrupt Eocene-Oligocene molluscan faunal change in the Pacific Northwest: IN Prothero, D.R., Ivany, L.C., and Nesbitt, E.A., Eds., From Greenhouse to Icehouse: The Marine Eocene-Oligocene Transition. Columbia Univ. Press, N.Y., p. 71-87.

Hurley, J.V. and Fluegeman, R.H. (2003) Late Middle Eocene glacioeustacy: stable isotopes and foraminifera from the Gulf Coastal Plain: IN Prothero, D.R., Ivany, L.C., and Nesbitt, E.A., Eds., From Greenhouse to Icehouse: The Marine Eocene-Oligocene Transition. Columbia Univ. Press, N.Y., p. 223-231.

Iturralde-Vinent, M.A. (2003) A brief account of the evolution of the Caribbean seaway: Jurassic to present: IN Prothero, D.R., Ivany, L.C., and Nesbitt, E.A., Eds., From Greenhouse to Icehouse: The Marine Eocene-Oligocene Transition. Columbia Univ. Press, N.Y., p. 386-396.

Ivany, L.C., Lohmann, K.C., and Patterson, W.P. (2003) Paleogene temperature history of the U.S. Gulf Coastal Plain inferred from $\delta^{18}O$ of fossil otoliths: IN Prothero, D.R., Ivany, L.C., and Nesbitt, E.A., Eds., From Greenhouse to Icehouse: The Marine Eocene-Oligocene Transition. Columbia Univ. Press, N.Y., p. 232-251.

Ivany, L.C., Van Simaeys, S., Domack, E.W., and Samson, S.D. (2006) Evidence for an earliest Oligocene ice sheet on the Antarctic Peninsula: Geology, 34, no. 5, 377-380.

Jarrard, R.D. and Arthur, M.A. (1989) Milankovitch paleoceanographic cycles in geophysical logs from ODP Leg 105, Labrador Sea and Baffin Bay: IN Srivastava, S.P., Arthur, M., Clement, B., et. al., Proc. ODP, Sci. Results, vol. 105: College Station, TX (Ocean Drilling Program).

Junge, F., Boettger, T., Morgenstern, P., and Kuehl, A. (2003) Comparative investigations into the upper Eocene and Quaternary palaeoenvironmental and palaeoclimate by geochemical studies of fluvial sediments and incorporated fossil tree trunks (central Germany): IN XVI INQUA congress; Shaping the Earth; A Quaternary Perspective, 79 pp.

Kar, R.K. (2000) Palynostratigraphy of the Tertiary sediments in North-east India with comments on the terminal Eocene events: The Paleobotanist: 49, no. 2, 281-292.

Katz, M.E. and Miller, K.G. (1996) Eocene to Miocene oceanographic provenance changes in a sequence stratigraphic framework : benthic foraminifers of the New Jersey margin: IN Mountain, G.S., Miller, K.G., Blum, P., Poag, C.W., and Twichell, D.C., Proc. ODP Scientific Results, vol. 150: College Station, TX (Ocean Drilling Program).

Kautz, C. and Ryan, P. (2002) The mineralogical record of climate change in the John Day Formation, central Oregon: G.S.A. Abstracts with Programs, 34, no. 5, p. 26.

Kominz, M.A., Miller, K.G., and Browning, J.V. (1998) Long-term and short term global Cenozoic sea-level estimates, Geology, v. 26, no. 4, 311-314.

Kvacek, Z. (2002) Late Eocene landscape, ecosystems and climate in northern Bohemia with particular reference to the locality of Kuclin near Bilina: Bulletin of the Czech Geological Survey: 77, no. 3, 217-236.

Lavelle, M. (2000) Direct Evidence for a major expansion of the East Antarctic ice sheet at 33 Ma: American Geophysical Union Fall 2000 Meeting, Abstract No. OS21E-08.

Lawver, L.A. and Gahagan, L.M. (2003) Evolution of Cenozoic seaways in the circum-Antarctic region: Palaeogeog., Palaeoclim., Palaeoecol., 198, no. 1-2, 11-37.

Lear, C.H., Bailey, T.R., Pearson, P.N., Coxall, H.K., and Rosenthal, Y. (2008) Cooling and ice growth across the Eocene-Oligocene transition: Geology, v. 36, no. 3, 251-254.

Lister, G.S., Etheridge, M.A., and Symonds, P.A. (1986) Detachment faulting and the evolution of passive continental margins: Geology, 14, 246-250.

Liu, G. and Yang, R. (1999) Pollen assemblages of the late Eocene Nadu Formation from the Bose Basin of Guangxi, southern China: Palynology, 23, 97-114.

Loeblich, A.R. and Tappan, H. (1988) Foraminiferal Genera and their Classification. Van Nostrand Reinhold.

McHugh, C.M.G. (1997) Effects of relative sea level changes on diagenesis of Eocene sediment: New Jersey slope and coastal plain: IN Miller, K.G. and Snyder, S.W. (Eds.), Proc. ODP, Sci. Results, 150X: College Station, TX, 25-49.

McHugh, C.M.G., Ryan, W.B.F., and Schreiber, B.C. (1993) The role of diagenesis in exfoliation of submarine canyons, AAPG Bull., V. 77, No. 2, 145-172.

McHugh, C.M.G., Snyder, S.W., Deconinck, J-F., Saito, Y., Katz, M.E., and Aubry, M-P. (1996) Upper Eocene tektites of the New Jersey continental margin, site 904, IN Mountain, G.S., Miller, K.G., Blum, P., and Twichell, D.C. (Eds.), Proc. O.D.P., Scientific Results, Vol. 150, 241-265.

McHugh, C.M.G., Snyder, S.W., and Miller, K.G. (1998) Upper Eocene ejecta of the New Jersey continental margin reveal dynamics of Chesapeake Bay impact: Earth and Planetary Science Letters, 160, 353-367.

McKenszie, D. (1978) Some remarks on the development of sedimentary basins: Earth and Planetary Science Letters, 40, 25-32.

Miller, K.G., Browning, J.W., Kominz, M.A., Wright, J.D., Sugarman, P.J., Mountain, G.S., Hernandez, J.C., Olsson, R.K., and Feigenson, M.D. (2002) Ocean Drilling Program, Sequences, and Global Sea-Level Change: Comparison of Icehouse vs. Greenhouse Eustatic Changes: www.gcssepm.org/pubs/2002_ab_30.htm.

Miller, K.G., Fairbanks, R.G., and Mountain, G.S. (1987) Tertiary oxygen isotope synthesis, sea level history, and continental margin erosion, Paleoceanography, v. 2, no. 1, 1-19.

Miller, K.G., Mountain, G.S., Browning, J.V., Kominz, M., Sugarman, P.J., Christie-Blick, N., Katz, M.E., and Wright, J.D. (1998) Cenozoic global sea level, sequences, and the New Jersey transect: results from coastal plain and continental slope drilling: Reviews of Geophysics, 36, no. 4, 569-601.

Miller, K.G., Mountain, G.S., and Shipboard Party (1996) Drilling and Dating New Jersey Oligocene-Miocene Sequences: Ice Volume, Global Sea Level, and Exxon Records, Science, v. 271, 1092-1095.

Miller, K.G., Mountain, G.S., and Shipboard Scientific Party (1994) Introduction: IN Mountain, G.S., Miller, K.G., Blum, et al., Proc. ODP, Init. Repts., 150: College Station, TX., 5-20.

Miller, K.G. and Sugarman, P.J. (1995) Correlating Miocene sequences in onshore New Jersey boreholes (ODP Leg 150X) with global $\delta^{18}O$ and Maryland outcrops, Geology, v. 23, no. 8, 747-750.

Miller, K.G., Sugarman, P.J., Browning, J.V., et al. (1998) 1. Bass River Site: IN Miller, K.G., Sugarman, P.J., Browning, et al., Proc. ODP, Init. Repts., 174AX, College Station, TX.

Miller, K.G., Wright, J.D., and Faribanks, R.G. (1991) Unlocking the Ice House: Oligocene-Miocene oxygen isotopes, eustacy, and margin erosion: Jour. Geophys. Res., v. 96, NO. B4, 6829-6848.

Mix, A.C. (1987) The Oxygen-Isotope Record of Glaciation, IN Ruddiman, W.F., Wright, H.E. Jr., (Eds.). North America and Adjacent Oceans During The Last Deglaciation: Boulder, Co., Geol. Soc. Amer., The Geo. of N. Amer. K-3

Moss, G. and McGowran, B. (1999) Sequence biostratigraphy in "greenhouse" and "icehouse" worlds; a valid proxy for sea level change?: A.A.P.G. Annual Meeting Expanded Abstracts, 1999, p. A97.

Mountain, G.S., Miller, K.G., Blum, P., et al. (1994) Proc. ODP, Init. Repts., 150: College Station, TX., 885 pp.

Myers, J.A. (2003) Terrestrial Eocene-Oligocene vegetation and climate in the pacific northwest: IN Prothero, D.R., Ivany, L.C., and Nesbitt, E.A., Eds., From Greenhouse to Icehouse: The Marine Eocene-Oligocene Transition. Columbia Univ. Press, N.Y., p. 171-185

Nebelsick, J.H., Rasser, M., and Bassi, D. (1999) The marine Eocene-Oligocene transition as recorded in shallow water, Tethyan carbonates: G.S.A. Abstracts with Programs, 31, no.7, p.310.

Nebelsick, J.H., Rasser, M., and Bassi, D. (2003) The development of facies patterns of Middle Eocene to Lower Oligocene circum-alpine, shallow water carbonate environments: IN Prothero, D.R., Ivany, L.C., and Nesbitt, E.A., Eds., From Greenhouse to Icehouse: The Marine Eocene-Oligocene Transition. Columbia Univ. Press, N.Y., p. 471-491.

Nesbitt, E.A. (1999) Changes in marine neritic paleoassemblages of the northeastern Pacific margin in response to the Eocene-Oligocene global climate shift: G.S.A. Abstracts with Programs, 31, no. 7, p. 310.

Nilsen, E.B., Anderson, L.D., and Delaney, M.L. (2003) Paleoproductivity, nutrient burial, climate change and the carbon cycle in the western equatorial Atlantic across the Eocene/Oligocene boundary: Paleoceanography, 18, no. 3, 11 pp.

O'Brien, P.E., Cooper, A.K., Richter, C., Macphail, M., and Truswell, E.M. (2000) Milestones in Antarctic ice sheet history; preliminary results from Leg 188 drilling in Prydz Bay, Antarctica: JOIDES Journal, 26, no. 2, 4-10.

Oboh-Ikuenobe, F.E., and Jaramillo, C.A. (2003) Palynological patterns in uppermost Eocene to Lower Oligocene sedimentary rocks in the U.S. Gulf Coast: IN Prothero, D.R., Ivany, L.C., and Nesbitt, E.A., Eds., From Greenhouse to Icehouse: The Marine Eocene-Oligocene Transition. Columbia Univ. Press, N.Y., p. 269-282.

O'Neil, J.R., Clayton, R.N., and Mayeda, T.K. (1969) Oxygen isotope fractionation in divalent metal carbonates: J. Chem. Phys., 51, 5547-5558.

Pagani, M., Zachos, J.C., Freeman, K.H., Tipple, B., and Bohaty, S. (2005) Marked decline in atmospheric carbon dioxide concentrations during the Paleogene: Science, 308, 600-603.

Paillard, D., Labeyrie, L., and Yiou, P. (1996) Macintosh program performs time-series analysis. EOS Trans., AGU vol. 77, 379.

Palike, H., Shackelton, N.J., and Roehl, U. (2001) Astronomical forcing in late Eocene marine sediments: Earth and Planetary Science Letters, 193, no. 3-4, p. 589-602.

Pazzaglia, F.J. and Gardner, T.W. (2000) Late Cenozoic landscape evolution of the US Atlantic passive margin: insights into a North American Great Escarpment: IN Summerfield, M.A. (Ed.), Geomorphology and Global Tectonics, Chap. 13, 283-306.

Pearson, P.N., Bart, E., van Dongen, B.E., Nicholas, C.J., Pancost, R.D., Schouten, S., Singano, J.M., and Wade, B.S. (2007) Stable warm tropical climate through the Eocene Epoch: Geology, v. 35, no. 3, 211-214.

Pekar, S.F., Miller, K.G., and Kominz, M.A. (2000) Reconstructing the stratal geometry of latest Eocene to Oligocene sequences in New Jersey: resolving a patchwork distribution into a clear pattern of progradation, Sedimentary Geology, 134, 93-109.

Poag, C.W. and Commeau, J.A. (1995) Paleocene to middle Miocene planktic foraminifera of the southwestern Salisbury Embayment, Virginia and Maryland: Journal of Foraminiferal Research, 25, no.2, 134-155.

Poag, C.W., Mankinen, E., and Norris, R.D. (2003) Late Eocene impacts: geological record, correlation, and paleoenvironmental consequences: IN Prothero, D.R., Ivany, L.C., and Nesbitt, E.A., Eds., From Greenhouse to Icehouse: The Marine Eocene-Oligocene Transition. Columbia Univ. Press, N.Y., p. 495-510.

Pratson, L.F. and Haxby, W.F. (1996) What is the slope of the U.S. continental slope?: Geology, 24, no. 1: 3-6.

Prentice, M.L. and Mathews, R.K. (1988) Cenozoic ice-volume history: Development of a composite oxygen isotope record, Geology, v.16, 963-966.

Prothero, D.R. (1994) The Eocene-Oligocene Transition: Paradise Lost. Columbia Univ. Press, New York, 281 pp.

Purton, L.M.A. and Brasier, M.D. (1997) Gastropod carbonate $\delta^{18}O$ and $\delta^{13}C$ values record strong seasonal productivity and stratification shifts during the late Eocene in England: Geology, 25, no. 10, 871-874.

Pusz, A.E., Miller, K.G., Wright, J.D., Browning, J.V., Wade, B.S. and Kent, D.V. (2006) Upper Eocene microtektites discovered in Alabama: a first-order correlation to the GPTS: Abstract, G.S.A. Annual Meeting, Oct. 2006, Philadelphia Pa.

Retallack, G.J. (2002) Paleosol compared with deep sea-records of Cenozoic global paleoclimatic change: G.S.A. Abstracts with Programs, 34, no. 6, p. 63-64.

Robert, C., Diester-Haass, L., and Chamley, H. (2002) Late Eocene-Oligocene oceanographic development at southern high latitudes, from terrigenous and biogenic particles; a comparison of Kerguelen Plateau and Maud Rise, ODP Sites 744 and 689: Marine Geology, 191, no. 1-2, 37-54.

Robinson, E. (2003) Upper Paleogene larger foraminiferal succession on a tropical carbonate bank, Nicaragua rise, Caribbean region: IN Prothero, D.R., Ivany, L.C., and Nesbitt, E.A., Eds., From Greenhouse to Icehouse: The Marine Eocene-Oligocene Transition. Columbia Univ. Press, N.Y., p. 294-302.

Roth-Nebelsick, A., Utescher, T., Mosbrugger, V., Diester-Haass, L., and Walther, H. (2004) Changes in atmospheric CO_2 concentrations and climate from the late Eocene to early Miocene; palaeobotanical reconstruction based on fossil floras from Saxony, Germany: Palaeogeog., Palaeoclim., Palaeoecol., 205, no. 1-2, 43-67.

Schellenberg, S.A. (1999) Deep-ocean ostracode response to the Eocene-Oligocene transition; high resolution records from the Southern Ocean (ODP sites 744 and 689): G.S.A. Abstracts with Programs 31, no. 7, p. 310.

Serra, O. (1989) Formation Microscanner Image Interpretation. Schlumberger Educational Services, Houston, TX, 117 pp.

Shackleton, N.J. (1974) Attainment of isotopic equilibrium between ocean water and the benthonic foraminifera genus *Uvigerina*: Isotopic changes in the ocean during the last glacial: Colloq. Int. C.N.R.S. 219, 203-210.

Shipboard Scientific Party (2000) Leg 189 Preliminary Report: The Tasmanian Seaway Between Australia and Antarctica Paleoclimate and Paleoceanography. ODP Prelim. Rpt., 89 [On-line].

Shipboard Scientific Party (2001) Leg 188 summary: Prydz Bay-Cooperation Sea, Antarctica. IN O'Brien, P.E., Cooper, A.K., Richter, C., et.al., *Proc. ODP, Init. Repts*., 188: College Station TX (Ocean Drilling Program), 1-65.

Shipboard Scientific Party (2001) Leg 189 summary: The Tasmanian Gateway. IN Exon, N.F., Kennet,J.P., Malone, M.J., et. al., *Proc. ODP, Init. Repts*., 189: College Station TX (Ocean Drilling Program),1-98.

Shipboard Scientific Party (2004) Leg 208 summary. IN Zachos, J.C., Kroon, D., Blum, P. et al., *Proc. ODP, Init. Repts*., 208: College Station TX (Ocean Drilling Program), 1-112.

Snyder, S.W. (1996) Data report: abundance patterns of planktonic foraminifers: site 904, LEG 150: IN Mountain, G.S., Miller, K.G., and Blum, P., Poag, C.W., and Twichell, D.C. (Eds.), Proc. ODP, Sci. Results, 150: College Station, TX., 455-460.

Snyder, S.W., Miller, K.G., and Saperson, Esfir (1996) Paleogene and Neogene planktonic foraminiferal biostratigraphy of the New Jersey continental slope: Sites 902, 903, and 904 (LEG 150): IN Mountain, G.S., Miller, K.G., Blum, P., Poag, C.W., and Twichell, D.C. (Eds.), Proc. ODP, Sci. Results, 150: College Station, TX., 3-15.

Snyder, S.W., and Waters, V.J. (1985) Cenozoic planktonic foraminifera biostratigraphy of the Goban Spur region, DSDP Leg 80: IN DeGracianski and Poag, C.W., Eds., Initial Reports of the Deep Sea Drilling Project, 80, 439-472.

Spezzaferri, S., Basso, D., and Coccioni, R. (2002) Late Eocene planktonic foraminiferal response to an extraterrestrial impact at Massignano GSSP (northeastern Apennines, Italy): Journal of Foraminiferal Research, 32, no. 2, 188-199.

Squires, R.L. (2003) Turnovers in marine gastropod faunas during the Eocene-Oligocene transition, west coast of the United States: IN Prothero, D.R., Ivany, L.C., and Nesbitt, E.A., Eds., From Greenhouse to Icehouse: The Marine Eocene-Oligocene Transition. Columbia Univ. Press, N.Y., p. 14-35.

Steckler, M.S. (2000) Reconstruction of the Cenozoic stratigraphy at the New Jersey margins; the interaction of climate, sediment supply and sea level: G.S.A. Abstracts with Programs, 32, no.1, p. 76.

Steckler, M.S., Mountain, G.S., Miller, K.G., and Christie-Blick, N. (1999) Reconstruction of Tertiary progradation and clinoform development on the New Jersey passive margin by 2-D backstripping, Marine Geology, 154, 399-420.

Steckler, M.S. and Watts, A.B. (1978) Subsidence of the Atlantic-type continental margin off New York: Earth and Planetary Science Letters, 41, 1-13.

Strand, K., Passchier, S., and Nasi, J. (2003) Implications of quartz grain microtextures for onset Eocene/Oligocene glaciation in Prydz Bay, ODP

Site 1166, Antarctica: Palaeogeog., Palaeoclim., Palaeoecol., 198, no. 1-2, 101-111.

Terry, D.O. Jr. (2001) Paleopedology of the Chadron Formation of northwestern Nebraska; implications for paleoclimatic change in the North American midcontinent across the Eocene-Oligocene boundary: Palaeogeog., Palaeoclim., Palaeoecol., 168, no.1-2, 1-38.

Thunell, R.C., Curry, W.B., and Honjo, S. (1983) Seasonal variation in the flux of planktonic foraminifera: time series sediment trap results from the Panama Basin: Earth and Planetary Sci. Ltrs., 64, 44-55.

Vail, P.R. and Mitchum, R.M. (1977) Seismic Stratigraphy and Global Changes of Sea-Level, Part 1, Overview, IN Payton, C.E. (Ed.), AAPG Memoir 26 Seismic Stratigraphy – Applications to Hydrocarbon Exploration, p. 51-52.

Van Morkoven, F.P., Berggren, W.A., and Edwards, A.S. (1987). Cenozoic Cosmopolitan Deep-Water Benthic Foraminifera. Bulletin Des Centres de Recherches Exploration-Production Elf-Aquitaine, Memoir v. 11, 421 pp.

Wade, B., Kroon, D., and Norris, R.D. (2001) Orbitally forced climate change in late mid-Eocene time at Blake Nose (Leg 171B); evidence from stable isotopes in Foraminifera: Geol. Soc. Lond. Special Publication 183, 273-291.

Wang, D. (1999) Late Eocene sporopollen and paleoclimate, paleoenvironment of the Yuanqu Basin, Shanxi: Continental Dynamics, 4, no.2, 29-38.

Weedon, G. (2003) Time-Series Analysis and Cyclostratigraphy: Examining stratigraphic records of environmental cycles. Cambridge Univ. Press, 259 pp.

Wilson, G.S., Florindo, F., Roberts, A.P., Sagnotti, L., and Verosub, K.L. (1999) Magnetostratigraphic and environmental magnetic records of Antarctic paleoclimate from Eocene-Oligocene glaciomarine sediments, Victoria Land Basin, Antarctica: G.S.A. Abstracts with Programs, 31, no.7, p. 309.

Yancey, T.E. and Elsik, W.C. (1999) The palynological record of late Eocene climate change and terrestrial palynostratigraphy, Northwest Gulf of Mexico: Abstracts with Programs, G.S.A., 31, no. 7, 309-310.

Zachos, J.C, Quinn, T.M., Salamy, K.A. (1996) High-resolution (10^4 years) deep-sea foraminiferal stable isotope records of the Eocene-Oligocene climate transition: Paleoceanography, v. 11, no. 3, 251-266.

Zachos, J., Pagani, M., Sloan, L., Thomas, E., and Billups, K. (2001) Trends, rhythms, and aberrations in global climate 65 Ma to present: Science, 292, 686-693.

Zachos, J.C., D. Kroon, P. Blum, et al. (2004) Proc. ODP, Init. Repts., 208, College Station, TX (Ocean Drilling Program).